Aggregation, adsorption and toxicity of fullerene C60 nanoparticles in the activated sludge process(Dissertation_全文)

AUTHOR(S):

Yang, Yongkui

Aggregation, adsorption and toxicity of fullerene C_{60} nanoparticles in the activated sludge process

YONGKUI YANG

2013

Aggregation, adsorption and toxicity of fullerene C_{60} nanoparticles in the activated sludge process

（活性汚泥法におけるフラーレン C_{60} ナノ粒子の凝集、吸着と毒性に関する研究）

YONGKUI YANG

A Dissertation submitted in partial fulfillment of

the requirements for the degree of

Doctor of Engineering

Department of Environmental Engineering

Graduate School of Engineering

Kyoto University

Kyoto, Japan

March 2013

ABSTRACT

Fullerene C_{60} nanoparticles are expected to have promising potential for the application in wide fields such as the optics, sensors, electronics and coating in industry, and the cosmetics, clothing, sunscreen in consumer products. The growing production and use of C_{60} will inevitably result in their entering into the environment. The aqueous C_{60} aggregate (nC_{60}) presented the toxicity on a wide range of organisms partially due to the oxidative stress by producing the reactive oxygen species. This raises recent concerns about the environmental risks and human health. Once released, the wastewater treatment plant would be a key route for nC_{60} discharge into the environment. However, it is still unclear about the fate of nC_{60} in the activated sludge process. Moreover, as an emerging pollutant with nanoscale size, the aggregation of nC_{60} in wastewater could affect their fate during the wastewater treatment as well as the toxicity. However, no information is available on size aggregation of nC_{60} in wastewater. If nC_{60} has an adverse antibacterial effect on the activated sludge, it will greatly affect the removal of organic matters and nutrients in wastewater. Based on the background above, the size aggregation in wastewater, adsorption on different wastewater sludges and toxicity on activated sludge were investigated in this study.

Firstly, two types of nC_{60} were prepared using the toluene exchange (tol/nC_{60}) and extended stirring (aqu/nC_{60}) techniques. Two types of nC_{60} demonstrated very similar size distribution with an average size of 154 and 144 nm for aqu/nC_{60} and tol/nC_{60}, respectively. Both nC_{60} were negatively charged in Milli-Q water at pH 5.6. The tol/nC_{60} was used for studies of nC_{60} fate in the activated sludge process because of less time-consuming and high production. And the aqu/nC_{60} was used for the studies on toxicity because this preparation method could mostly represent the real transition of C_{60} to water environment during the production and consumption of C_{60} nanoparticle. In addition, the tol/nC_{60} was also used for the studies on toxicity to investigate the effect of preparation methods on nC_{60} toxicity.

And the nC_{60} extraction in wastewater was evaluated using the liquid-liquid extraction (LLE) or solid phase extraction (SPE) methods. And the method detection limits (MDL) of nC_{60} in wastewater were determined using the HPLC-UV/vis system

with LLE or SPE. The LLE method gave a MDL of 1.07 μg/L with a recovery of > 90 %. And the SPE gave a MDL of 0.03 μg/L with a recovery of > 64 %. Based on the annual wastewater and the production of C_{60} in Japan, the nC_{60} concentration was estimated to be 0.020 μg/L in the raw wastewater. And no nC_{60} was detected in the influent from a domestic WWTP in Japan.

And then the developed methods were used to investigate the fate of nC_{60} in the activated sludge process. It included two parts: the nC_{60} size aggregation in wastewater and their adsorption behavior on the wastewater sludges. This was the first study to investigate the effects of pH, ionic strength and dissolved organic matter (DOM) on nC_{60} aggregation in wastewater. The nC_{60} remained relatively stable up to 24 h under environmentally relevant values of ionic strength and pH. This finding suggested the potential for nC_{60} discharge from wastewater treatment plants in effluent and subsequent long-distance transport in water environment. At high ionic strength (>100 mM) or under acidic conditions (pH 3), the absolute ζ potential of the nC_{60} was reduced to ≲20 mV from an initial ~30 mV, increasing the size of aggregates up to the micrometer scale. The nC_{60} aggregation behavior varied among wastewater samples. These results showed the aquatic conditions could affect the aggregation behavior of nC_{60} in wastewater which might consequently influence their fate during the wastewater treatment process.

The second part investigated the adsorption behavior of nC_{60} on the different sludges. The adsorption mechanism was explained by modeling the adsorption isotherm and kinetics, analyzing the correlation of nC_{60} adsorption coefficients and surface properties of sludge samples, as well as the effect of influencing factors on the adsorption on sludge. The adsorption on the primary and activated sludge well followed the Freundlich model indicating the adsorption occurred at multi-layer and on the heterogeneous surface of the sludges. The high correlation with linear partitioning model suggested the partitioning process played an important role in the adsorption process on the sludge such as the hydrophobic-hydrophobic interactions. The activated sludge had a much higher Freundlich coefficient (k_F) and linear partitioning coefficient (k_d) than those for the primary sludge indicating their higher adsorption capacity. It could be attributed to the higher hydrophobicity and lower absolute ζ potential of

activated sludge which could contribute to the adsorption of nC_{60} by increasing the attractive force and reducing the repulsive forces, respectively. The pH values greatly affected the adsorption process, decreasing the adsorption of nC_{60} from 86% at pH 3 to 26% at pH 11 after 1 h of mixture. At MLSS concentrations of 1000 and 2000 mg/L, which are common in the conventional activated sludge process, the reduction of nC_{60} in the aqueous phase after 1 h of mixture reached up to 48 and 74%, respectively, demonstrating high removal efficiency. The adsorption coefficients of k_F and k_d showed consistent correlations with the surface properties: positive correlation with relative hydrophobicity and ζ potential, negative with sludge size. These results showed both the electrostatic repulsions and hydrophobic attractions were involved in the nC_{60} adsorption on the activated sludge, as well as sludge size.

In addition, the sequencing batch reactor (SBR) was used to investigate the effect of aqu/nC_{60} on treatment performance of activated sludge process. The toxicity of aqu/nC_{60} on activated sludge was indicated using the nitrifying sludge and bioluminescent bacteria. And the tol/nC_{60} was also used to investigate the effect of preparation methods on nC_{60} toxicity. After exposure of 0.100 and 0.500 mg/L nC_{60} for 10 days, no significant effect was observed on the water quality of treated wastewater by the SBR, and on the sludge growth and settlement properties. The adsorption amount of nC_{60} was calculated to be 7.63 mg (nC_{60})/g (MLSS) at the exposure level studied. Therefore at this adsorption level, the nC_{60} had no significant effect on the treated performance by the SBR and the activated sludge. The aqu/nC_{60} presented no significant toxicity to the nitrification sludge and bioluminescent bacteria at 8.4 mg/L (maximum concentration studied). In contrast, the EC_{20} of tol/nC_{60} was obtained to be 4.89 mg/L (3 h) for the nitrification inhibition and 3.44 mg/L (30 min) for Microtox® test, respectively. Both the nitrification inhibition and Microtox® test showed the nC_{60} toxicity was greatly affected by the preparation method. This might be attributed to the difference in the physicochemical characteristics of nC_{60} prepared by different methods. Therefore, it is necessary to consider the effect of preparation methods on the physicochemical characteristics of nC_{60} when evaluating their toxicity.

Finally, a fate model based on the steady-state mass balance was developed by combing the primary and secondary treatments and then used to model the nC_{60} fate in

the activated sludge process. The nC_{60} removal efficiency increased with increase in the removal of suspended solids during the primary treatment. The increase in HRT, MLVSS and decrease in SRT could contribute to the removal of nC_{60} by increasing the discharge of excess activated sludge and adsorption capacity by the fresh sludge. The predicted no effect concentrations (PNEC) of nC_{60} were calculated to be 0.18 μg/L and 0.763 mg/g for the aquatic organism and activated sludge, respectively. Under the conventional operational conditions of activated sludge process, the nC_{60} concentration in secondary effluent and activated sludge would not exceed the PNEC until the nC_{60} in influent increase to be 0.35 μg/L and 0.16 mg/L, respectively. These exposure levels of the nC_{60} were much higher than the estimated nC_{60} concentration of 0.020 μg/L in raw wastewater based on the current production amount of C_{60} nanoparticle. However, due to high toxicity of nC_{60} on the human cell line and high assessment factor due to the uncertainties in the extrapolation for the human being, the remaining nC_{60} in treated wastewater might pose the potential risk on human health. Also, the rapid increase in C_{60}'s production and use will increase the potential of higher exposure to human beings. Therefore, it is necessary to further investigate the nC_{60}'s fate during different wastewater treatment processes.

TABLE OF CONTENTS

LIST OF FIGURES

LIST OF TABLES

CHAPTER I

INTRODUCTION

1.1 Research background

The nanotechnology market is expected to grow to 1 trillion US dollar by 2015 (Aitken et al., 2006). In 2011 the numbers of nanotechnology consumer products reached up to 1317 which increased by nearly 521% since 2006 (Woodrow Project on Emerging Nanotechnologies, 2012). Fullerene C_{60}, the most commonly-produced and -used fullerene nanoparticles, is expected to have promising potential for the application in wide fields such as the optics, sensors, electronics and coating in industry, and the cosmetics, clothing, sunscreen in consumer products (Murayama et al., 2004). The growing production and use of C_{60} will inevitably result in their entry into the environment, raising recent concerns about environmental risks and human health (Isaacson et al., 2009). C_{60} molecule can form stable nanoscale aggregates (nC_{60}) in water at mg/L level further higher than its molecule solubility of 7.96 ng/L (Ma and Bouchard, 2009) indicating its potential transport and exposure in water environment. Previous studies have showed the toxicity of the nC_{60} on the liver carcinoma cell (Sayes et al., 2004), bacteria (Lyon et al., 2006) and fish (Kim et al., 2010) partially due to the oxidative stress by producing the reactive oxygen species (ROS).

Once introduced into the wastewater, the wastewater treatment plant (WWTP) would be a key route for nC_{60} discharge into the environment. However, due to analytical difficulty it is still unclear whether the conventional WWTP can provide an efficient barrier or not. The quantification method have been developed for the tap water (Chen et al., 2008), surface water (Bouchard and Ma, 2008) and also organic matter-containing artificial water (Hyung and Kim, 2009). After extraction using the soxhlet, liquid-liquid or solid phase extraction, the C_{60} is usually quantified by the UV detector or mass spectrometry. The extraction efficiency might be greatly affected when treating the complex wastewater matrices. Therefore, it is needed to evaluate and establish an appropriate method for nC_{60} quantification in the wastewater.

C_{60} has been detected in the commercial cosmetics ranging from 0.04 to 1.1 μg/g (Benn et al., 2011), suggesting the potential pathway of C_{60} from consumer products to the wastewater streams. Given their non-biodegradation in the aerobic/anaerobic systems (Hartmann et al., 2011; Kummerer et al., 2011) and high hydrophobicity, the adsorption on the sludge might play an important role in the fate and removal of nC_{60} during the wastewater treatment. One study showed high adsorption of nC_{60} on the activated sludge (Kiser et al., 2010). However, the mechanisms of nC_{60} adsorption on sludge and their influencing factors during the wastewater treatment process are still unclear. Besides, it is necessary to clarify the nC_{60} adsorption on primary sludge during the primary wastewater treatment which could contribute to the control of the discharge of nC_{60} into the water environment. On the other hand, as an emerging contaminant (USEPA, 2009) with the nanoscale size, the toxic effect of nC_{60} was reported to be size-dependent (Lyon et al., 2006). Therefore it is necessary to consider not only the mass removal of nC_{60} during the wastewater treatment but also their size aggregation in wastewater. Also, the treatment process based on the size exclusion such as membrane filtration might be greatly affected by particle aggregation in wastewater. Therefore the information on size aggregation of nC_{60} in wastewater could help to predict their fate by different treatment process as well as the toxic effect.

The nC_{60} showed the antibacterial effect on the Gram-negative *Escherichia coli*, the Gram-positive *Bacillus subtilis*, and *Peseudomona Putida* (Lyon et al., 2005; Lyon et al., 2006). This suggested the potential of adverse effect of nC_{60} on the activated sludge. If so, it would greatly affect the removal of organic matters and nutrient compounds in wastewater. Therefore, the research is needed to evaluate the effect of nC_{60} on the treatment performance of activated sludge process as well as the potential toxicity on the activate sludge.

1.2 Research objectives

The main objective was to investigate the nC_{60} fate in the activated sludge process and the potential effect of nC_{60} exposure on performance of wastewater treatment. The specific objectives were as follows:

1) To establish the method for the nC_{60} quantification in wastewater

2) To investigate the nC_{60} fate in the activated sludge process including by studies on nC_{60} size aggregation in the wastewater and their adsorption on the wastewater sludges

3) To evaluate the potential effect of nC_{60} on the performance of activated sludge process and toxicity on the activated sludge

1.3 Research structure

This dissertation consisted of seven chapters. The study in each chapter was described as follows:

In Chapter I, the research background, the objectives and structure of this study were described.

In Chapter II, the literature review was conducted about the current knowledge on the application of fullerene nanoparticles, the quantification method in water samples, toxicity on the microorganisms, and the fate of fullerene nanoparticles in the activated sludge process.

In Chapter III, two types of nC_{60} aqueous suspension were prepared using different techniques for the following studies. And the detection and quantification limits of nC_{60} in wastewater samples were determined using the liquid-liquid extraction and solid phase extraction combined with the HPLC-UV/vis system.

In Chapter IV, the fate of nC_{60} in activated sludge process was investigated including two aspects, i.e., the size aggregation in wastewater and adsorption behavior on wastewater sludge. The aggregation behavior of nC_{60} in filtrated wastewater was investigated by analyzing the effects of pH, ionic strength and dissolved organic matter. The second part investigated the adsorption behavior of nC_{60} on the different sludge

samples, and explained the adsorption mechanism by modeling the adsorption isotherm and kinetics, analyzing the correlation of nC_{60} adsorption coefficients and surface properties of sludge samples.

In Chapter V, the effects of nC_{60} on treatment performance of activated sludge process were investigated using a sequential batch reactor. And the toxicity of nC_{60} on the activated sludge was indicated by investigating their effects on the nitrifying sludge and fluorescent bacteria.

In Chapter VI, a fate model based on the steady-state mass balance was used to investigate the nC_{60} fate in the activated sludge process. The Freundlich adsorption coefficients, obtained from Chapter IV, were used to determine the nC_{60} concentration in the effluent and excess sludge. The effects of HRT, SRT and MLVSS on the nC_{60} treatment were investigated as well as the relative contribution of each unit (i.e., primary treatment and secondary treatment) for the nC_{60} removal.

Chapter VII summarized the conclusions from this study and recommendations for future studies.

And the structure of this study was summarized in **Fig.1.1** as follows:

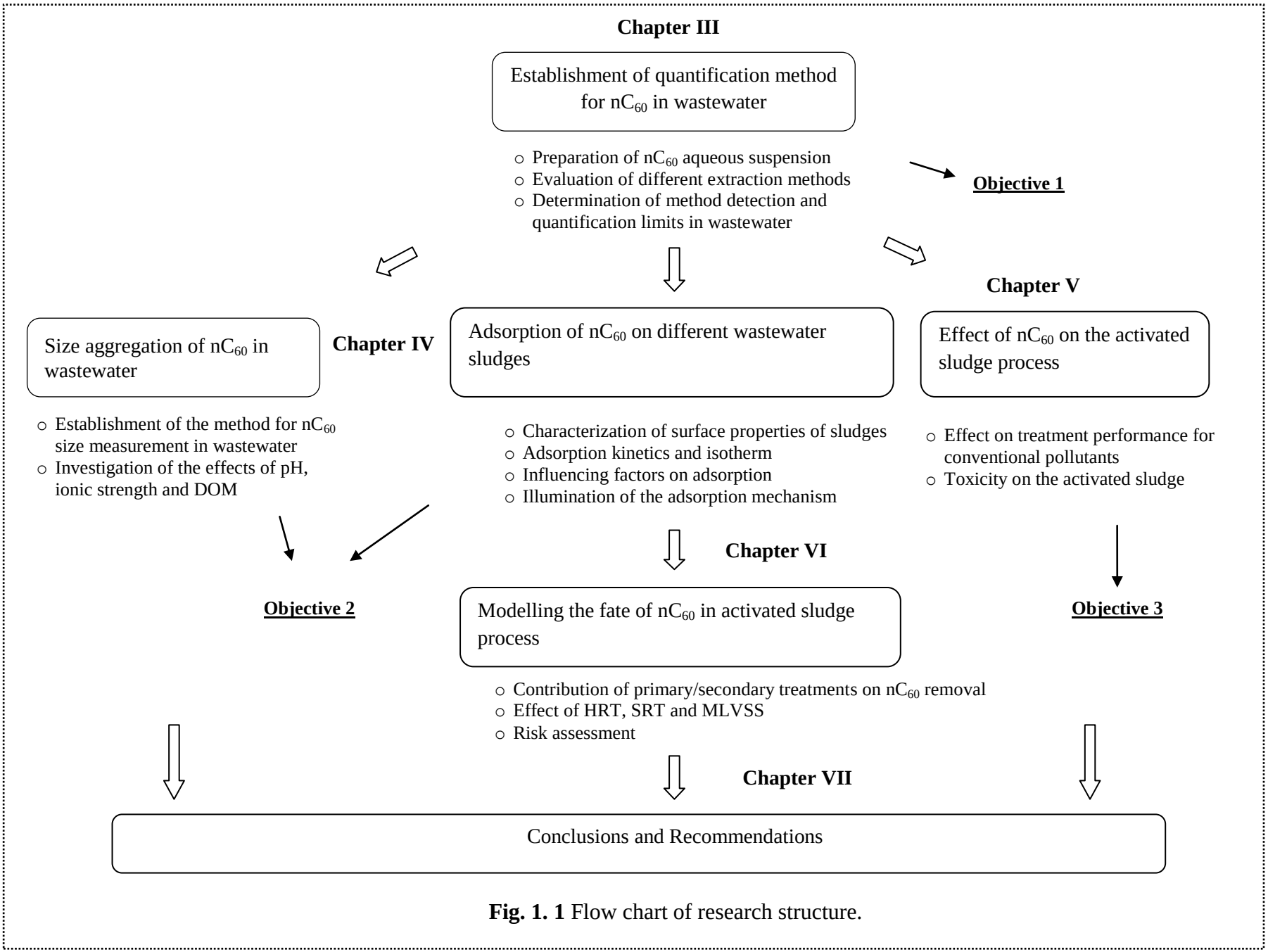

Fig. 1. 1 Flow chart of research structure.

1.4 References

Aitken, R.J., Chaudhry, M.Q., Boxall, A.B.A., Hull, M., 2006. Manufacture and use of nanomaterials: current status in the UK and global trends. Occupational Medicine Oxford 56 (5), 300–306.

Benn, T.M., Westerhoff, P., Herckes, P., 2011. Detection of fullerenes (C_{60} and C_{70}) in commercial cosmetics. Environmental Pollution 159 (5), 1334–1342.

Bouchard, D., Ma, X., 2008. Extraction and high-performance liquid chromatographic analysis of C_{60}, C_{70} and [6,6]-phenyl C_{61}-butyric acid methyl ester in synthetic and natural waters. Journal of Chromatography A 1203 (2), 153–159.

Chen, Z., Westerhoff, P., Herckes, P., 2008. Quantification of C_{60} fullerene concentrations in water. Environmental Toxicology and Chemistry 27 (9), 1852–1859.

Fortner, J.D., Lyon, D.Y., Sayes, C.M., Boyd, a M., Falkner, J.C., Hotze, E.M., Alemany, L.B., Tao, Y.J., Guo, W., Ausman, K.D., Colvin, V.L., Hughes, J.B., 2005. C_{60} in water: nanocrystal formation and microbial response. Environmental Science & Technology 39 (11), 4307–4316.

Hartmann, N.B., Buendia, I.M., Bak, J., Baun, A., 2011. Degradability of aged aquatic suspensions of C_{60} nanoparticles. Environmental Pollution 159 (10), 3134–3137.

Hyung, H., Kim, J.H., 2009. Dispersion of C_{60} in natural water and removal by conventional drinking water treatment processes. Water Research 43 (9), 2463–2470.

Isaacson, C.W., Kleber, M., Field, J.A., 2009. Quantitative analysis of fullerene nanomaterials in environmental systems: a critical review. Environmental Science & Technology 43 (17), 6463–6474.

Kang, S., Mauter, M.S., Elimelech, M., 2009. Microbial cytotoxicity of carbon-based nanomaterials: implications for river water and wastewater effluent. Environmental Science & Technology 43 (7), 2648–2653.

Kim, K.T., Jang, M.H., Kim, J.Y., Kim, S.D., 2010. Effect of preparation methods on toxicity of fullerene water suspensions to Japanese medaka embryos. Science of the Total Environment 408 (22), 5606–5612.

Kiser, M. a, Ryu, H., Jang, H., Hristovski, K., Westerhoff, P., 2010. Biosorption of nanoparticles to heterotrophic wastewater biomass. Water Research 44 (14), 4105–4114.

Kummerer, K., Menz, J., Schubert, T., Thielemans, W., 2011. Biodegradability of organic nanoparticles in the aqueous environment. Chemosphere 82 (10), 1387–1392.

Lyon, D.Y., Adams, L.K., Falkner, J.C., Alvarez, P.J.J., 2006. Antibacterial activity of fullerene water suspensions: effects of preparation method and particle size. Environmental Science & Technology 40 (14), 4360–4366.

Lyon, D.Y., Fortner, J.D., Alvarez, P.J., 2005. Fullerene water suspensions display antibacterial properties. Abstracts of Papers of the American Chemical Society 230, U1522–U1522.

Ma, X., Bouchard, D., 2009. Formation of aqueous suspensions of fullerenes. Environmental Science & Technology 43 (2), 330–336.

Murayama, H., Tomonoh, S., Alford, J.M., Karpuk, M.E., 2004. Fullerene production in tons and more: from science to industry. Fullerenes Nanotubes and Carbon nanostructures 12 (1–2), 1–9.

Oberdorster, E., Zhu, S.Q., Blickley, T.M., McClellan-Green, P., Haasch, M.L., 2006. Ecotoxicology of carbon-based engineered nanoparticles: effects of fullerene (C_{60}) on aquatic organisms. Carbon 44 (6), 1112–1120.

Sayes, C.M., Fortner, J.D., Guo, W., Lyon, D., Boyd, A.M., Ausman, K.D., Tao, Y.J., Sitharaman, B., Wilson, L.J., Hughes, J.B., West, J.L., Colvin, V.L., 2004. The differential cytotoxicity of water-soluble fullerenes. Nano Letters 4 (10), 1881–1887.

USEPA, Emerging Contaminants-Nanomaterials. Fact Sheet, 2009.

Woodrow Project on Emerging Nanotechnologies. The project on emerging nanotechnoglies. 2012. http://www.nanotechproject.org/.

Zhu, S.Q., Oberdorster, E., Haasch, M.L., 2006. Toxicity of an engineered nanoparticle (fullerene, C_{60}) in two aquatic species, Daphnia and fathead minnow. Marine Environmental Research 62, S5–S9.

CHAPTER II

LITERATURE REVIEW

2.1 Introduction of fullerene nanoparticles

2.1.1 Properties and applications

With rapid development of the nanotechnology, the global production of engineered nanomaterials is expected to increase to 58,000 tons by 2020 (Nowack and Bucheli, 2007) with an estimated economic market of one trillion dollars in 2015 (Aitken et al., 2006). The number of nanotechnology consumer products has increased by around five times in the past five years (Woodrow Project on Emerging Nanotechnologies, 2012). By 2014, more than 15% of all products on the global market are likely to be produced based on the nanotechnology (Bystrzejewska-Piotrowska et al., 2009).

As of 2011, the class of fullerenes and other carbon-based nanomaterials are ranked as the second among all the nanomaterials used in the nanotechnology-based consumer products, as shown in **Fig. 2.1**. The Fullerene C_{60} is the most common-produced and -used fullerene nanoparticles, consists of 60 carbon atoms arranged in 20 hexagons and 12 pentagons that form a cage structure with a size approximately 1 nm. C_{60} has the promising properties such as the special electrical, optical properties, high strength and radical scavenging (Wang et al., 2010). Therefore, the C_{60} is predicted to be applied in wide fields from the industry to the daily consumer products. **Table 2.1** shows the current and promising potential of application for the fullerenes related to their unique characteristics (Duclos et al., 1991; Sherigara et al., 2003; NEDO project, 2009).

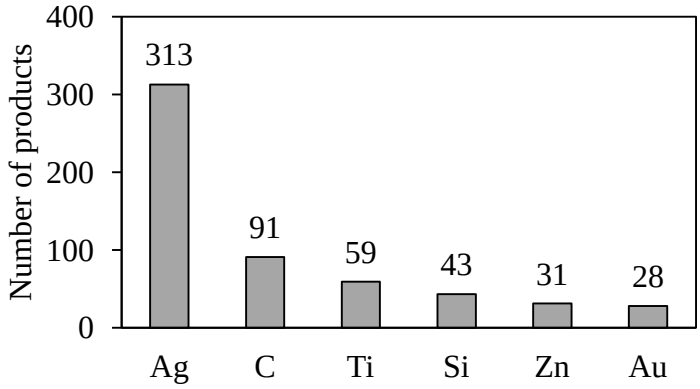

Fig. 2. 1 Number of products associated with specific materials. (Woodrow Project on Emerging Nanotechnologies, 2012).

Table 2. 1 The current and potential application of fullerenes

Unique property	Current application	Potential uses
High strength	Tennis racket, badminton racket	
Lubricity	Engine oil	
Radical scavenging capability	Cosmetics	
Electron acceptor		Solar energy cell Fuel cell
DNA photocleavage		Drug delivery
High adsorption		Environmental remediation

2.1.2 Preparation of nanoscale nC_{60} aqueous suspensions

Pristine C_{60} is highly hydrophobic and has very low solubility in water (7.96 ng/L) (Jafvert and Kulkarni, 2008). However, recent findings showed the C_{60} molecule could form stable nanoscale C_{60} aqueous suspensions (usually termed as nC_{60}) via the organic

solvent exchange method resulting a size ranged from several to hundred nanometers. The nC_{60} preparation were attempted by using a wide range of organic solvent such as the benzene (Scrivens et al., 1994; Yamakoshi et al., 1994), tetrahydrofuran (THF) (Deguchi et al., 2001; Brant et al., 2005) and dimethylsulfoxide (Wei et al., 1997). Recently, the toluene-based exchange method were widely used for studies of nC_{60}' fate and toxicities due to high yield and control of aggregate size (Brant et al., 2006; Lyon et al., 2006; Chen et al., 2008; Kim et al., 2010; Wang et al., 2010). This technique dissolves the C_{60} powder in the solvents and then disperses this solution into water followed by removing the organic solvent via evaporation or sonication. Another new technique directly dissolves or disperses the C_{60} powder into the water by the extended mixing using the shaking or stirring (Brant et al., 2006; Dhawan et al., 2006; Chen and Elimelech, 2009; Hyung and Kim, 2009; Kang et al., 2009; Kim et al., 2010). This technique simulates more likely conditions that the C_{60} discharge into the environment during the consumption and production, thus making it much more appropriate for toxicity studies of C_{60}. However, this preparation is extremely time-consuming and concentration-limited (Zhang et al., 2009; Pycke et al., 2011).

2.1.3 Toxicity of C_{60}

Although the toxicity mechanism is still not clarified for most nanoparticles, the previous studies showed some favorable explanation (**Fig. 2.2)**. The mechanisms included the release of hazardous impurities, the interrupt electron transport and the production of reactive oxygen species which could cause the DNA damage, disruption of membrane/their potential and proteins damage (Klaine et al., 2008). As of the fullerene C_{60}, it might cause toxicity related to one or several of these mechanisms above mentioned. One widely reported mechanism was due to the oxidative stress dependent or independent of the production of reactive oxygen species (Sayes et al., 2004; Lyon et al., 2008). **Table 2.2** reviewed the recent finding on the toxicity of nC_{60} to the aquatic microorganisms. The toxic effect concentration spanned over a wide range from sub mg/L to several hundred mg/L even using the same test microorganisms. Although no consistent conclusions on the relationship between the nC_{60} toxicity and preparation method, the lower toxicity was found on the nC_{60} suspensions prepared by

the direct dispersion in water by stirring without any solvent. It indicated that the toxicity of nC_{60} depended on the physicochemical properties of nC_{60} due to different preparation methods. Duncan et al. (2008) found the characteristics of nC_{60} such as the size, shape and surface charge dependent on the solvent used. The properties of nC_{60} could be affected by the specific procedures such as the initial ratio of C_{60} powder: water: organic solvent, even the mixture speeds (Brant et al., 2006). The specific toxicity mechanism were related to the lipid peroxidation (Oberdorster et al., 2006), the oxidative damage to the cellular membrane (Sayes et al., 2004), oyster embryonic development and lysosomal destabilization (Ringwood et al., 2009), as well as the increase in the heart rate, hopping frequency and appendage movement (Lovern et al., 2007). In addition, nC_{60} have displayed antibacterial effects with a minimal inhibitory concentration of 0.5 to 1 mg/L, and 1.5 to 3 mg/L against the Gram-negative *E.coli* and the Gram-positive *B.subtilis* (Lyon et al., 2005).

Previous studied reported nC_{60} toxicity on human cells. Sayes et al. (2004) found nC_{60} was toxic to human cell lines (HDF/HepG2) at 20 µg/L level might due to the membrane peroxidation by ROS. And the LC_{50} was observed to be 2 to 50 µg/L for human dermal fibroblasts, human liver carcinoma and neuronal astrocytes (Sayes et al., 2005). Totsuka et al. (2009) reported the dose dependent increase of micronuclei in human lung carcinoma cells (A549) at the exposure level of 0.02 to 200 mg/L.

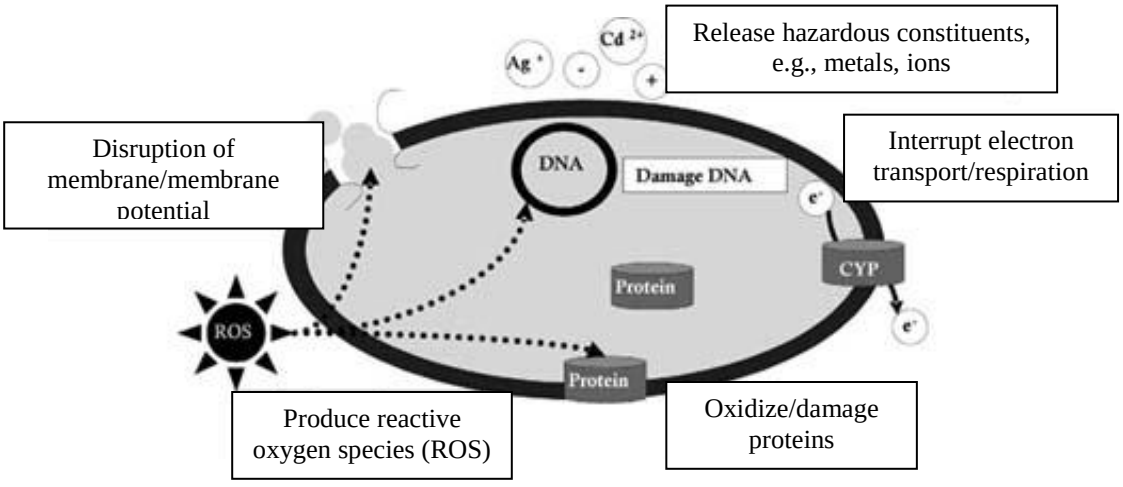

Fig. 2. 2 Possible mechanism of the toxicity of nanomaterials to the bacteria (Klaine et al., 2008).

Table 2. 2 Toxicity of nC_{60} to the aquatic microorganism and human cell

Test organism	nC_{60} preparation	Endpoint and effect	References
Daphnia magna	THF/Sonication	EC_{50} (Sonication): 7.9 mg/L EC_{50} (THF): 0.46 mg/L	(Lovern and Klaper, 2006)
Daphnia magna	THF	EC_{50} (THF): 0.8 mg/L; EC_{50} (Stir) >35 mg/L	(Zhu et al., 2006)
Daphinia magna	THF	Increase in heart rate at 0.26 mg/L	(Lovern et al., 2007)
Daphinia magna	Stirring	Increase in phenanthrene toxicity at 5 to 8 mg/L	(Baun et al., 2008)
Daphinia pulex	THF	No acute toxicity up to 100 mg/L but increase in the catalase	(Klaper et al., 2009)
Psedudomona putida/Bacillus subtilis	THF	Growth inhibiting at 0.5 and 0.75 mg/L	(Fang et al., 2007)
Escherichia coli	THF	Protein oxidation, interruption of cellular respiration	(Lyon and Alvarez, 2008)
Bacillus subtilis	Stir/Toluene/ THF	MIC at mg/L level with an order of THF>Stir>Toluene method	(Lyon et al., 2006)
Japanese medaka embryos	Toluene	30% of mortality at 0.8 mg/L	(Kim et al., 2010)
Human cell line (HDF/HepG2)	THF	Great super-anion production in acellular conditions	(Sayes et al., 2004)
Human dermal fibroblasts, human liver carcinoma, neuronal astrocytes	THF	Disruption in cellular function by lipid peroxidation	(Sayes et al., 2005)
Human lung carcinoma cells (A549)	Tween 80	Resulting in increase in the micronuclei frequency, DNA damage	(Totsuka et al., 2009)

2.1.4 Quantification method in water

The methods for nC_{60} quantification in aqueous samples usually consist of two steps (i.e., extraction and detection). The quantification method has been developed firstly for the biological samples such as the plasma (Santa et al., 1995; Xia et al., 2006) and blood (Moussa et al., 1997), and recently for the aqueous samples such as the pure water and tap water (Chen et al., 2008), surface water (Bouchard and Ma, 2008; van Wezel et al., 2011) and also organic matter-containing artificial water (Hyung and Kim,

2009). Two extraction methods, the liquid-liquid extraction (LLE) and solid phase extraction (SPE), were used for the extraction of nC_{60} from the samples. The LLE method is a traditional method for extracting non-polar compounds from the aqueous phases into the non-polar solvents (Pycke et al., 2011). Toluene is the most widely used organic solvent for the LLE of nC_{60} from the samples due to high solubility of C_{60} in the toluene and relatively low toxicity among the solvents that can greatly dissolve the C_{60}. The LLE could give a recovery from 33 to 94% dependent on the water matrix and concentration factors (Pycke et al., 2011). And the SPE method has been recently attempted to extract nC_{60} from the water samples using the Sep-Pak C18 (Bouchard and Ma, 2008) and Strata C18-E (Chen et al., 2008) cartridges in several previous studies. The extraction efficiency ranged from 9 to 78%. After extraction into the toluene from aqueous samples, the C_{60} is usually quantified by the UV detector at the wavelength of 300 to 400 nm or mass spectrometry at m/z of 720 after the HPLC separation system.

The LLE is most widely used for nC_{60} extraction, but this method needs large volume of toluene solvent if extracting nC_{60} from large volume samples. Therefore, the SPE is expected to be a promising method to allow the analysis of the nC_{60} in the environmental samples with a high concentration factor. The nC_{60} concentration in the treated wastewater was estimated to be several ng/L level based on a probabilistic material flow analysis from a life cycle perspective in the US and Europe (Gottschalk et al., 2009). Both the LLE and SPE methods available combined with the UV or MS detection systems are still difficult to quantify the occurrence concentration in the environmental samples. When treating the wastewater samples, the extraction efficiency might be affected by the complex matrices. And the quantification of nC_{60} in wastewater is still a barrier hindering the studies of nC_{60} fate in the wastewater treatment process.

2.1.5 Position of this research

From the literature reviewed, it can be known that the fullerene C_{60} has been already used in the consumer products, industrial and research area, and their production and consumption are expected to rapidly increase in the next few years. A number of studies reported the toxicity of C_{60} on microorganism from the gene level to

aquatic organisms. Therefore, once released into the water environment intentionally or unintentionally during the production and use, the C_{60} might pose the potential risks on the human health and the environment. However, it is still unclear whether the conventional wastewater treatment plant can provide an efficient barrier from their discharge into the environment, primary due to quantification limit. In Chapter III, a quantification method was established for nC_{60} in the wastewater.

2.2 Fate of nC_{60} in the activated sludge process

The fullerene C_{60} is just recently being introduced into consumer products such as the cosmetics and the composite for the sport goods. Therefore, only few studies were published on their fate in wastewater treatment plants. Farre et al. (2010) firstly and only reported the occurrence concentration in the suspended solids in the wastewater effluent. Half of the samples from 22 wastewater treatment plants in Spain contained fullerene C_{60} with a concentration up to μg/L level, although no information was determined on the source of C_{60} (Farre et al., 2010). The nC_{60} concentrations in the treated effluent were predicted to be 5.2 and 4.6 ng/L, in Europe and USA, respectively, based on the probabilistic material flow analysis from a life-cycle aspect (Gottschalk et al., 2009). The fate of nC_{60} might be affected by the size aggregation, biodegradation and adsorption behavior in the wastewater treatment process considering their properties of colloids and organic carbon structure (Brar et al., 2010).

2.2.1 Aggregation of nC_{60} in wastewater

The interactions between the pollutants and activated sludge play an important role in the fate of the pollutants in the activated sludge process. The adsorption behavior of nC_{60} on the activated sludge could be affected by their surface properties such as size and surface charge (Brar et al., 2010; Kiser et al., 2010; Gomez-Rivera et al., 2012). On the other hand, the size aggregation also could affect the efficiency of nC_{60} removal during the membrane treatment process the main removal mechanism of which is the size exclusion, as shown in **Fig. 2.3.** Although recent studies have been conducted on the aggregation behavior in artificial aqueous samples, the aggregation of nC_{60} in

wastewater is still unknown. Chen and Elimelech (2006) investigated the aggregation and deposition kinetics of nC_{60} in pure water and reported the critical coagulation concentration of 120 mM for the NaCl and 4.8 mM for the $CaCl_2$. The aggregation behavior of nC_{60} was in good agreement with Derjaguin-Landau-Verwey-Overbeek (DLVO) theory. In the presence of humic acid, the fullerene nanoparticles were effectively stabilized which was shown by the increase in the critical coagulation concentrations (Chen and Elimelech, 2007). And Li et al. (2009b) also found the natural organic matter could enhance the C_{60} dispersion during the simple mixture. However, the effect of cations varied with the type of ions showing the increasing NaCl could reduce the dispersion rate while the increasing calcium ions significantly increased the rate (Li et al., 2009b).

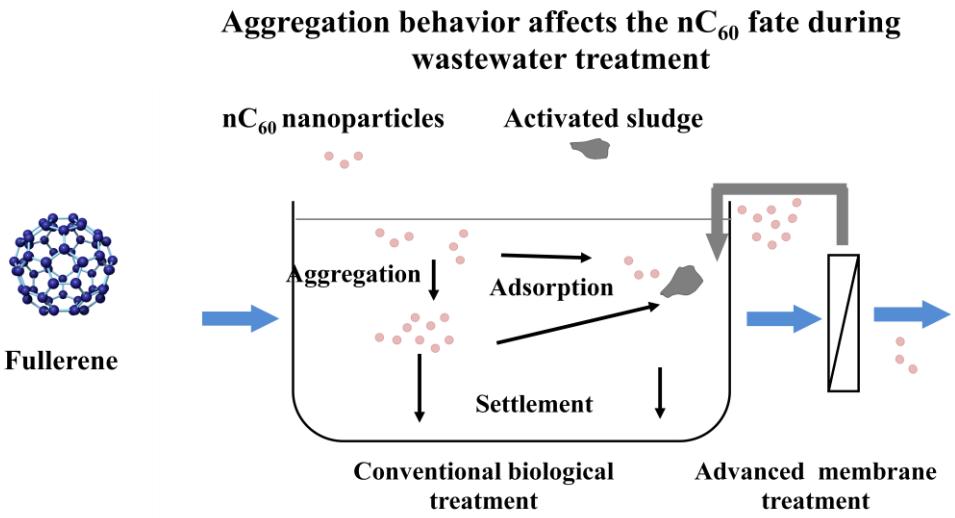

Fig. 2.3 Fate of fullerene nC_{60} during the wastewater treatment process as a function of size aggregation.

2.2.2 Biodegradation of nC_{60} by the activated sludge

Although not enough information was available on the biodegradation of fullerene nanoparticles in the wastewater environment, the C_{60} is considered to be not biodegraded under environmental conditions. Nyberg et al. (2008) investigated the

potential for anaerobic biodegradation of C_{60} by monitoring the production of CO_2 and CH_4 but no biodegradation of C_{60} was found for a few months. According to the closed bottle test of OECD method based on the oxygen consumption, the biodegradability of a series of organic nanoparticles was investigated. The fullerene were not biodegraded up to 28 days (Kummerer et al., 2011). One recent study assessed the biodegradability of C_{60} (20 mg/L) under aerobic condition using the activated sludge (30 mg TSS/L). No mineralization was observed over 58 days and nC_{60} can be classified as not readily biodegradable according to the OECD 301F test procedure (Hartmann et al., 2011).

2.2.3 Adsorption behavior of nC_{60} on the sludge

The non-degradability of nC_{60} reviewed above suggested the adsorption behavior on the activated sludge could play an important role in the fate and transport of nC_{60} during the wastewater treatment and consequently control their discharge through the treated wastewater. Kiser et al. (2010) reported the high adsorption of nC_{60} on the activated sludge using the batch experiments, but the adsorption mechanism was not yet determined. Here we summarized the literature from the perspectives of the adsorption mechanism and the influencing factors on the adsorption which included but not limited to the fullerene nC_{60}.

2.2.3.1 Adsorption mechanisms

In general, the adsorption processes between the particles are controlled by the attractive forces such as the Van der waals forces and hydrophobic interactions, and the repulsive forces such as the electrostatic repulsion (Gentry et al., 2008). Van der waals force mainly comes from the favorable interaction due to the dynamic distribution of charge. The hydrophobic interactions refer to the tendency of non-polar groups to associate in the aqueous environment. For the electrostatic interaction, the activated sludge generally is negatively charged with a zeta potential ranged from 0 to –40 mV (Mikkelsen, 2003; Meng et al., 2006; Zhou et al., 2010). The negative charges come primarily from lipoteichoic acids and lipopolysaccharides as well as the extracellular polymeric substances on the surface of bacteria (Gentry et al., 2008).

2.2.3.2 Influencing factors

Effect of pH

pH could affect the surface charge of particles by the protonation and deprotonation process (Reddad et al., 2002). And the extent of effects depends on the point of zero of charge (pzc) of particles. One study investigated the effect of pH on the adsorption of negative-charged on Perfluorinated compounds (PFCs) on the activated sludge (Zhou et al., 2010). The activated sludge had a negative surface charge at pH from 2 to 9 with a pzc value of ~pH 2.2. At lower pH, the absolute ζ potential of sludge decreased resulting in the increase in the adsorption of PFCs due to the decrease in the electrostatic repulsion between the PFCs and activated sludge. And Ma and Bouchard (2009) reported the nC_{60} was negatively charged in water and their absolute ζ potential of nC_{60} in water decreased from ~45 mV to zero with the decreasing pH values from 10 to 1. Therefore, the nC_{60} adsorption on the wastewater sludge might be affected by pH via changing the ζ potential of both the wastewater sludge and nC_{60}.

Effect of ionic strength

The ionic strength in solution could affect the adsorption process between the particles by altering the diffuse double layer and/or neutralized the surface charge. Until now, the effect of ionic strength on the adsorption is still in debate. Theoretically, for the particles with like charge, an increase in ionic strength will decrease the adsorption capacity. While, for the particles with opposite charge, an increase in ionic strength will increase the adsorption (German-heins, 2000). The absolute zeta potential of nC_{60} was greatly reduced from ~50 mV to ~10 mV with the increase of NaCl solution from 0.0001 to 0.1 M (Brant et al., 2005). And the obvious increase in size was observed in NaCl solution with an ionic strength > 0.05 mM (Fortner et al., 2005b). Therefore, the ionic strength might affect the nC_{60}' adsorption on sludge by not only changing the surface charge of both particles but also the size aggregation of nC_{60}.

Effect of sludge concentration

The increase in the sludge concentration could contribute to the adsorption by increasing the adsorption sites. Zhao et al. (2008) found the adsorption of Biosphenol A greatly increased at higher sludge concentration.

Effect of dissolved organic matter

The dissolved organic matter (DOM) is readily to be adsorbed on the particles and could affect the fate of particles due to the combined effect of the electrostatic, steric and hydrophobic effects (Li et al., 2009a; Qu et al., 2010). Hyung and Kim (2009) found the DOM might adsorb on the surface of nC_{60} and consequently improved the stability of nC_{60} by the steric and electrostatic stabilization. The presence of natural organic matter (NOM) could decrease in the removal of nC_{60} during the coagulation/flocculation/sedimentation process mightily due to the competitive interaction between NOM and the coagulant (Hyung and Kim, 2009). Kim and Lee (2008) found the surfactants could improve the stability of nC_{60}. The addition of surfactants in the wastewater inhibited the removal of cerium oxide nanoparticle in the activated sludge treatment process (Limbach et al., 2008).

2.2.4 Position of this research

According to the literature reviewed above, we can understand the nC_{60} size could be affected by the aquatic conditions such as the pH, ionic strength, dissolved organic matter and so on. However, it is still unclear on the aggregation behavior of nC_{60} in the wastewater. On the other hand, the size aggregation might affect the fate of nC_{60} in the wastewater treatment process such as the adsorption on activated sludge and size exclusion by membrane process. Therefore the size aggregation of nC_{60} in wastewater was conducted in Chapter IV.

In addition, as known above no degradation happened in the sludge under the aerobic and anaerobic conditions over time up to several months, and therefore the adsorption will greatly control the fate of nC_{60} in the wastewater treatment process. Very little information was available on the adsorption behavior on the activated sludge.

The adsorption mechanism is still unclear. In Chapter IV, the study was conducted on the contribution of adsorption on primary and activated sludges, the effect of surface properties of wastewater sludges on the adsorption, the effect of aquatic and operational conditions such as the pH, ionic strength and sludge concentrations. And the adsorption mechanism was estimated by modeling the kinetics and isotherm adsorption, and correlating the adsorption with surface properties of different sludges.

2.3 Effect of nC_{60} on the activated sludge process

2.3.1 Toxicity of nC_{60} on the bacteria and microorganism community

Lyon et al. (2005) reported the minimal inhibitory concentration of 0.5 to 1 mg/L, and 1.5 to 3 mg/L for nC_{60} against the Gram-negative *Escherichia coli* and Gram-positive *Bacillus subtilis*. And the fraction with smaller size of nC_{60} had greater antibacterial activity on *Bacillus subtilis* (Lyon et al., 2006). The bacteria of *Peseudomona Putida* showed the response in lipid composition, membrane fluidity and membrane phase behavior after exposure of nC_{60} from 0.01 to 0.75 mg/L (Fang et al., 2007). Besides of pour culture of bacteria, Kang et al. (2009) reported about 30% inactivation of microorganism in wastewater samples after 1 h exposure to nC_{60}-coated filter. In addition, Nyberg et al. (2008) investigated the impact of nC_{60} on the microbial community structure of anaerobic sludge after exposure of 0.321 mg/kg biomass (dry weight) for a few months. No significant change was observed on the community structure by denaturing gradient gel electrophoresis (DGGE), using primer sets targeting the small subunit rRNA genes of Bacteria, Archaea, and Eukarya (Nyberg et al., 2008).

2.3.2 Position of this research

As the literature reviewed above, the nC_{60} have displayed antibacterial effects at sub-mg/L level on a wide range of bacteria. It suggested the potential of adverse effect of nC_{60} on the activated sludge in the wastewater treatment process. Although some studies were attempted on the effect of nC_{60} on the anaerobic sludge, the information was very limited on the activated sludge. Moreover, the potential inhibition on nitrification process, which is very sensitive to the emerging pollutant, will greatly affect the treatment of NH_4^+–N in the wastewater. Chapter V investigated the effect of nC_{60} on the treatment performance of organic matters and nutrient compounds and toxicity on the activated sludge.

2.4 References

Aitken, R.J., Chaudhry, M.Q., Boxall, A.B.A., Hull, M., 2006. Manufacture and use of nanomaterials: current status in the UK and global trends. Occupational Medicine Oxford 56 (5), 300–306.

Baun, A., Sorensen, S.N., Rasmussen, R.F., Hartmann, N.B., Koch, C.B., 2008. Toxicity and bioaccumulation of xenobiotic organic compounds in the presence of aqueous suspensions of aggregates of nanoC_{60}. Aquatic Toxicology 86 (3), 379–387.

Bouchard, D., Ma, X., 2008. Extraction and high-performance liquid chromatographic analysis of C_{60}, C_{70} and [6,6]-phenyl C_{61}-butyric acid methyl ester in synthetic and natural waters. Journal of Chromatography A 1203 (2), 153–159.

Brant, J., Lecoanet, H., Wiesner, M.R., 2005. Aggregation and deposition characteristics of fullerene nanoparticles in aqueous systems. Journal of Nanoparticle Research 7 (4-5), 545–553.

Brant, J.A., Labille, J., Bottero, J.Y., Wiesner, M.R., 2006. Characterizing the impact of preparation method on fullerene cluster structure and chemistry. Langmuir 22 (8), 3878–3885.

Brar, S.K., Verma, M., Tyagi, R.D., Surampalli, R.Y., 2010. Engineered nanoparticles in wastewater and wastewater sludge - Evidence and impacts. Waste Management 30 (3), 504–520.

Bystrzejewska-Piotrowska, G., Golimowski, J., Urban, P.L., 2009. Nanoparticles: their potential toxicity, waste and environmental management. Waste Management 29 (9), 2587–2595.

Chen, K.L., Elimelech, M., 2006. Aggregation and deposition kinetics of fullerene (C_{60}) nanoparticles. Langmuir 22 (26), 10994–11001.

Chen, K.L., Elimelech, M., 2007. Influence of humic acid on the aggregation kinetics of fullerene (C_{60}) nanoparticles in monovalent and divalent electrolyte solutions. Journal of Colloid and Interface Science 309 (1), 126–134.

Chen, K.L., Elimelech, M., 2009. Relating colloidal stability of fullerene (C_{60}) nanoparticles to nanoparticle charge and electrokinetic properties. Environmental Science & Technology 43 (19), 7270–7276.

Chen, Z., Westerhoff, P., Herckes, P., 2008. Quantification of C_{60} fullerene concentrations in water. Environmental Toxicology and Chemistry 27 (9), 1852–1859.

Deguchi, S., Alargova, R.G., Tsujii, K., 2001. Stable dispersions of fullerenes, C_{60} and C_{70}, in water. preparation and characterization. Langmuir, 17(19), 6013–6017.

Dhawan, A., Taurozzi, J.S., Pandey, A.K., Shan, W., Miller, S.M., Hashsham, S.A, Tarabara, V.V., 2006. Stable colloidal dispersions of C_{60} fullerenes in water: evidence for genotoxicity. Environmental Science & Technology 40 (23), 7394–7401.

Duclos, S.J., Brister, K., Haddon, R.C., Kortan, A.R., Thiel, F.A., 1991. Effects of Pressure and Stress on C_{60} fullerite to 20 Gpa. Nature 351 (6325), 380–382.

Duncan, L.K., Jinschek, J.R., Vikesland, P.J., 2008. C_{60} colloid formation in aqueous systems: effects of preparation method on size, structure, and surface charge. Environmental Science & Technology 42 (1), 173–178.

Fang, J.S., Lyon, D.Y., Wiesner, M.R., Dong, J.P., Alvarez, P.J.J., 2007. Effect of a fullerene water suspension on bacterial phospholipids and membrane phase behavior. Environmental Science & Technology 41 (7), 2636–2642.

Farre, M., Perez, S., Gajda-Schrantz, K., Osorio, V., Kantiani, L., Ginebreda, A., Barcelo, D., 2010. First determination of C_{60} and C_{70} fullerenes and N-methyl fulleropyrrolidine C_{60} on the suspended material of wastewater effluents by liquid chromatography hybrid quadrupole linear ion trap tandem mass spectrometry. Journal of Hydrology 383 (1-2), 44–51.

Fortner, J.D., Lyon, D.Y., Sayes, C.M., Boyd, a M., Falkner, J.C., Hotze, E.M., Alemany, L.B., Tao, Y.J., Guo, W., Ausman, K.D., Colvin, V.L., Hughes, J.B., 2005a. C_{60} in water: Nanocrystal formation and microbial response. Environmental Science & Technology 39 (11), 4307–4316.

Fortner, J.D., Lyon, D.Y., Sayes, C.M., Boyd, A.M., Falkner, J.C., Hotze, E.M., Alemany, L.B., Tao, Y.J., Guo, W., Ausman, K.D., Colvin, V.L., Hughes, J.B., 2005b. C_{60} in water: Nanocrystal formation and microbial response. Environmental Science & Technology 39 (11), 4307–4316.

Gentry, T., Maier, R.M., Pepper, I.L., Gerba, C.P., 2008. Environmental microbiology. Academic press.

German-heins, J., Flury, M., 2000. Sorption of brilliant blue FCF in soils as affected by pH and ionic strength. Geoderma 97, 87–101.

Gomez-Rivera, F., Field, J.A., Brown, D., Sierra-Alvarez, R., 2012. Fate of cerium dioxide (CeO_2) nanoparticles in municipal wastewater during activated sludge treatment. Bioresource Technology 108, 300–304.

Gottschalk, F., Sonderer, T., Scholz, R.W., Nowack, B., 2009. Modeled environmental concentrations of engineered nanomaterials (TiO_2, ZnO, Ag, CNT, Fullerenes) for different regions. Environmental Science & Technology 43 (24), 9216–9222.

Hartmann, N.B., Buendia, I.M., Bak, J., Baun, A., 2011. Degradability of aged aquatic suspensions of C_{60} nanoparticles. Environmental Pollution 159 (10), 3134–3137.

Hyung, H., Kim, J.H., 2009. Dispersion of C_{60} in natural water and removal by conventional drinking water treatment processes. Water Research 43 (9), 2463–2470.

Jafvert, C.T., Kulkarni, P.P., 2008. Buckminsterfullerene's (C_{60}) octanol-water partition coefficient (K_{ow}) and aqueous solubility. Environmental Science & technology 42 (16), 5945–5950.

Kang, S., Mauter, M.S., Elimelech, M., 2009. Microbial cytotoxicity of carbon-based nanomaterials: Implications for river water and wastewater effluent. Environmental Science & Technology 43 (7), 2648–2653.

Kim, K.T., Jang, M.H., Kim, J.Y., Kim, S.D., 2010. Effect of preparation methods on toxicity of fullerene water suspensions to Japanese medaka embryos. Science of the Total Environment 408 (22), 5606–5612.

Kiser, M. a, Ryu, H., Jang, H., Hristovski, K., Westerhoff, P., 2010. Biosorption of nanoparticles to heterotrophic wastewater biomass. Water Research 44 (14), 4105–4114.

Klaine, S.J., Alvarez, P.J.J., Batley, G.E., Fernandes, T.F., Handy, R.D., Lyon, D.Y., Mahendra, S., McLaughlin, M.J., Lead, J.R., 2008. Nanomaterials in the environment: behavior, fate, bioavailability, and effects. Environmental Toxicology and Chemistry 27 (9), 1825–1851.

Klaper, R., Crago, J., Barr, J., Arndt, D., Setyowati, K., Chen, J., 2009. Toxicity biomarker expression in daphnids exposed to manufactured nanoparticles: changes in toxicity with functionalization. Environmental Pollution 157 (4), 1152–1156.

Kummerer, K., Menz, J., Schubert, T., Thielemans, W., 2011. Biodegradability of organic nanoparticles in the aqueous environment. Chemosphere 82 (10), 1387–1392.

Lee, J., Kim, J.H., 2008. Effect of encapsulating agents on dispersion status and photochemical reactivity of C_{60} in the aqueous phase. Environmental Science & Technology 42 (5), 1552–1557.

Li, Q., Xie, B., Hwang, Y.S., Xu, Y., 2009a. Kinetics of C_{60} fullerene dispersion in water enhanced by natural organic matter and sunlight. Environmental Science & Technology 43 (10), 3574–3479.

Li, Q.L., Xie, B., Hwang, Y.S., Xu, Y.J., 2009b. Kinetics of C_{60} Fullerene dispersion in water enhanced by natural organic matter and sunlight. Environmental Science & Technology 43 (10), 3574–3579.

Limbach, L.K., Bereiter, R., Müller, E., Krebs, R., Galli, R., Stark, W.J., 2008. Removal of oxide nanoparticles in a model wastewater treatment plant: influence of agglomeration and surfactants on clearing efficiency. Environmental Science & Technology 42 (15), 5828–5833.

Lovern, S.B., Klaper, R., 2006. Daphnia magna mortality when exposed to titanium dioxide and fullerene (C_{60}) nanoparticles. Environmental Toxicology and Chemistry 25 (4), 1132–1137.

Lovern, S.B., Strickler, J.R., Klaper, R., 2007. Behavioral and physiological changes in Daphnia magna when exposed to nanoparticle suspensions (titanium dioxide, nanoC_{60}, and C_{60}HxC_{70}Hx). Environmental Science & Technology 41 (12), 4465–4470.

Lyon, D.Y., Adams, L.K., Falkner, J.C., Alvarez, P.J.J., 2006. Antibacterial activity of fullerene water suspensions: Effects of preparation method and particle size. Environmental Science & Technology 40 (14), 4360–4366.

Lyon, D.Y., Alvarez, P.J.J., 2008. Fullerene water suspension (nC_{60}) exerts antibacterial effects via ROS-independent protein oxidation. Environmental Science & Technology 42 (21), 8127–8132.

Lyon, D.Y., Brunet, L., Hinkal, G.W., Wiesner, M.R., Alvarez, P.J.J., 2008. Antibacterial activity of fullerene water suspensions (nC_{60}) is not due to ROS-mediated damage. Nano Letters 8 (5), 1539–1543.

Lyon, D.Y., Fortner, J.D., Alvarez, P.J., 2005. Fullerene water suspensions display antibacterial properties. Abstracts of Papers of the American Chemical Society 230, U1522–U1522.

Ma, X., Bouchard, D., 2009. Formation of aqueous suspensions of fullerenes. Environmental Science & Technology 43 (2), 330–336.

Meng, F., Zhang, H., Yang, F., Zhang, S., Li, Y., Zhang, X., 2006. Identification of activated sludge properties affecting membrane fouling in submerged membrane bioreactors. Separation and Purification Technology 51 (1), 95–103.

Mikkelsen, L.H., 2003. Applications and limitations of the colloid titration method for measuring activated sludge surface charges. Water Research, 37(10):2458–2466.

Moussa, F., Pressac, M., Genin, E., Roux, S., Trivin, F., Rassat, A., Ceolin, R., Szwarc, H., 1997. Quantitative analysis of C_{60} fullerene in blood and tissues by high-performance liquid chromatography with photodiode-array and mass spectrometric detection. Journal of Chromatography B 696 (1), 153–159.

Murayama, H., Tomonoh, S., Alford, J.M., Karpuk, M.E., 2004. Fullerene production in tons and more: from science to industry. Fullerenes Nanotubes and Carbon Nanostructures 12 (1-2), 1–9.

NEDO project. Research and development of nanoparticle characterization methods. 2009.

Nowack, B., Bucheli, T.D., 2007. Occurrence, behavior and effects of nanoparticles in the environment. Environmental Pollution 150 (1), 5–22.

Nyberg, L., Turco, R.F., Nies, L., 2008. Assessing the impact of nanomaterials on anaerobic microbial communities. Environmental Science & Technology 42 (6), 1938–1943.

Oberdorster, E., Zhu, S.Q., Blickley, T.M., McClellan-Green, P., Haasch, M.L., 2006. Ecotoxicology of carbon-based engineered nanoparticles: Effects of fullerene (C_{60}) on aquatic organisms. Carbon 44 (6), 1112–1120.

Pycke, B.F.G., Benn, T.M., Herckes, P., Westerhoff, P., Halden, R.U., 2011. Strategies for quantifying C_{60} fullerenes in environmental and biological samples and implications for studies in environmental health and ecotoxicology. TrAC Trends in Analytical Chemistry 30 (1), 44–57.

Qu, X.L., Hwang, Y.S., Alvarez, P.J.J., Bouchard, D., Li, Q.L., 2010. UV irradiation and humic acid mediate aggregation of aqueous fullerene (nC_{60}) nanoparticles. Environmental Science & Technology 44 (20), 7821–7826.

Reddad, Z., Gerente, C., Andres, Y., Le Cloirec, P., 2002. Adsorption of several metal ions onto a low-cost biosorbent: kinetic and equilibrium studies. Environmental Science & Technology 36 (9), 2067–2073.

Ringwood, A.H., Levi-Polyachenko, N., Carroll, D.L., 2009. Fullerene Exposures with Oysters: embryonic, adult, and cellular responses. Environmental Science & Technology 43 (18), 7136–7141.

Santa, T., Yoshioka, D., Homma, H., Imai, K., Satoh, M., Takayanagi, I., 1995. High-performance liquid-chromatography of fullerence (C_{60}) in plasma using Ultraviolet and mass-spectrometric detection. Biological & Pharmaceutical Bulletin 18 (9), 1171–1174.

Sayes, C.M., Fortner, J.D., Guo, W., Lyon, D., Boyd, A.M., Ausman, K.D., Tao, Y.J., Sitharaman, B., Wilson, L.J., Hughes, J.B., West, J.L., Colvin, V.L., 2004. The differential cytotoxicity of water-soluble fullerenes. Nano Letters 4 (10), 1881–1887.

Sayes, C.M., Gobin, A.M., Ausman, K.D., Mendez, J., West, J.L., Colvin, V.L. (2005). Nano-C_{60} cytotoxicity is due to lipid peroxidation. Biomaterials 26, 7587–7595.

Scrivens, W.A., Cassell, A.M., North, B.L., Tour, J.M., 1994. Single-column purification of gram quantities of C_{70}. Journal of the American Chemical Society 116 (15), 6939–6940.

Sherigara, B.S., Kutner, W., D'Souza, F., 2003. Electrocatalytic properties and sensor applications of fullerenes and carbon nanotubes. Electroanalysis 15 (9), 753–772.

Totsuka, Y., Higuchi, T., Imai, T., Nishikawa, A., Nohmi, T., Kato, et al., 2009. Genotoxicity of nano/microparticles in in vitro micronuclei, in vivo comet and mutation assay systems. Particle and Fibre Toxicology 6:23, doi:10.1186/1743-8977-6-23.

van Wezel, A.P., Moriniere, V., Emke, E., ter Laak, T., Hogenboom, A.C., 2011. Quantifying summed fullerene nC_{60} and related transformation products in water using LC LTQ Orbitrap MS and application to environmental samples. Environment International 37(6), 1063–1067.

Wang, C., Shang, C., Westerhoff, P., 2010. Quantification of fullerene aggregate nC_{60} in wastewater by high-performance liquid chromatography with UV-vis spectroscopic and mass spectrometric detection. Chemosphere 80 (3), 334–339.

Wei, X.W., Wu, M.F., Qi, L., Xu, Z., 1997. Selective solution-phase generation and oxidation reaction of C_{60}^{n-} (n=1, 2) and formation of an aqueous colloidal solution of C_{60}. Journal of the Chemical Society-Perkin Transactions 2(7), 1389–1393.

Woodrow Project on Emerging Nanotechnologies. The project on emerging nanotechnoglies. 2012. http://www.nanotechproject.org/.

Xia, X.R., Monteiro-Riviere, N.A., Riviere, J.E., 2006. Trace analysis of fullerenes in biological samples by simplified liquid-liquid extraction and high-performance liquid chromatography. Journal of Chromatography A 1129 (2), 216–222.

Yamakoshi, Y.N., Yagami, T., Fukuhara, K., Sueyoshi, S., Miyata, N., 1994. Solubilization of Fullerenes into water with polyvinylpyrrolidone applicable to biological Tests. Journal of the chemical society-chemical communications (4), 517–518.

Zhang, B., Cho, M., Hughes, J.B., Kim, J.H., 2009. Translocation of C_{60} from aqueous stable colloidal aggregates into surfactant micelles. Environmental Science & Technology 43 (24), 9124–9129.

Zhao, J., Li, Y., Zhang, C., Zeng, Q., Zhou, Q., 2008. Sorption and degradation of bisphenol A by aerobic activated sludge. Journal of Hazardous Materials 155 (1-2), 305–311.

Zhou, Q., Deng, S.B., Yu, Q., Zhang, Q.Y., Yu, G., Huang, J., He, H.P., 2010. Sorption of perfluorooctane sulfonate on organo-montmorillonites. Chemosphere 78 (6), 688–694.

Zhu, S.Q., Oberdorster, E., Haasch, M.L., 2006. Toxicity of an engineered nanoparticle (fullerene, C_{60}) in two aquatic species, Daphnia and fathead minnow. Marine Environmental Research 62, S5–S9.

CHAPTER III

PREPARATION OF nC_{60} AQUEOUS SUSPENSION AND QUANTIFICATION IN WASTEWATER

3.1 Introduction

With the rapid increase in the production and consumption, the nC_{60} nanoparticles might find their ways to the aquatic environment. It has caused the recent concerns on the environmental risks and human health. Once entering into the wastewater, the wastewater treatment plant (WWTP) would be an important route for nC_{60} discharge in the aquatic environment (Isaacson et al., 2009). The nC_{60} concentration was predicted to be 5.2 and 4.6 ng/L in treated effluent in WWTP in Europe and US, respectively (Gottschalk et al., 2009). However, it is still unclear on the occurrence, fate and transport of nC_{60} during the wastewater treatment process. The main reason is due to the limitation on the quantification method for the low concentration in the complex wastewater matrix. The quantification method of nC_{60} was firstly developed for the solid samples such as the carbon soot (Jinno and Kohrikawa, 1998) and sediment (Heymann et al., 1996) and the biological samples such as the plasma (Xia et al., 2006) and tissues (Moussa et al., 1997). More recently, some studies were attempted to quantify the nC_{60} in simple aqueous matrix such as tap water (Chen et al., 2008), NOM containing artificial water (Hyung and Kim, 2009) and surface water (Bouchard and Ma, 2008). The extraction method included the Soxhlet extraction, liquid-liquid extraction (LLE) and solid phase extraction (SPE) combined with the HPLC-UV/vis or MS detectors. However, very few studies were conducted on the extraction and detection of nC_{60} from the wastewater partially due to the complex matrices.

The objectives of this chapter are to a) prepare the nC_{60} aqueous suspension for the studies on the fate and toxicity in the activated sludge process in the following chapters; b) to evaluate the extraction efficiencies of LLE and SPE for the nC_{60} in wastewater samples and c) to establish the optimized quantification method for this study according

to the quantification limit and linear range. The research content of this chapter was shown in **Fig. 3.1**.

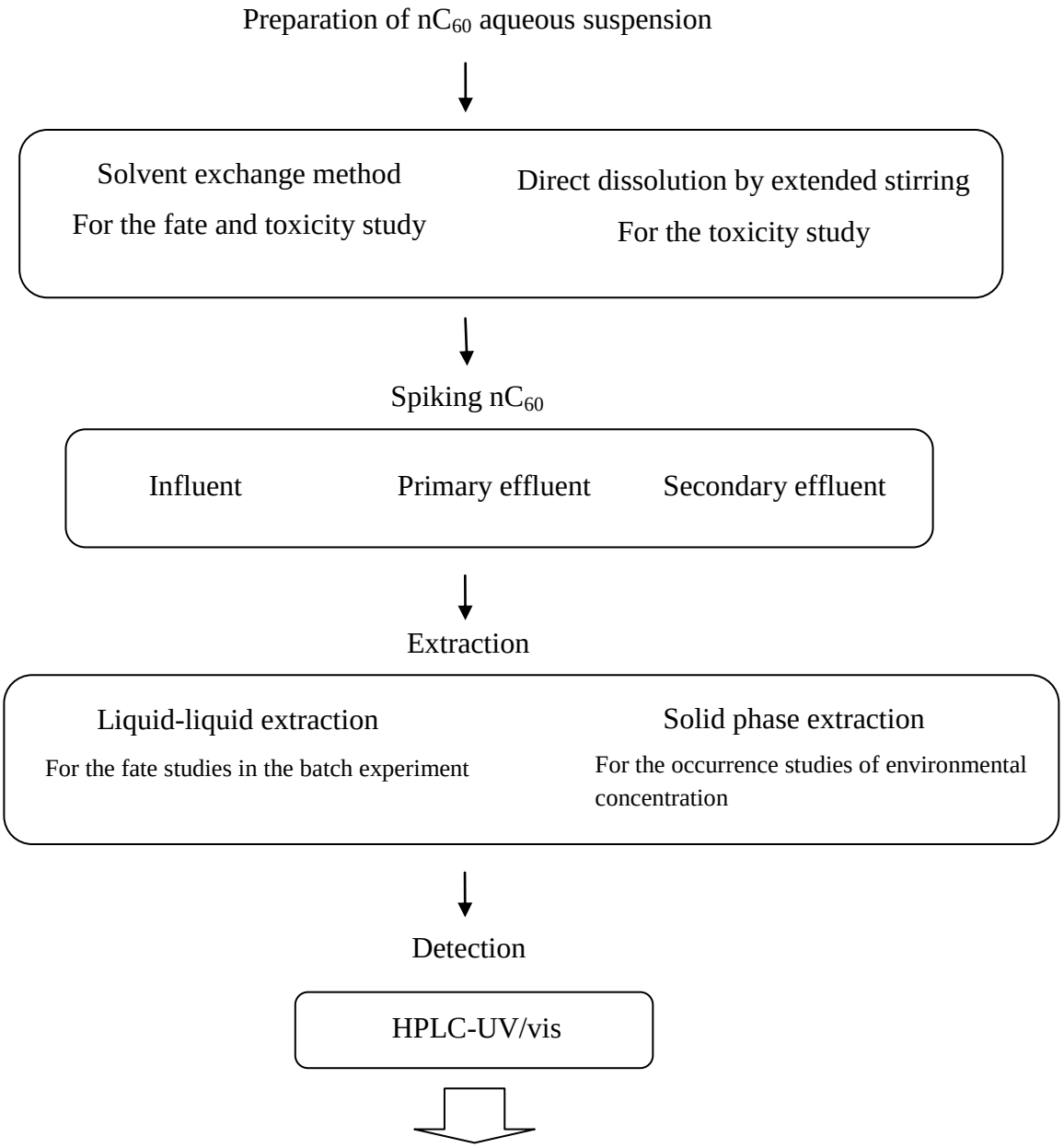

- Prepare the nC_{60} aqueous suspension and Characterize their properties
- Evaluate the extraction efficiency from the wastewater samples by two methods
- Determine the method detection and quantification limits in wastewater

Fig. 3. 1 The research structure of Chapter III.

3.2 Materials and methods

3.2.1 Preparation of nC_{60} aqueous suspension and quantification in Milli-Q water

Two types of nC_{60} aqueous suspensions were prepared for the fate and toxicity studies. One was prepared using the toluene-based solvent exchange technique and the resulted nC_{60} was denoted as tol/nC_{60}. The other type was prepared by extended stirring for long time without any organic solvent which was denoted as aqu/nC_{60}. The tol/nC_{60} was used for studies of nC_{60} fate during the wastewater treatment process because of less time-consuming and high production. And the aqu/nC_{60} via the direct dissolution in water, which could mostly represent the real transition of C_{60} to water environment during the production and consumption of C_{60} nanoparticles, was used for the toxicity test. In addition, the tol/nC_{60} was also used for toxicity studies to investigate the effect of preparation methods on nC_{60} toxicity. The tol/nC_{60} was prepared as follows: C_{60} powder (99.9% purity; SES Research, USA) was dissolved in toluene (HPLC grade; Wako, Japan) to give a 1000 mg/L C_{60} solution. And then 40 mL of the stock C_{60} toluene solution was added to 100 mL Milli-Q water. The toluene was removed by sonication in an ultrasonicator (AS ONE, Japan). And the aqu/nC_{60} was produced by adding 200 mg of powder C_{60} to 300 mL of Milli-Q water (Millipore, USA) and then mixing with a magnetic stirrer at 500 rpm for three weeks.

Both the resulted yellow suspensions were sequentially filtered through a glass filter (1.0 μm pore size; Pall Life Sciences, USA) and a cellulose acetate filter (0.45 μm pore size; Advantec, Japan). The filtrate was stored in the dark at 4 °C for use. The nC_{60} concentrations in both nC_{60} suspensions were quantified as following procedures: 5 mL of the nC_{60} aqueous suspensions was thoroughly mixed with 0.56 mL NaCl (10%) solution followed by adding 5 mL toluene as the extraction solvent. The mixture was agitated at 200 rpm for 30 min on a horizontal shaker. And then the toluene phase and aqueous phase was separated by settlement. The C_{60} concentration in toluene was quantified at 332 nm by UV/visible spectrometer (UV-2500PC, Shimadzu, Japan). A calibration curve was obtained by a series of C_{60} toluene standard solutions. The prepared tol/C_{60} by the solvent exchange method had a concentration of ~18 mg/L, while the aqu/C_{60} concentration was only round

0.5 mg/L. Therefore, the aqu/C_{60} suspensions were concentrated using a N1100 rotary evaporator (EYELA, Japan) followed by the 0.45 μm filtration. The aqu/C_{60} was finally concentrated to a concentration of ~18 mg/L by repeating the evaporating and filtration procedures.

3.2.2 Wastewater samples

Three wastewater samples, influent (IF), primary effluent (PE) and secondary effluent (SE) were collected from a domestic WWTP in Japan, which applied a conventional activated sludge treatment process. All the wastewater samples were filtrated through 1.0 μm GF/B filter and then stored at 4 °C for use.

3.2.3 Extraction method

Two extraction methods, LLE and SPE, were evaluated by spiking the prepared tol/nC_{60} suspension into the wastewater samples.

3.2.3.1 Liquid-liquid extraction

5 mL of wastewater sample was placed in a 10 mL glass test tube followed by spiking the different amounts of tol/nC_{60} suspensions ranged from 2 to 500 μg/L. And then 0.56 mL of 10% NaCl was added to destabilize the tol/nC_{60} for facilitating the extraction of tol/nC_{60} from the water into the toluene phase. After adding 3 mL toluene, the mixture was shaken at 200 rpm for 30 min using a horizontal shaker. The toluene phase was separated by the settlement for 1 h. And then 2 mL toluene was collected to a vial for C_{60} quantification through HPLC-UV/vis systems.

3.2.3.2 Solid phase extraction

The tol/nC_{60} has the combined property of hydrophobic (C_{60} molecule) and hydrophilic (nC_{60} aggregate) in water and was characterized as the weak acid. According to those characteristics, three types of cartridges were investigated in this study; those were Waters Oasis HLB (200 mg), Agilent SampliQ-SAX (150 mg) and SampliQ-SCX (150 mg). Waters Oasis HLB is a hydrophilic-lipophilic-balanced reversed phase sorbent for the acids, bases and neutrals. The Agilent SampliQ-SAX cartridge is a mixed polymer with both anion exchange and reversed

phase properties for both acidic and neutral compounds. And the Agilent SampliQ-SCX is sulfonic acid modified polymer with both ion exchange and reverse phase properties both basic and neutral compounds. All the cartridges were preconditioned sequentially with 6 mL methanol and 6 mL Milli-Q water. Firstly, the extraction efficiency (recovery) of three types of cartridges was studied by extracting the tol/nC_{60} in Milli-Q water samples. And then the cartridge with highest recovery was selected and the extraction conditions were optimized by adjusting the pH and salt addition. Finally, the optimized extraction method was applied to determine the recovery, detection limit, and quantification limit of tol/nC_{60} in different wastewater samples. The detailed procedure as follows:

For optimization of extraction, tol/nC_{60} was spiked into 100 mL of Milli-Q water to a final concentration of 5 µg/L. And for the evaluation of recovery, detection and quantification limit, a series of tol/nC_{60} concentration ranged from to 0.05 to 5.17 µg/L were spiked into 100 mL of wastewater samples. And the water samples containing tol/nC_{60} were passed through the cartridges at a flow rate of 5 mL/min using a Charatec Sep-Pak concentrator (SPC 10-C, Chratec, Kyoto, Japan). And around 10 mL Milli-Q water was used to rinse the flasks and internal line systems of concentrator. The cartridges were dried completely using a vacuum manifold for 3 h. The analyses were then eluted from the cartridge with 8 mL toluene. The toluene extracts were concentrated to a volume of around 1 mL by a gentle flow of nitrogen gas at 55 °C. The complete evaporation of toluene was avoided because the extraction efficiency could reduce due to the aggregate formation and/or adsorption to the glassware surface according to the results of the preliminary experiments. The volume was then adjusted to 2 mL by weighing. The extract was collected and transferred to a vial for HPLC-UV/vis analysis.

3.2.4 Chromatographic separation and detection

C_{60} in the toluene was separated and quantified by the HPLC-UV/visible system (LC-10AD, Shimadzu, Japan). nC_{60} was separated in a triacontyl (C30) silica-gel column (250 mm×4.6 mm i.d. packed with 5-µm particles; Nomura Chemical, Japan) by isocratic elution at a flow rate of 1 mL/min in a mobile phase of acetonitrile and toluene (65:35, v/v) at 30 °C with an injection volume of 20 µL. C_{60} was quantified at 332 nm by the UV-vis detector.

3.2.5 Method validation

The accuracy and precision of the method were determined from the spiking experiments. The calibration curve was obtained by a series of standard solutions (C_{60} in toluene) prepared by the stock C_{60} toluene solutions. Recovery of extraction was determined by the ratio of detected and spiked amount. The method detection limit (MDL) and method quantification limit (MQL) were calculated from the standard deviation of measurement of five replicates samples at the lowest concentration with the variation coefficient of less than 20% (Komori et al., 2004; Kim and Tanaka, 2009; Kumar et al., 2009).

3.2.6 Analysis

The photon count rate (kilo counts per second: kcps) and size (hydrodynamic diameter) of nC_{60} were determined by dynamic light scattering in a Zetasizer Nano ZS (Malvern Instruments, UK) as shown in **Fig. 3.2**. The 633-nm laser is used as a light source and the intensity of light scattered by the particles is measured as the photon count rate by a detector at 173°. The particle size is determined by analyzing the fluctuation of scattered light intensity by particles undergoing Brownian motion (Malvern manual, 2009). The measurement position from the cell wall and attenuation index for laser power are automatically adjusted to ensure that the measured count rate is suitable for the requirements of the detector and then obtain the best signal to noise ratio. The derived count rate (DCR) is a calculated scattering intensity representing the scattering intensity that would be measured at detector in the absence of laser light attenuation filter. The DCR is fairly stable for a sample with stable size over time and then may be used to determine the relative concentration of particles. The same instrument was used to measure the electrophoretic mobility which was subsequently calculated into Zeta (ζ) potential using the Smoluchowski equation. The UV absorbance of the stock C_{60} toluene solution and nC_{60} suspension in water was measured using a UV-2500 spectrophotometer (Shimadzu, Japan).

a

b

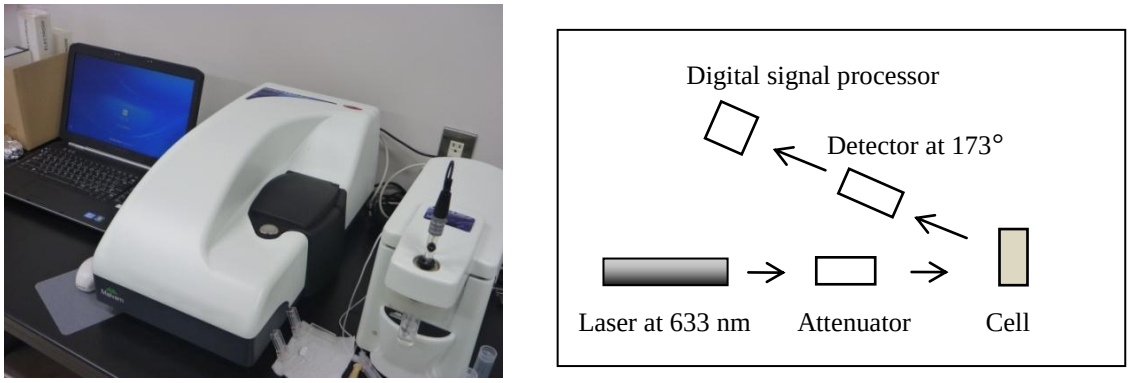

Fig. 3. 2 The Zetasizer Nano ZS analyzer (a) and its optical configurations for dynamic light scattering measurement (b).

3.3 Results and discussions

3.3.1 Characterization of nC_{60} aqueous suspension prepared by different techniques

Fig. 3.3 shows the UV−visible absorption spectra of aqu/nC_{60} (7 mg/L) and tol/nC_{60} (14 mg/L). Both nC_{60} shows the absorption peaks at 260 and 350 nm for the electronic structure of molecular C_{60} cage (Lee et al., 2009), and a broad absorption band at 450−550 nm for the aggregated C_{60}−C_{60} interactions (Fortner et al., 2005). Similar findings have also been reported for nC_{60} prepared via tetrahydrofuran (THF) (Fortner et al., 2007). However, the ratio of absorbance at 260, 350 and 450 nm varied with the nC_{60} types suggesting the difference in the structure and composition of nC_{60} aggregates (Brant et al., 2006).

Two types of nC_{60} demonstrated very similar size distribution with an average size of 154 and 144 nm for aqu/nC_{60} and tol/nC_{60}, respectively, as shown in **Fig. 3.4**. Both nC_{60} were negatively charged at pH 5.6 (**Fig. 3.5**), which is in agreement with the reported results of nC_{60} prepared using similar methodologies (Brant et al., 2006).

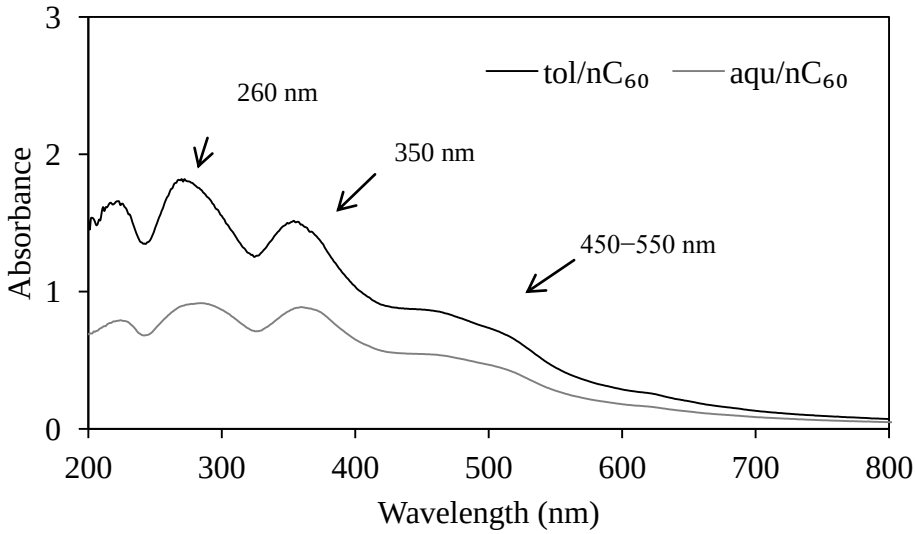

Fig. 3. 3 UV−visible absorption spectra of prepared nC_{60}.

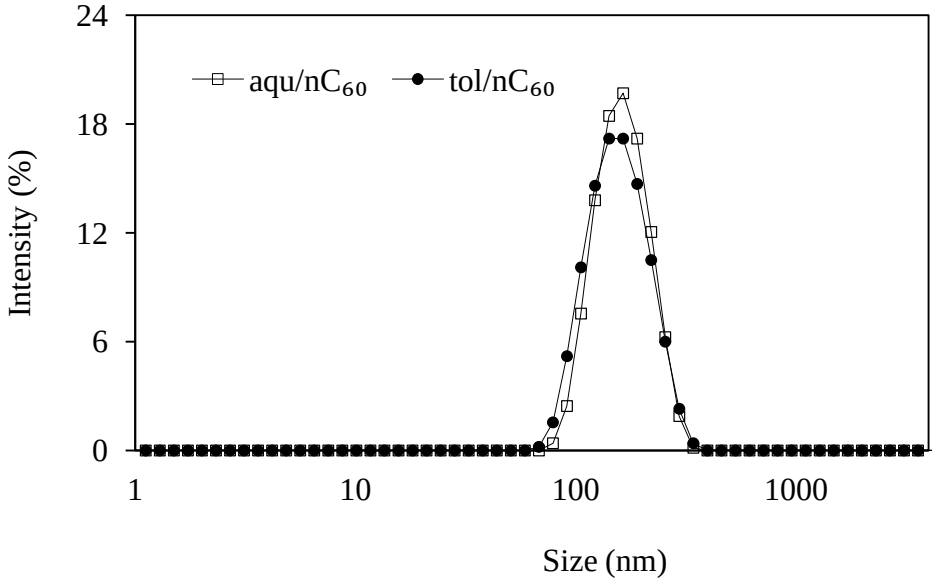

Fig. 3. 4 Size distribution of prepared nC_{60}.

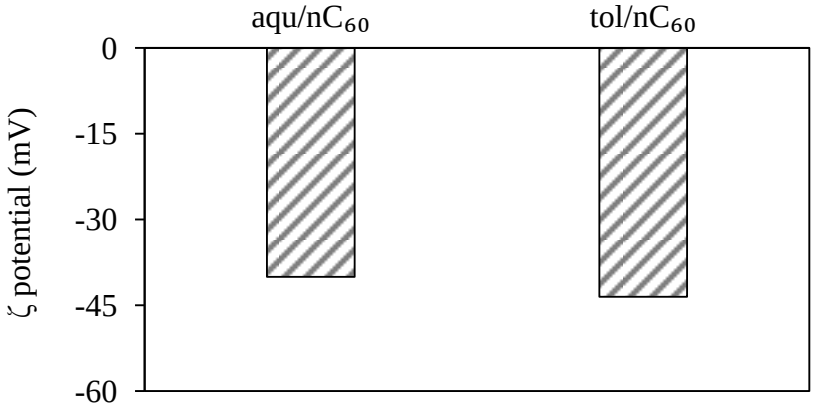

Fig. 3. 5 ζ potential of prepared nC_{60}.

3.3.2 Analytical accuracy for tol/nC_{60} by LLE

The tol/nC_{60} was spiked into the wastewater samples to a series of final concentrations ranged from 2 to 500 µg/L (n = 5). As shown in **Table 3.1**, the nC_{60} recoveries were all higher than 90% and only slight difference was found among three wastewater samples. It indicated the LLE extraction could provide high recovery and was not significantly affected by the wastewater matrices. The coefficient of variation (CV) decreased with the decrease in the spiked concentrations. And the lowest concentration with a CV less than 20% was the spiked level of 5 µg/L which was used to determine the method detection and quantification limits of tol/nC_{60} in wastewater. The method detection limit was ranged from 0.89 to 1.07 µg/L and the method quantification limit was ranged from 2.97 to 3.55 µg/L for three wastewater samples (**Table 3.2**).

As shown in **Fig. 3.6**, HPLC column and UV detector could gave a sharp peak for C_{60} extracted from the wastewater and no unaccepted matrix effect was observed from the wastewater. And **Fig. 3.7** showed the correlation of peak area against spiked concentrations in different wastewater samples. The linear correlations were found in a wide linear range from 2 to 500 µg/L. And the correlation coefficients (R^2) for three wastewater samples were all higher than 0.99, indicating the comparable recovery over the concentrations studied and potential application for the tol/nC_{60} quantification in wastewater as the calibration curves.

Table 3. 1 Recovery of tol/nC_{60} at different concentrations in wastewaters by LLE

Spiked Conc. (µg/L)	Influent			Primary Effluent			Secondary Effluent		
	Measured Conc. (µg/L)	CV (%)	Recovery (%)	Measured Conc. (µg/L)	CV (%)	Recovery (%)	Measured Conc. (µg/L)	CV (%)	Recovery (%)
2	1.81	21	91	1.92	18	96	1.90	17	95
5	4.5	7	90	4.53	7	91	4.61	8	92
10	9.14	8	91	9.52	8	95	9.15	5	91
30	27.22	4	91	28.36	5	95	27.24	3	91
100	90.17	5	90	92.69	1	93	93.28	2	93
200	180.07	2	90	182.80	2	91	187.28	3	94
350	318.80	2	91	318.45	5	91	327.64	3	94
500	457.84	5	92	467.43	2	93	476.56	2	95
Average	-	-	91	-	-	93	-	-	93

Table 3. 2 Calculated method detection limit (MDL) and method quantification limit (MQL) of tol/nC_{60} in different wastewater samples by LLE

Limit (µg/L)	Spiked nC_{60} Conc. (µg/L)	Influent		Primary effluent		Secondary effluent	
		Measured (µg/L)	Standard derivation	Measured (µg/L)	Standard derivation	Measured (µg/L)	Standard derivation
	5	4.50	0.32	4.53	0.30	4.61	0.36
MDL		0.97		0.89		1.07	
MQL		3.22		2.97		3.55	

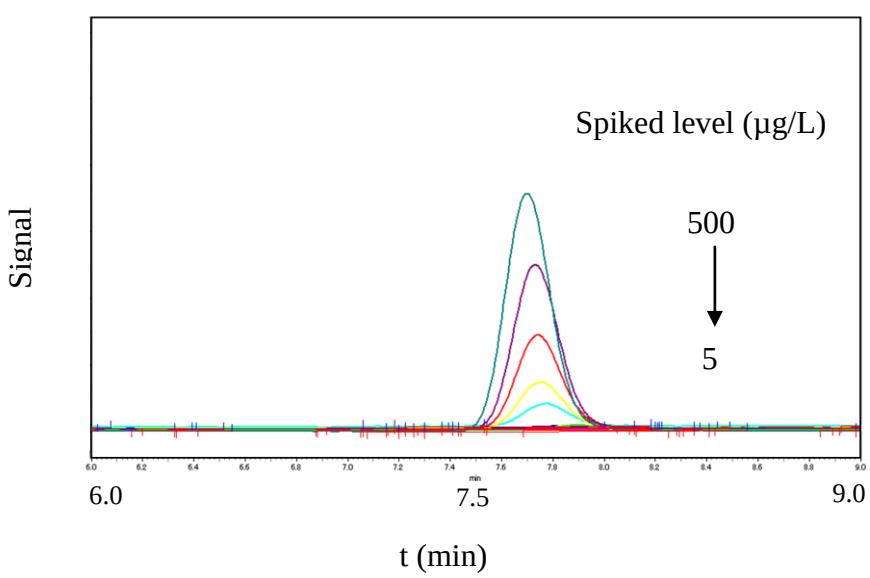

Fig. 3. 6 HPLC-UV/vis spectrum of C_{60} extracted from the tol/nC_{60} spiked influent wastewater.

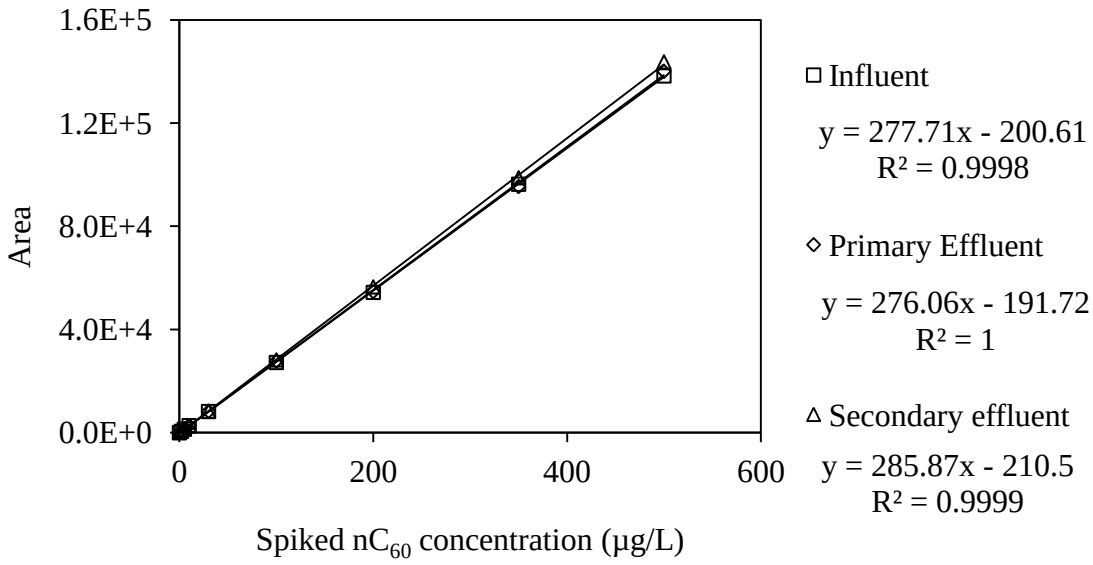

Fig. 3. 7 Calibration curves of peak area against spiked tol/nC_{60} concentrations in different wastewater samples by LLE.

3.3.3 Analytical accuracy for tol/nC_{60} by SPE

Three types of solid phase extraction cartridges were evaluated to recover the tol/nC_{60} in the Milli-Q water samples. The HLB cartridge yielded the highest

recovery (57%), compared to the recovery of 35% and 16% for the SAX and SCX cartridges, respectively (**Fig. 3.8**). It might be attributed to the hydrophilic and lipophilic property for both the sorbent materials in HLB cartridge and the nC_{60} nanoparticles. And then the pretreatment of pH adjusting and salt addition were investigated to optimize the solid phase extraction. As shown in **Fig. 3.9**, **t**he recovery of tol/nC_{60} from Oasis HLB cartridge at pH 3 was about 80% which was significantly higher than the other pH conditions. The absolute charge of tol/nC_{60} was reduced at lower pH which could decrease the electrostatic repulsive between the tol/nC_{60} and sorbent materials in the cartridge and consequently improved the nonpolar-nonpolar interactions. On the other hand, the salt addition did not show significant effect on the recovery of tol/nC_{60} from water samples by SPE using Oasis HLB cartridge (**Fig. 3.10**). It might be explained that the salt addition could not only improve the retention on the cartridge by destabilizing the tol/nC_{60} but also increase the loss of adsorption on the glassware or internal system of concentrators. As a result, no significant change in tol/nC_{60} recovery was observed at different concentrations of salts.

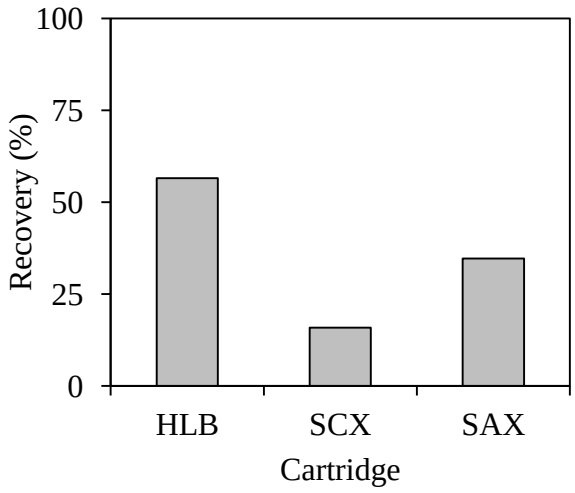

Fig. 3. 8 Recovery of tol/nC_{60} in Milli-Q water samples by different type of cartridges.

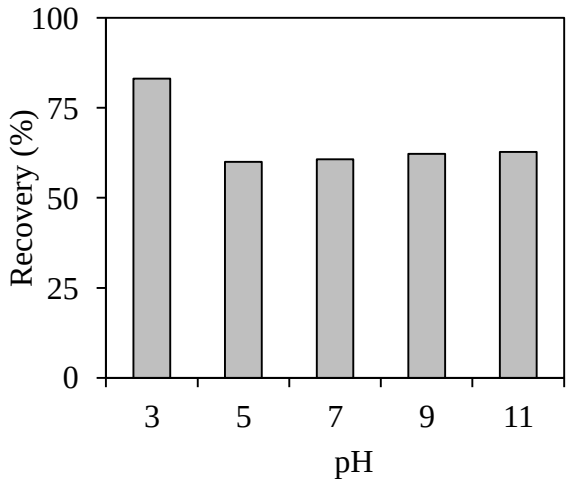

Fig. 3. 9 Effect of pH on the recovery of tol/nC_{60} in Milli-Q water samples.

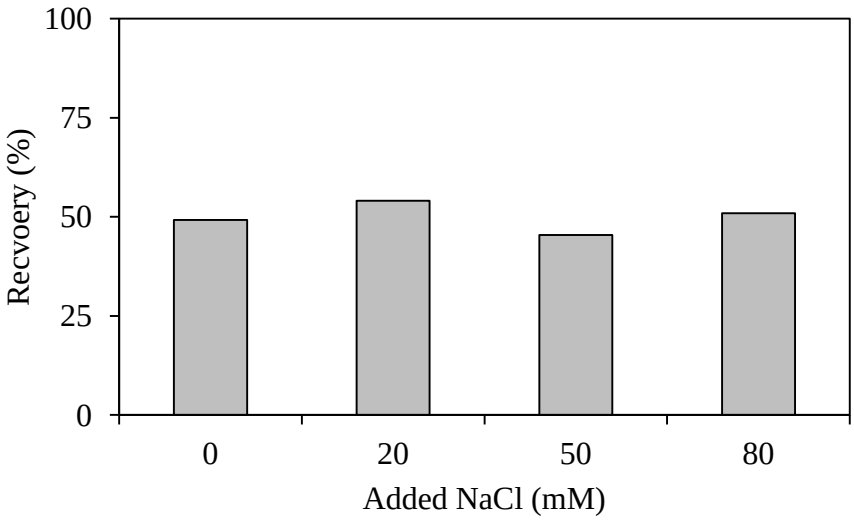

Fig. 3. 10 Effect of ionic strength on the recovery of tol/nC_{60} in Milli-Q water samples.

Based on the results of optimization experiments, the extraction conditions for tol/nC_{60} were established as follows: the HLB cartridge, pH 3 and no salt addition. And the recovery of tol/nC_{60} in wastewater samples was evaluated by a series of spiking experiments. Seven levels of aqueous C_{60} solution from 0.05 to 5.17 µg/L were prepared by diluting the tol/nC_{60} into the filtrated wastewater samples. The recovery decreased with decrease in the spiked tol/nC_{60} concentration for all the three wastewater samples (**Table 3.3**). At the spiked concentration, the average recoveries were 75, 74 and 80% for the influent, primary effluent and secondary effluent samples, respectively. And the CV values increased with decrease in the spiked concentrations. The spiking level of 0.10 µg/L was the lowest level with the CV values lower than 20%. This level was used to calculate the method detection limit and quantification limit. As shown in **Table 3.4**, the method detection limit ranged from 0.02 to 0.03 µg/L, while the method quantification limit was from 0.08 to 0.10 µg/L for wastewater samples. The method quantification limits by SPE was ~30 times lower than those obtained by the LLE due to the higher concentration factors. This suggested the potential application of SPE for determining the occurrence concentration of nC_{60} in environmental wastewater samples. **Fig. 3.11** showed the linearity of calibration curve of peak area against the spiked tol/nC_{60} concentration. High correlation coefficients (R^2) were obtained for SPE from all the three wastewater samples.

Table 3. 3 Recoveries of tol/nC_{60} at different concentrations in wastewaters by SPE

Spiked conc.(µg/L)	Influent			Primary Effluent			Secondary Effluent		
	Measured conc. (µg/L)	Recovery (%)	CV (%)	Measured conc. (µg/L)	Recovery (%)	CV (%)	Measured conc. (µg/L)	Recovery (%)	CV (%)
0.05	0.03	64	18	0.03	65	22	0.04	70	16
0.10	0.07	70	14	0.07	67	15	0.07	72	11
0.21	0.15	73	10	0.15	74	8	0.17	79	6
0.52	0.38	74	3	0.39	75	5	0.41	79	3
1.03	0.84	81	1	0.80	77	5	0.85	83	3
2.07	1.69	82	2	1.65	80	3	1.76	85	3
5.17	4.27	83	2	4.31	83	2	4.60	89	1
Average		75			74			80	

Table 3. 4 Calculated method detection limit (MDL) and method quantification limit (MQL) of tol/nC_{60} in different wastewater samples by SPE

Limit (µg/L)	Spiked conc. (µg/L)	Influent		Primary effluent		Secondary effluent	
		Measured conc. (µg/L)	Standard derivation	Measured conc. (µg/L)	Standard derivation	Measured conc. (µg/L)	Standard derivation
	0.10	0.07	0.01	0.07	0.01	0.07	0.008
MDL		0.03		0.03		0.02	
MQL		0.10		0.10		0.08	

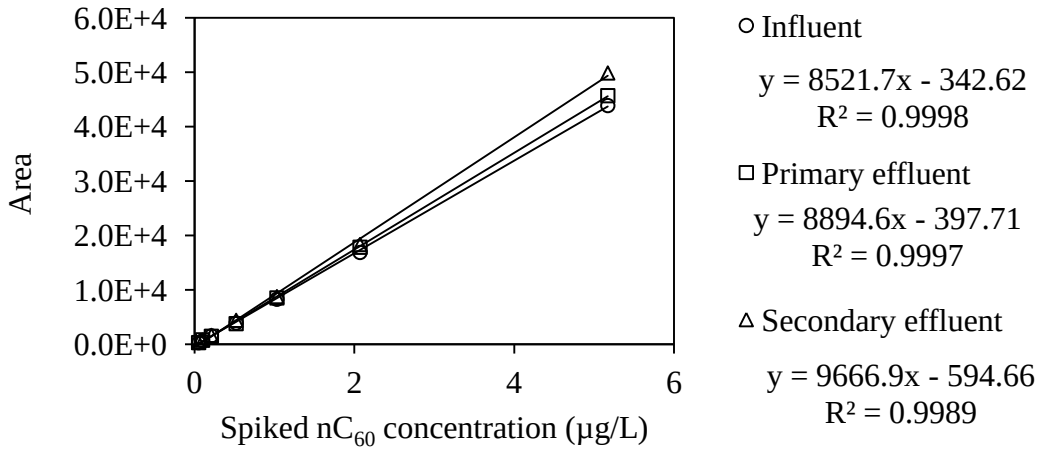

Fig. 3. 11 Calibration curves of peak area against spiked tol/nC_{60} concentrations in different wastewater samples by SPE.

3.3.4 Application of SPE for the environmental samples

The nC_{60} concentration in influent wastewater from a WWTP, treating the domestic wastewater, was measured using the optimized SPE extraction method with HPLC-UV/vis system. **Fig. 3.12** showed the UV/vis chromatography at wavelength of 332 nm for the C_{60} in the influent and 0.10 µg/L nC_{60}-spiked sample. No peak of C_{60} was detected in the influent compared to that in the 0.10 µg/L nC_{60}-spiked sample. The results indicated the environmental concentration of nC_{60} in influent was less than the method quantification limit of 0.10 µg/L.

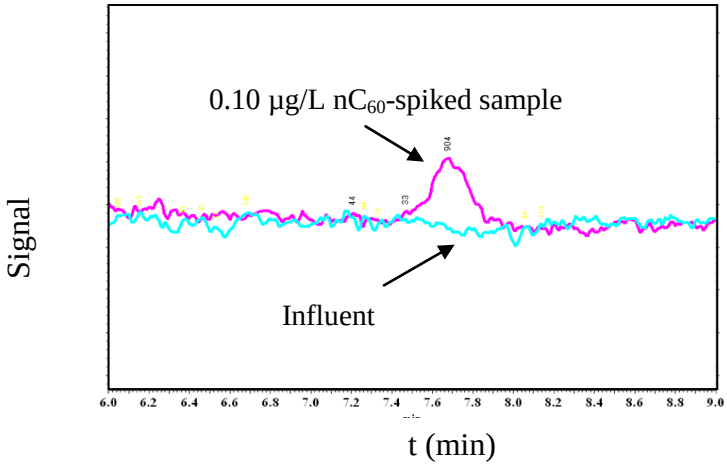

Fig.3. 12 HPLC-UV/vis chromatography of C_{60} in the influent and 0.10 µg/L nC_{60}-spiked samples.

3.3.5 Estimation of nC_{60} concentration in the raw wastewater in Japan

The nC_{60} concentration in the raw wastewater was estimated based on the wastewater amount and the production of fullerene C_{60} in Japan, as well as the life cycle perspective for each application of nC_{60}. The annual production was 2 ton in 2006 (The Ministry of Environment of Japan, 2009). At present, the main application of fullerene nC_{60} was estimated to be 80, 12.5 and 7.5% for the composites, cosmetics and research & development, respectively (The National Institute of Advanced Industrial Science and Technology, 2009). And the wastewater was 14.5×10^9 m^3/year in 2008 (The Japan Sewage Works Association, 2012). The percent fraction of nC_{60} release into different compartments via each application was estimated according to the life cycle of nC_{60} and wastewater treatment service coverage in Japan (Gottschalk et al., 2009; The Ministry of Land, Infrastructure, Transport and Tourism of Japan, 2012). The information was detailed in **Table 3.5**.

Table 3. 5 The data and parameters for estimating the nC_{60} concentration in the raw wastewater

Application	Total production (ton/year)	Contribution of each application (%)	Release coefficient of C_{60} into different compartments			Wastewater ($\times 10^9$ m^3/year)
			WWTP	Wastewater incineration plant+Landfill	Surface water	
Composites	2	80	0	1	0	14.5
Cosmetics		12.5	0.88	0	0.12	
Research & Development		7.5	0.50	0.50	0	

The nC_{60} concentration in the raw wastewater was estimated using the following equation,

$$C_{nC60} = \sum_{i}^{3} M \times D_i \times P_i / Q \quad (3.1)$$

where C_{nC60} is the estimated concentration in raw wastewater; the M is the production of nC_{60} per year, the D_i is the percent contribution of each application, P_i is the percent release of nC_{60} into the wastewater treatment plant; Q is the annual wastewater in Japan; i is the type of application.

The nC_{60} was calculated to be 0.020 μg/L in the raw wastewater. The real concentration in the liquid phase in wastewater could be lower than the value estimated above, given the adsorption on the suspended solids in the raw wastewater.

3.4 Conclusions

Previous studies have developed the quantification methods for nC_{60} in the simple aqueous samples such as the pure water, tap water, surface water and organic matter-containing artificial water. The liquid-liquid extraction (LLE) method was mostly used for extracting nC_{60} from these aqueous samples. However, very few studies were attempted to quantify the nC_{60} in wastewater because of complex matrices. In this chapter, two types of nC_{60} aqueous suspension were prepared using the toluene exchange and extended stirring techniques. The recoveries were evaluated for extracting nC_{60} from different wastewater samples using the LLE method. In addition, the solid phase extraction (SPE) method was also evaluated by investigating three types of extraction cartridges. And the method detection and quantification limits of nC_{60} in wastewater samples were determined using the HPLC-UV/vis detection system for both LLE and SPE. The main conclusions as follows:

(1) Two types of nC_{60} demonstrated very similar size distribution with an average size of 154 and 144 nm for aqu/nC_{60} and tol/nC_{60}, respectively. Both nC_{60} were negatively charged in Milli-Q water at pH 5.6. The tol/nC_{60} was used for the fate studies in the Chapter IV because of less time-consumption and high yield of the preparation method. The aqu/nC_{60} was used to investigate the toxicity on the activated sludge in Chapter V because it could well represent the discharge of nC_{60} into the water environment during the production and use of C_{60} nanoparticles. In addition, the tol/nC_{60} was also used for toxicity studies to investigate the effect of preparation methods on the nC_{60} toxicity.

(2) The liquid-liquid extraction of nC_{60} from wastewater samples could give a high recovery of > 90% and good linear correlation (R^2 > 0.99) at the concentration ranged from 2 to 500 μg/L. The method detection limit was ranged from 0.89 to 1.07 μg/L and the method quantification limit was ranged from 2.97 to 3.55 μg/L for wastewater samples.

(3) The solid phase extraction of nC_{60} from wastewater samples could give a recovery of > 64% and good linear correlation (R^2 > 0.99) at the concentration ranged from 0.05 to 5.17 μg/L. The recovery of nC_{60} from the wastewater samples here was significantly higher than the published ones primarily

because of the high extraction efficiency of HLB solid phase cartridge. The method detection limit ranged from 0.02 to 0.03 μg/L, while the method quantification limit was from 0.08 to 0.10 μg/L for wastewater samples. The method detection limit was 10 times lower than the reported ones because of the high extraction efficiency of HLB cartridge and high concentrations factors.

(4) The nC_{60} concentration in the domestic influent wastewater from a domestic WWTP was measured using the optimized SPE extraction method with HPLC-UV/vis system. The nC_{60} concentration was lower than 0.10 μg/L (the method quantification limit). In addition, the nC_{60} concentration in the raw wastewater was estimated based on the annual wastewater and the production of fullerene C_{60} in Japan, as well as the life cycle perspective for each application of C_{60}. The nC_{60} was calculated to be 0.020 μg/L in the raw wastewater. The real concentration in the liquid phase in wastewater could be much lower, given the adsorption on the suspended solids in the raw wastewater.

(5) By comparison of two types of extraction methods, the LLE has much higher recovery and wider range of linear calibration curves than those of SPE. Therefore, the LLE was used for the fate studies in the Chapter IV.

3.5 References

Bouchard, D., Ma, X., 2008. Extraction and high-performance liquid chromatographic analysis of C_{60}, C_{70}, and [6,6]-phenyl C_{61}-butyric acid methyl ester in synthetic and natural waters. Journal of Chromatography A 1203 (2), 153–159.

Brant, J.A., Labille, J., Bottero, J.Y., Wiesner, M.R., 2006. Characterizing the impact of preparation method on fullerene cluster structure and chemistry. Langmuir 22 (8), 3878–3885.

Chen, Z., Westerhoff, P., Herckes, P., 2008. Quantification of C_{60} fullerene concentrations in water. Environmental Toxicology and Chemistry 27 (9), 1852–1859.

Farre, M., Perez, S., Gajda-Schrantz, K., Osorio, V., Kantiani, L., Ginebreda, A., Barcelo, D., 2010. First determination of C_{60} and C_{70} fullerenes and N-methylfulleropyrrolidine C_{60} on the suspended material of wastewater effluents by liquid chromatography hybrid quadrupole linear ion trap tandem mass spectrometry. Journal of Hydrology 383 (1-2), 44–51.

Fortner, J.D., Kim, D.-I., Boyd, A.M., Falkner, J.C., Moran, S., Colvin, V.L., Hughes, J.B., Kim, J.H., 2007. Reaction of water-stable C_{60} aggregates with ozone. Environmental Science & Technology 41 (21), 7497–7502.

Fortner, J.D., Lyon, D.Y., Sayes, C.M., Boyd, a M., Falkner, J.C., Hotze, E.M., Alemany, L.B., Tao, Y.J., Guo, W., Ausman, K.D., Colvin, V.L., Hughes, J.B., 2005. C_{60} in water: nanocrystal formation and microbial response. Environmental Science & Technology 39 (11), 4307–4316.

Gottschalk, F., Sonderer, T., Scholz, R.W., Nowack, B., 2009. Modeled environmental concentrations of engineered nanomaterials (TiO_2, ZnO, Ag, CNT, Fullerenes) for different regions. Environmental Science & Technology 43 (24), 9216–9222.

Heymann, D., Korochantsev, A., Nazarov, M.A., Smit, J., 1996. Search for fullerenes C_{60} and C_{70} in Cretaceous-Tertiary boundary sediments from Turkmenistan, Kazakhstan, Georgia, Austria, and Denmark. Cretaceous Research 17 (3), 367–380.

Hyung, H., Kim, J.H., 2009. Dispersion of C_{60} in natural water and removal by conventional drinking water treatment processes. Water Research 43 (9), 2463–2470.

Isaacson, C.W., Kleber, M., Field, J.A., 2009. Quantitative analysis of fullerene nanomaterials in environmental systems: a critical review. Environmental Science & Technology 43 (17), 6463–6474.

Jinno, K., Kohrikawa, C., 1998. Supercritical and subcritical fluid extraction of fullerenes from carbon soot. Chimica Oggi-Chemistry Today 16 (1-2), 9–15.

Kim, I., Tanaka, H., 2009. Photodegradation characteristics of PPCPs in water with UV treatment. Environment International 35 (5), 793–802.

Komori, K., Tanaka, H., Okayasu, Y., Yasojima, M., Sato, C., 2004. Analysis and occurrence of estrogen in wastewater in Japan. Water Science and Technology 50 (5), 93–100.

Kumar, V., Nakada, N., Yasojima, M., Yamashita, N., Johnson, A.C., Tanaka, H., 2009. Rapid determination of free and conjugated estrogen in different water matrices by liquid chromatography-tandem mass spectrometry. Chemosphere 77 (10), 1440–1446.

Lee, J., Cho, M., Fortner, J.D., Hughes, J.B., Kim, J.H., 2009. Transformation of aggregate C_{60} in the aqueous phase by UV irradiation. Environmental Science & Technology 43 (13), 4878–4883.

Malvern manual, Zetasizer Nano Series User Manual, man 0317, issue 5.0, 2009.

Moussa, F., Pressac, M., Genin, E., Roux, S., Trivin, F., Rassat, A., Ceolin, R., Szwarc, H., 1997. Quantitative analysis of C_{60} fullerene in blood and tissues by high-performance liquid chromatography with photodiode-array and mass spectrometric detection. Journal of Chromatography B 696 (1), 153–159.

Smeraldi, J., Ganesh, R., Safarik, J., Rosso, D., 2012. Statistical evaluation of photon count rate data for nanoscale particle measurement in wastewaters. Journal of Environmental Monitoring 14 (1), 79–84.

The Japan Sewage Works Association, the annual wastewater and wastewater sludge, 2012. http://www.jswa.jp/data-room/data.html.

The Ministry of Environment of Japan, Guideline for prevention of environmental impact of the manufactured nanomaterials, 2009.

The National Institute of Advanced Industrial Science and Technology, Risk assessment of manufactured nanomaterials, 2009.

Xia, X.R., Monteiro-Riviere, N.A., Riviere, J.E., 2006. Trace analysis of fullerenes in biological samples by simplified liquid-liquid extraction and high-performance liquid chromatography. Journal of Chromatography A 1129 (2), 216–222.

CHAPTER IV

AGGREGATION BEHAVIOR OF nC_{60} IN WASTEWATER AND ADSORPTION BEHAVIOR OF nC_{60} ON WASTEWATER SLUDGES

4.1 Aggregation behavior of nC_{60} in wastewater

4.1.1 Introduction

Fullerene C_{60}, the most commonly-produced and -used fullerene nanoparticles, are expected to have promising potential for the application in commercial and scientific fields (Murayama et al., 2004). If nC_{60} are introduced, either intentionally or unintentionally, into industrial and domestic wastewater (Gottschalk et al., 2009; Brar et al., 2010), wastewater treatment plants can become an important route for nC_{60} discharge into waters. The ability of conventional activated sludge treatment processes to treat nC_{60} could be affected by the surface properties of nanoparticles, such as size aggregation and surface charge, by affecting the adsorption interactions between nanoparticles and activated sludge (Brar et al., 2010; Kiser et al., 2010; Gomez-Rivera et al., 2012). Membrane filtration, with pore sizes ranging from nanometer to micrometer scale, can be used to treat both primary (Abdessemed and Nezzal, 2003; Radjenovic et al., 2009; Kuo et al., 2010) and secondary effluents (Kim et al., 2002; Wang et al., 2005; Lee et al., 2007). Because size exclusion offers the best means to remove nC_{60}, the efficiency of removal might be greatly affected by particle aggregation in wastewater. However, the characteristics of nC_{60} aggregation in wastewater are still unknown.

The objective of this part was to understand the aggregation behavior of nC_{60} in wastewater. The aggregation of nC_{60} in filtered secondary effluent, aeration tank liquor, and primary effluent was investigated by measuring their size and zeta (ζ) potential, and the effects of pH, ionic strength and dissolved organic matter (DOM). The results are expected to provide useful information on the fate of nC_{60} during wastewater treatment and appropriate methods for improving nC_{60} treatment during wastewater treatment. The content structure of this part was shown in **Fig. 4.1.1.**

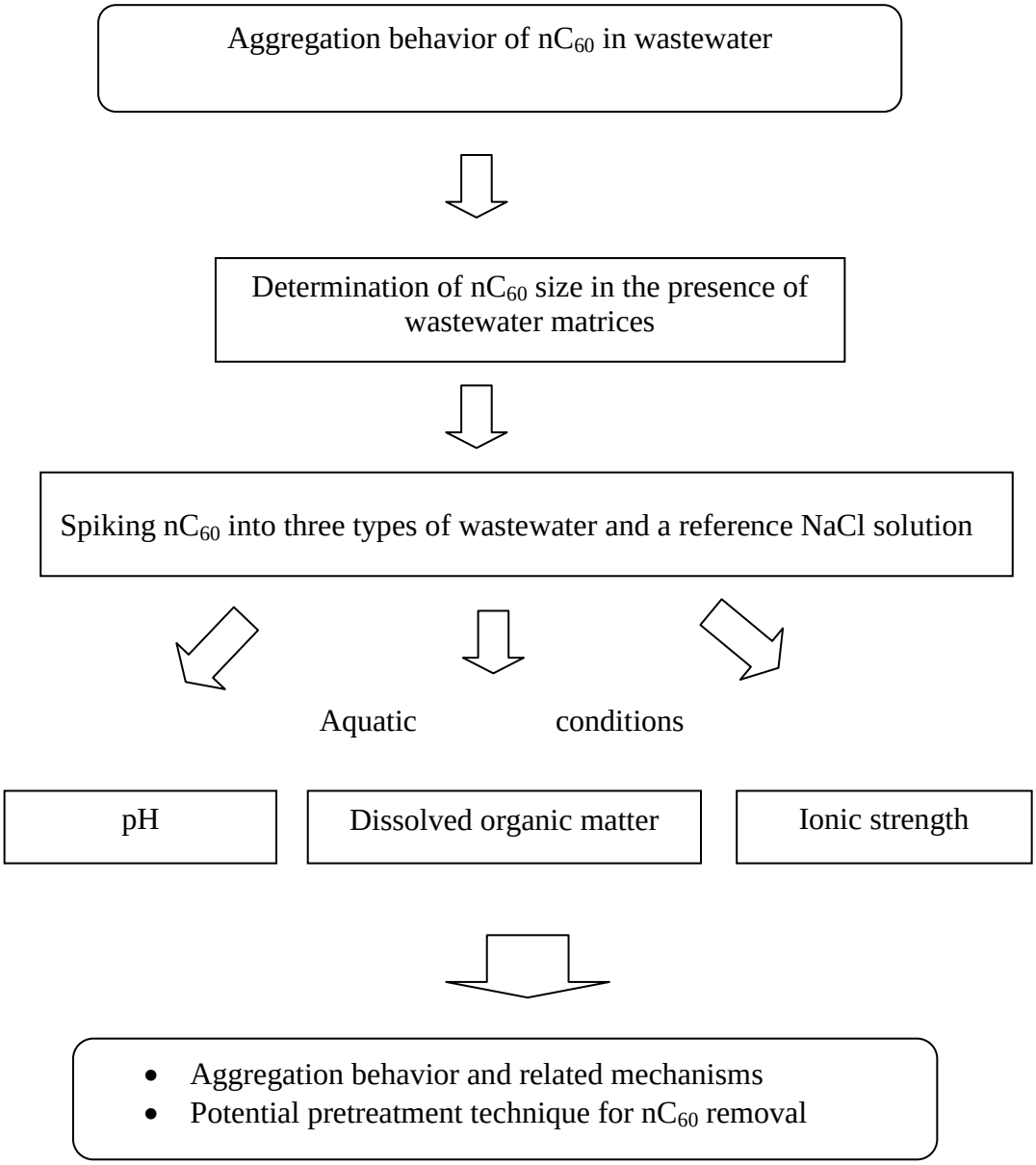

Fig. 4. 1. 1 The content structure of this part.

4.1.2 Materials and methods

4.1.2.1 Preparation and characterization of nC_{60} aqueous suspension

A suspension of nC_{60} was prepared by the toluene-based solvent exchange method, described in detail in Chapter III.

4.1.2.2 Water sample and isolation of dissolved organic matter from wastewater

Three wastewater samples were used: filtered primary effluent (PE), aeration tank liquor (AT), and secondary effluent (SE). All samples were collected from a municipal WWTP in Japan that applied the conventional activated sludge process. The samples or supernatant of activated sludge were sequentially filtered through a glass filter (1.0 μm pore size; Pall Life Sciences, USA) and a mixed cellulose ester filter (0.45 μm pore size; Advantec, Japan). In addition, a series of NaCl solutions were prepared to yield different ionic strengths using Milli-Q water. They were used as the reference water samples with similar ionic strength to that of wastewaters but no dissolved organic matter (DOM). The wastewater samples were characterized by the chemical compositions, electrical conductivity (EC), pH, and dissolved organic carbon (DOC) concentration.

The DOM was isolated from primary effluent by the following procedures. The 0.45-μm-filtrated wastewater was frozen at −30 °C and then concentrated using a FDU-1200 freeze drier (EYELA, Japan). The concentrated solution was desalted by the H^+ cation- (via converting the Dowex Marathon MSC (Na^+ form), Sigma Aldrich, USA) and OH^- anion- (Dowex Monosphere 550A (OH^- form), Wako, Japan) exchange resins. After filtrating again through a 0.45 μm mixed cellulose ester filter, the DOC concentration was determined with a TOC 5000A analyzer (Shimadzu, Japan).

4.1.2.3 Dynamic light scattering technique and determination of spiked nC_{60} concentration for aggregation studies

The results of preliminary experiments showed that the sizes of the nC_{60} and matrix particles in filtered wastewater were very close. However, the concentration of spiked nC_{60} should be high enough to mask the effect of the wastewater derived matrix particles. On the other hand, it should be low enough to reflect aggregation behavior at likely environmental levels. To select the optimum spiked nC_{60} concentration, the sizes of nC_{60} in water samples were measured using the dynamic light scattering technique. The 1.0-µm-filtered primary effluent was firstly investigated, because it has the highest derived count rate of matrix particles, by spiking nC_{60} to varying concentrations to test the effect on size measurements. Measurements were taken after 1 min to avoid increased aggregation with time. The optimum spike concentration was determined from the change in measured nC_{60} size with the increase in spike concentration. Then the derived count rate of matrix particles in three 0.45-µm-filtered wastewater samples was measured under all experimental conditions described in section 4.1.2.4. Finally, the effects of matrix particles were evaluated by comparing those results with the results from 1.0-µm-filtered primary effluent.

4.1.2.4 nC_{60} aggregation studies

Three experiments were conducted in Erlenmeyer flasks containing 25 or 50 mL water samples. The first experiment examined the time profile of nC_{60} aggregation in 0.45-µm-filtered wastewater samples up to 24 h and in 2.5 mM NaCl solution prepared as a reference solution with similar ionic strength to that of the wastewater but no dissolved organic matter. All water samples were adjusted to pH 7 with dilute NaOH or HCl solution. Then the samples were spiked with nC_{60} to 1 mg/L (as determined in sections 4.1.2.3 and 4.1.3.2) and shaken on a rotary shaker (120 rpm, 25 °C). The aggregate size was immediately examined at 1 min and at 2, 4, 6, and 24 h without settling. The second experiment examined the effects of pH and ionic strength on nC_{60} aggregation in 0.45-µm-filtered wastewater and NaCl reference samples. Water samples were adjusted to 0, 2.5, 10, 50, 100, or 500 mM NaCl and to a pH of 3, 5, 7, 9, or 11 with HCl or NaOH. The samples were spiked

with nC_{60} and shaken as above. The aggregate size was immediately measured after 1 h mixing without settling. Both the first and second experiments were performed in duplicate on samples collected on two separate dates. The third experiment examined the effect of DOM isolated from wastewater on the nC_{60} aggregation. The water samples were prepared by diluting the concentrated DOM solution to different DOC concentrations using the Milli-Q water, followed by adjusting to pH 7. And the water samples were spiked to 1 mg/L nC_{60} as above. After being mixed thoroughly for 1 min, 1 mL of test solutions were maintained at 25 °C internally controlled by the Zetasizer instrument and the nC_{60} size was measured every 5 min through the experiments. This experiment was performed in triplicate. For all the three experiments, the ζ potential was measured 1 min after nC_{60} spiking and mixing using a vortex mixer (TM-2000, LMS, Japan). And all the results in figures are the mean values of the replicates.

4.1.2.5 Other analysis

The size, size distribution, and ζ potential of nC_{60} was measured with the Zetasizer Nano ZS (Malvern Instruments, UK), detailed in Chapter III. The concentrations of Al^{3+}, Na^{+}, K^{+}, Ca^{2+}, and Mg^{2+} in wastewater were measured using the inductively coupled plasma mass spectrometry (7700X, Agilent Technology, Japan), and those of Cl^{-}, NO_3^{-}, NO_2^{-}, SO_4^{2-} and PO_4^{3-} using the ion chromatography (ICS-2000, Dionex, USA). And the HCO_3^{-} concentration was determined by the titration via the total alkalinity and phenolphthalein method. The electrical conductivity was measured with a CG 511B electrode **(**DKK-TOA, Japan), and the pH with an InLab413 SG/2m electrode (Mettler Toledo, Japan). The comparison of mean difference was analyzed by the one-way analysis of variance (ANOVA) (SPSS, Version 16.0, SPSS lnc., USA). And the ionic strength (IS) in water samples was calculated using the following equation (French et al., 2009):

$$I = \frac{1}{2}\sum_i C_i \times Z_i^2 \qquad (4.1.1)$$

Where I is the ionic strength of the ions in water (mM), C_i is the concentration of each ion in water (mM), the Z_i is the charge for each ion in water.

4.1.3 Results and discussions

4.1.3.1 Characterization of nC_{60} aqueous suspensions and water samples

The ζ potential showed that the nC_{60} suspension was negatively charged in the range of pH studied. The absolute values decreased with the decrease in pH from 11 to 1, with an isoelectric point around pH 1. It indicated the nC_{60} become unstable at acidic condition. The detailed information was shown in Chapter III.

Table 4.1.1 showed the chemical properties of water samples used in this study. The 0.45-μm-filtered wastewater samples had close pH, EC and IS, as well as nearly the same level of cations. But the primary effluent had a very high DOC concentration compared to the other two wastewaters. And the 2.5-mM NaCl solution has an electrical conductivity close to the wastewater samples. It was used as a reference sample to compare the aggregation behavior of nC_{60} in the presence/absence of dissolved organic matter in wastewater.

Table 4. 1. 1 Properties of water samples used in this study

Water sample	Chemical composition (mg/L)											DOC (mg/L)	pH	Electrical conductivity (mS/cm)	Ionic strength (*I*)
	Cl^-	NO_3^-	NO_2^-	SO_4^{2-}	HCO_3^-	PO_4^{3-}	Na^+	K^+	Mg^{2+}	Ca^{2+}	Al^{3+}				
Primary effluent	36.34	N.D.[a]	0.06	22.73	75.20	4.63	34.23	8.77	3.17	16.40	N.D.[b]	26.9	7.6	0.51	3.8
Aeration tank liquor	36.57	24.50	0.60	32.37	22.27	0.57	34.20	8.40	3.03	17.33	N.D.[b]	5.8	7.3	0.37	3.6
Secondary effluent	36.77	24.60	0.06	37.43	14.57	0.30	29.60	7.93	2.80	16.87	N.D.[b]	3.4	6.8	0.37	3.5
2.5-mM NaCl solution	–	–	–	–	–	–	–	–	–	–		–	5.6	0.35	2.5

N.D.[a]: not detected (detection limit: 0.2 mg/L)

N.D.[b]: not detected (detection limit: 0.1 mg/L)

–: not measured

4.1.3.2 Determination of nC_{60} spike concentration for aggregation studies

The derived count rate (DCR) with the unit of kilo counts per second (kcps) is the scattering intensity measured by the Zetasizer Nano ZS analyzer. The DCR is fairly stable for a sample with stable size over time and then may be used to determine the relative concentration of particles. Detailed information was shown in Chapter III. Matrix particles in 1.0-µm-filtered primary effluent were measured to be 2674 kcps in DCR (**Table 4.1.2**). The DCR of total particles (nC_{60} + matrix particles) increased and the size decreased as the nC_{60} concentration in 1.0-µm primary effluent increased (**Fig. 4.1.2**). At the spike level of 1 mg/L, the DCR of nC_{60} was around 10 times higher than that of the matrix particles, and the size of total particles stabilized at close to the nC_{60} size in Milli-Q water. Therefore, the effect of matrix particles could be ignored at such a high nC_{60} level. On the other hand, the DCR of matrix particles in wastewater samples under all experimental conditions did not exceed 2386 kcps, which was less than the value of 1.0-µm-filtered primary effluent (**Table 4.1.2**). Therefore, a spike level of 1 mg/L was used in all experiments, and the size of total particles in wastewater was reported as the nC_{60} size.

Table 4. 1. 2 Derived count rate of matrix particles in 0.45-μm-filtered wastewater samples as a function of pH and ionic strength after 1-h mixture, and in 1.0-μm-filtered primary effluent

Water sample	Filtration	Derived count rate (kcps)										
		pH					Added ionic strength (mM NaCl)					
		3	5	7	9	11	0	2.5	10	50	100	500
Secondary effluent		52	53	53	51	77	53	51	53	51	51	58
Aeration tank liquor	Filtration with 0.45 μm	88	75	80	87	221	80	79	83	80	76	78
Primary effluent		2000	1063	971	1002	2386	971	991	991	943	962	978
Primary effluent	Filtration with 1.0 μm			2674								

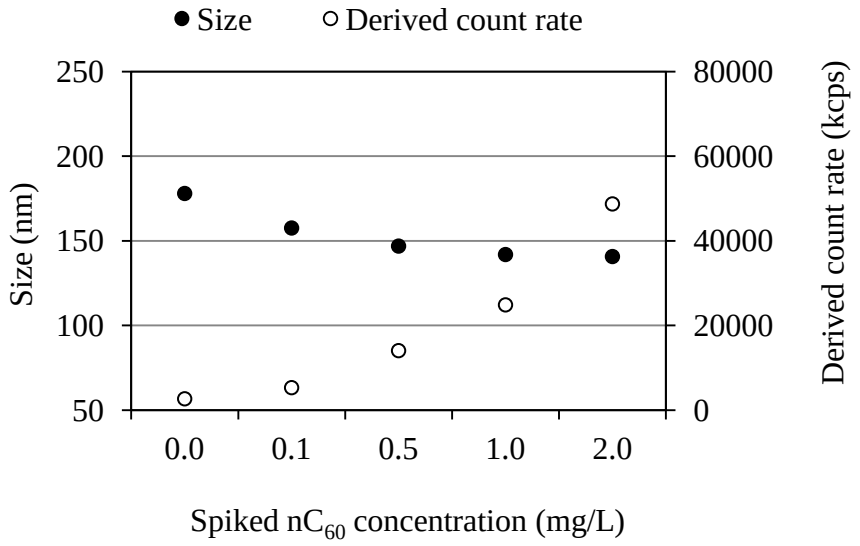

Fig. 4. 1. 2 Derived count rate and size of total particles (nC_{60} + matrix particles) in 1.0-μm-filtrated primary effluent as a function of spiked concentration.

4.1.3.3 Time profile of nC_{60} aggregation in wastewater

nC_{60} remained relatively stable without significant change in size up to 24 h in the reference NaCl solution and wastewater (**Fig. 4.1.3**). It suggested the potential of nC_{60} discharge with the treated wastewater and also subsequent long transport in the aquatic environment. The ζ potential of nC_{60} was −55 mV in 2.5-mM NaCl solution but only a mean value of −28 mV in wastewater (**Fig. 4.1.4**). As shown in **Table 4.1.1**, the wastewater samples had a mean value of 0.55 mM divalent (Mg^{2+} + Ca^{2+}) and 1.64 mM monovalent (Na^{+} + K^{+}) cations which might contribute to the reduction of absolute ζ potential. Zhang et al. (2008) found the stronger effects of divalent cations than monovalent ones on ζ potential of CdTe quantum dots nanoparticles in water. Also, Chen and Elimelech (2006) reported the nC_{60} had a much lower critical coagulation concentrations for Ca^{2+} (4.8 mM) than that for Na^{+} (120 mM). Therefore, the existing divalent cations in wastewater could efficiently reduce the ζ potential of nC_{60}. Even though no clear standard relates the ζ potential value to particle stability, the colloid system is considered to be unstable at a ζ potential of <20 mV. For all water samples,

the absolute ζ potential of nC_{60} was higher than 20 mV which could partially explain their stability in water up to 24 h. In addition, the dissolved organic matter in wastewater might contribute to the nC_{60}'s stability even at low absolute ζ potential compared to that in 2.5-mM NaCl solution. This part will be discussed in following section.

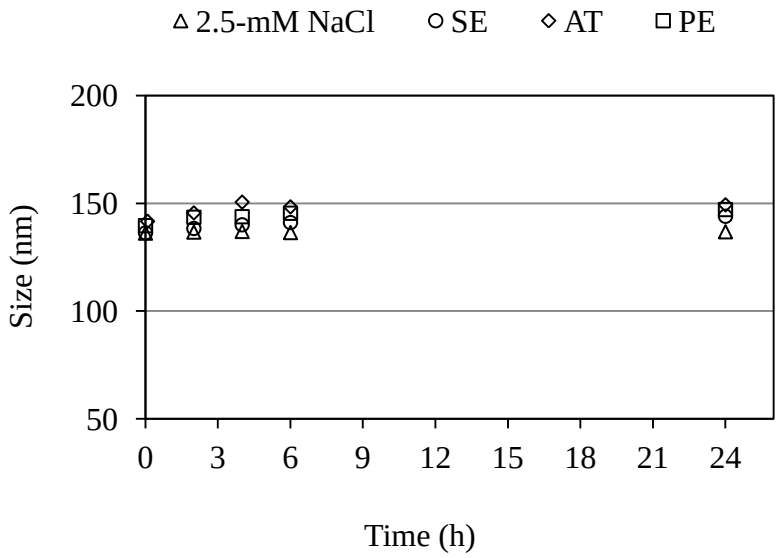

Fig. 4. 1. 3 Time profile of nC_{60} aggregation in water samples.
PE: primary effluent; AT: aeration tank liquor; SE: secondary effluent

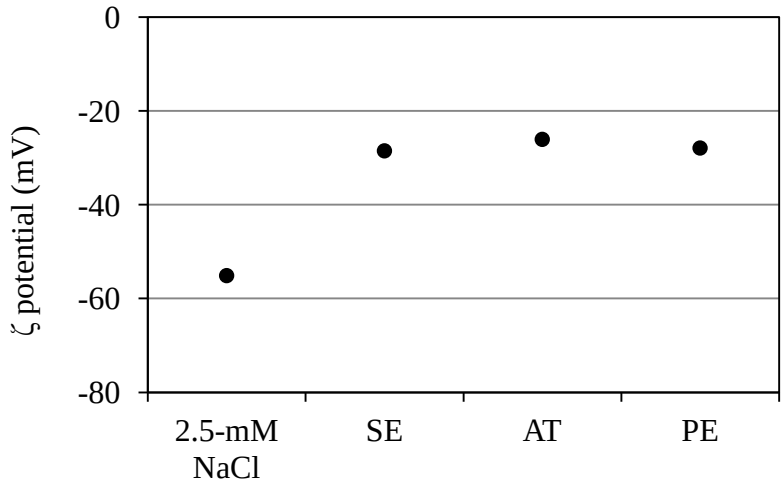

Fig. 4. 1. 4 ζ potential of nC_{60} in water samples.
PE: primary effluent; AT: aeration tank liquor; SE: secondary effluent

4.1.3.4 Aggregation of nC_{60} in wastewater

Effect of ionic strength on size and ζ potential

The nC_{60} retained its initial size at an added ionic strength of ≤50 mM, but obvious aggregation occurred in all the samples at ≥100 mM NaCl after 1 h (**Fig. 4.1.5**), which is comparable to the reported threshold destabilization concentration of ~120 mM for nC_{60} in pure water (Chen and Elimelech, 2006). The nC_{60} in Milli-Q water were obviously bigger than those in wastewater samples at 100 and 500 mM. At 500 mM, the size decreased in the order of Milli-Q > SE > AT > PE, opposite to the DOC concentration **(Table 4.1.1)**. In all samples, the size distribution became wider and the peak shifted to a bigger size as the ionic strength increased (**Fig. 4.1.6**).

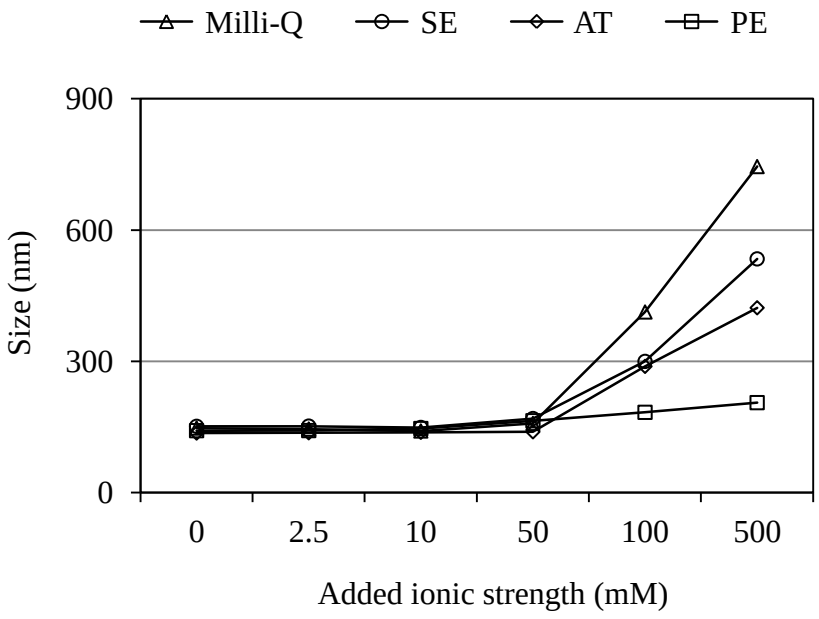

Fig. 4. 1. 5 nC_{60} size in water samples as a function of ionic strength after 1-h mixture.

PE: primary effluent; AT: aeration tank liquor; SE: secondary effluent

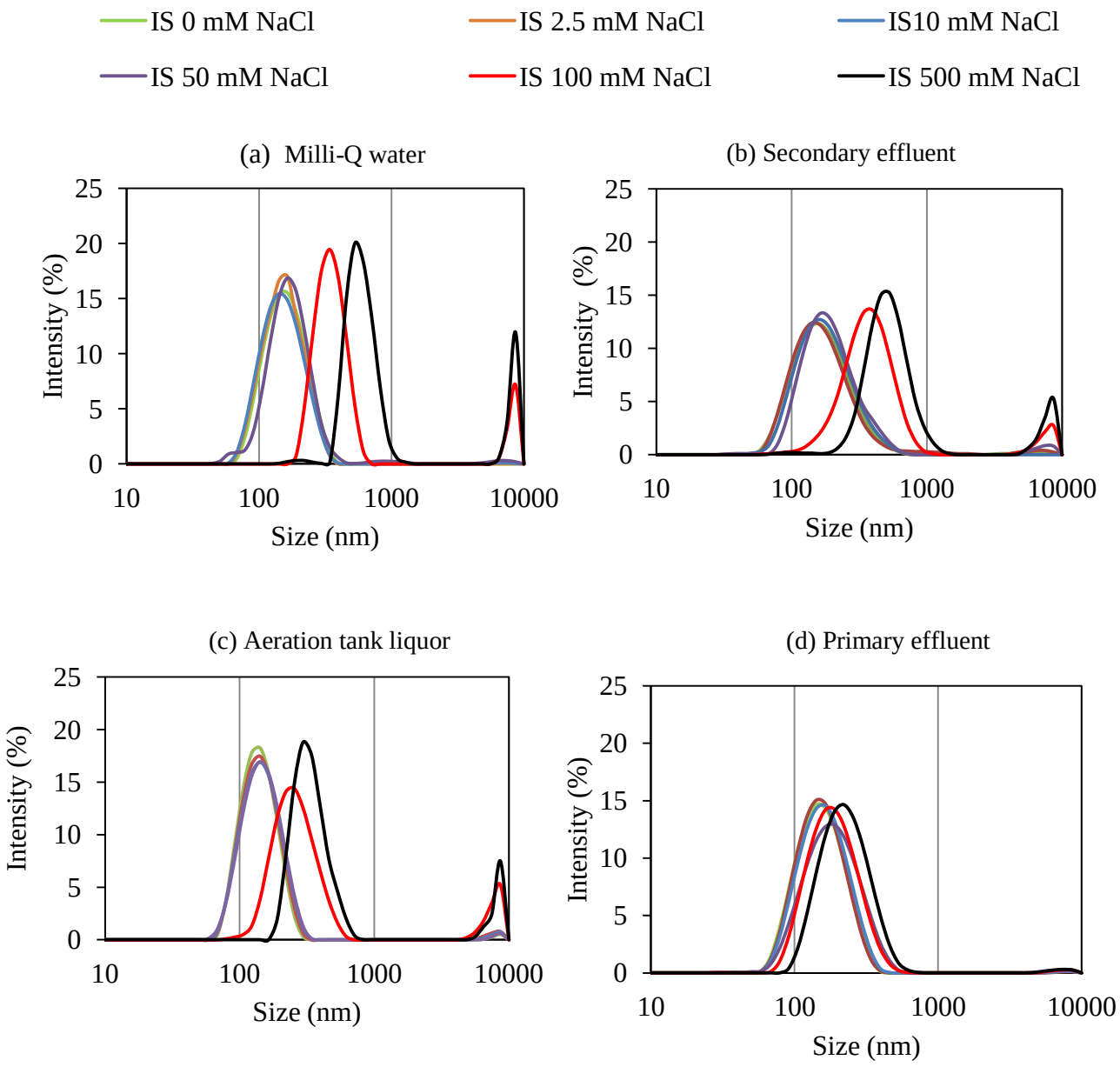

Fig. 4. 1. 6 Size distribution of nC_{60} in (a) Milli-Q water, (b) secondary effluent, (c) aeration tank liquor, and (d) primary effluent as a function of ionic strength (IS) after 1-h mixture.

In all the samples, the absolute ζ potential of nC_{60} decreased as the ionic strength increased (**Fig. 4.1.7)**. This decrease can be explained by the suppression of the electrical double layer and surface charge neutralization by the increased ionic strength (Brant et al., 2006; Zhang et al., 2008). The absolute ζ potential was >30 mV at 0–10 mM NaCl, but became ≲20 mV at 50–500 mM NaCl. At 500 mM NaCl, the ζ potential of nC_{60} in all samples was close to 0, indicating that the ionic strength was high enough to screen all surface charge. Yet despite the similar small values of ζ potential, the aggregation behavior differed widely (**Fig. 4.1.5)**, suggesting steric stabilization in addition to electrostatic stabilization.

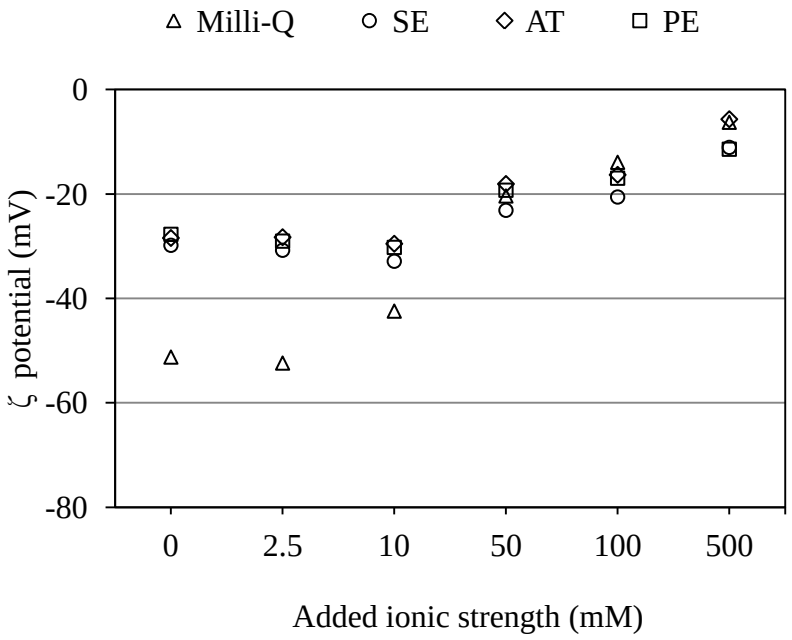

Fig. 4. 1. 7 ζ potential of nC_{60} in water samples as a function of ionic strength.
PE: primary effluent; AT: aeration tank liquor; SE: secondary effluent

Effect of pH on size and ζ potential

nC_{60} aggregates in all samples remained stable after 1 h at pH 5 to 11 (**Fig. 4.1.8**). At pH 3, however, sizes in wastewater increased to 2 to 3 times higher than that in 2.5 mM NaCl. In addition, aggregates were much larger in SE and AT than in PE at pH 3,

consistent with the results of nC_{60} aggregation with ionic strength (**Fig. 4.1.5**). The size distribution at different pH values was confirmed the nC_{60} aggregation at pH 3 by both shifting to a larger size and forming a second peak in the wastewater samples (**Fig. 4.1.9**).

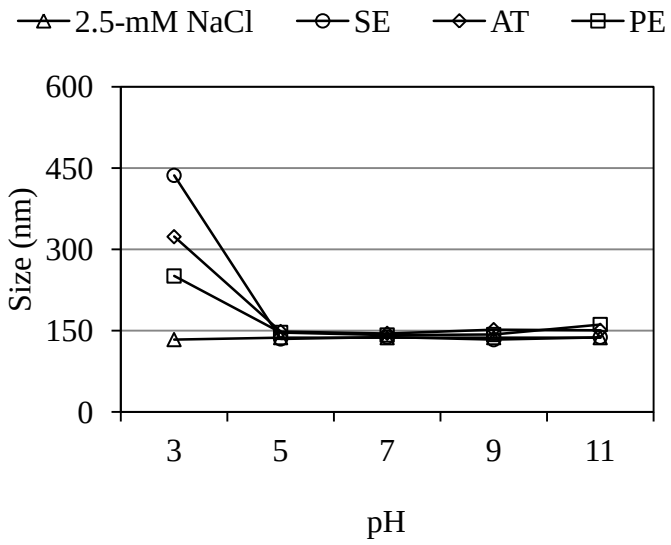

Fig. 4. 1. 8 nC_{60} size in water samples as a function of pH after 1-h mixture.

PE: primary effluent; AT: aeration tank liquor; SE: secondary effluent

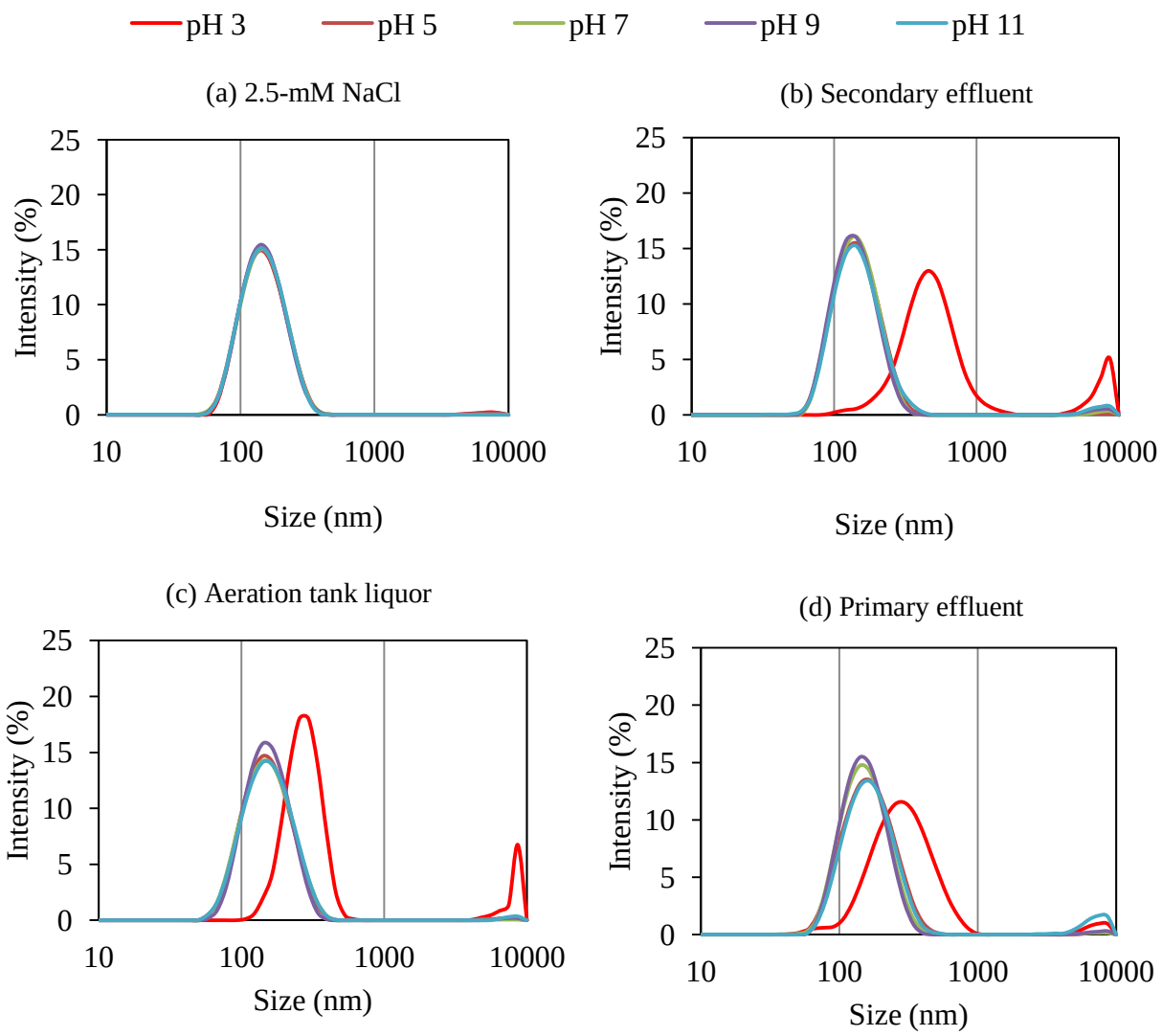

Fig. 4. 1. 9 Size distribution of nC_{60} in (a) 2.5-mM NaCl, (b) secondary effluent, (c) aeration tank liquor, and (d) primary effluent as a function of pH after 1-h mixture.

In all samples, the absolute ζ potential decreased as the pH decreased (**Fig. 4.1.10**). However, the decrease became more obvious under acidic condition indicating the neutralization reaction between the H^+ and acidic surface of nC_{60}. Andrievsky et al. (2002) proposed the hydrolysis complex structure of nC_{60} in water as $C_{60}\{mH_2O\cdot(nOH^-)\}^{n-}$. Compared to the nC_{60} in 2.5 mM NaCl solution, the pH (5−11) had moderate effect on ζ potential of nC_{60} in wastewater. It might be explained due to the lower absolute ζ potential of nC_{60} in wastewater because part of the surface charges has been already neutralized by the existing divalent and monovalent cations. In contrast, the absolute ζ potentials of nC_{60} in all samples were significantly decreased at pH 3 due to the high concentration of H^+. Among, it was <20 mV only at pH 3 in the wastewater samples; this result could partially explain the aggregate size increase (**Fig. 4.1.8**).

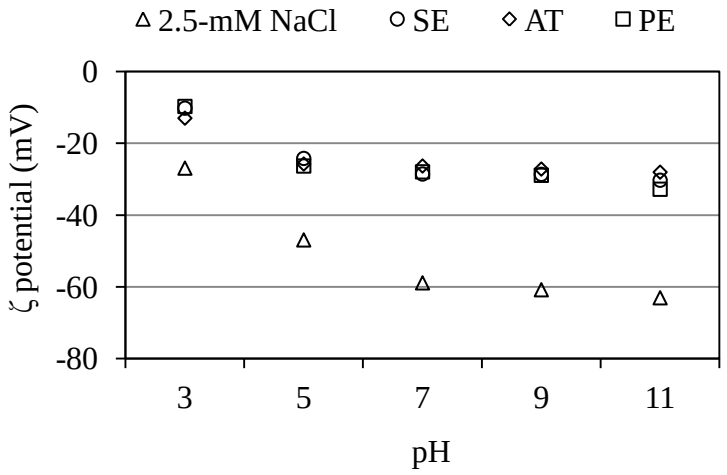

Fig. 4. 1. 10 ζ potential of nC_{60} in water samples as a function of pH.
PE: primary effluent; AT: aeration tank liquor; SE: secondary effluent

Effect of dissolved organic matter on size and ζ potential

Fig. 4.1.11 showed the aggregation kinetics of nC_{60} at different DOC concentrations under two levels of ionic strengths. The nC_{60} remained stable at all DOC concentrations without NaCl addition (**Fig. 4.1.11a**), and no effect of DOM was

observed on nC_{60} aggregation. However, the nC_{60} aggregation occurred in all water samples at 100 mM NaCl, and the aggregation rates of nC_{60} varied with the added DOM amounts (**Fig. 4.1.11b**). The aggregation rate decreased with the increase in DOC concentration, consistent with the results of nC_{60} aggregation behavior in the wastewater samples.

Without NaCl addition the absolute ζ potential of nC_{60} in DOM solutions was measured to ~50 mV (**Fig. 4.1.12a**) which was higher than those in wastewater samples (~30 mV, **Fig. 4.1.4 and 4.1.7**). This decrease indicated the strong effect of the existing cations in wastewater on ζ potential of nC_{60}. In addition, a significant increase in absolute ζ potential ($p = 0.023 < 0.050$) was observed at high DOC concentrations indicating the adsorption of DOM on nC_{60} aggregate. On the other hand, no significant change in ζ potential ($p = 0.245 > 0.050$) was observed at different DOC concentrations at 100 mM NaCl (**Fig. 4.1.12b**). Therefore, the decrease in aggregation rate at higher DOC concentrations would clearly be attributed to the steric effect due to the DOM since the charges have been effectively screened at such high NaCl concentrations. Similar results were also found in aggregation studies of titanium dioxide (Domingos et al., 2009; Thio et al., 2011), cerium dioxide nanoparticles (Li and Chen, 2012), and carbon nanotubes (Hyung et al., 2007), which remained dispersed in solution containing dissolved organic matter such as surfactants and natural organic matter even under high ionic strength. Recent studies also reported the natural organic matters (Suwannee River humic acid and fulvic acid) could enhance the C_{60} dispersion in the simulated natural water partially due to the steric hindrance effect (Chen and Elimelech, 2007; Li et al., 2009; Qu et al., 2010).

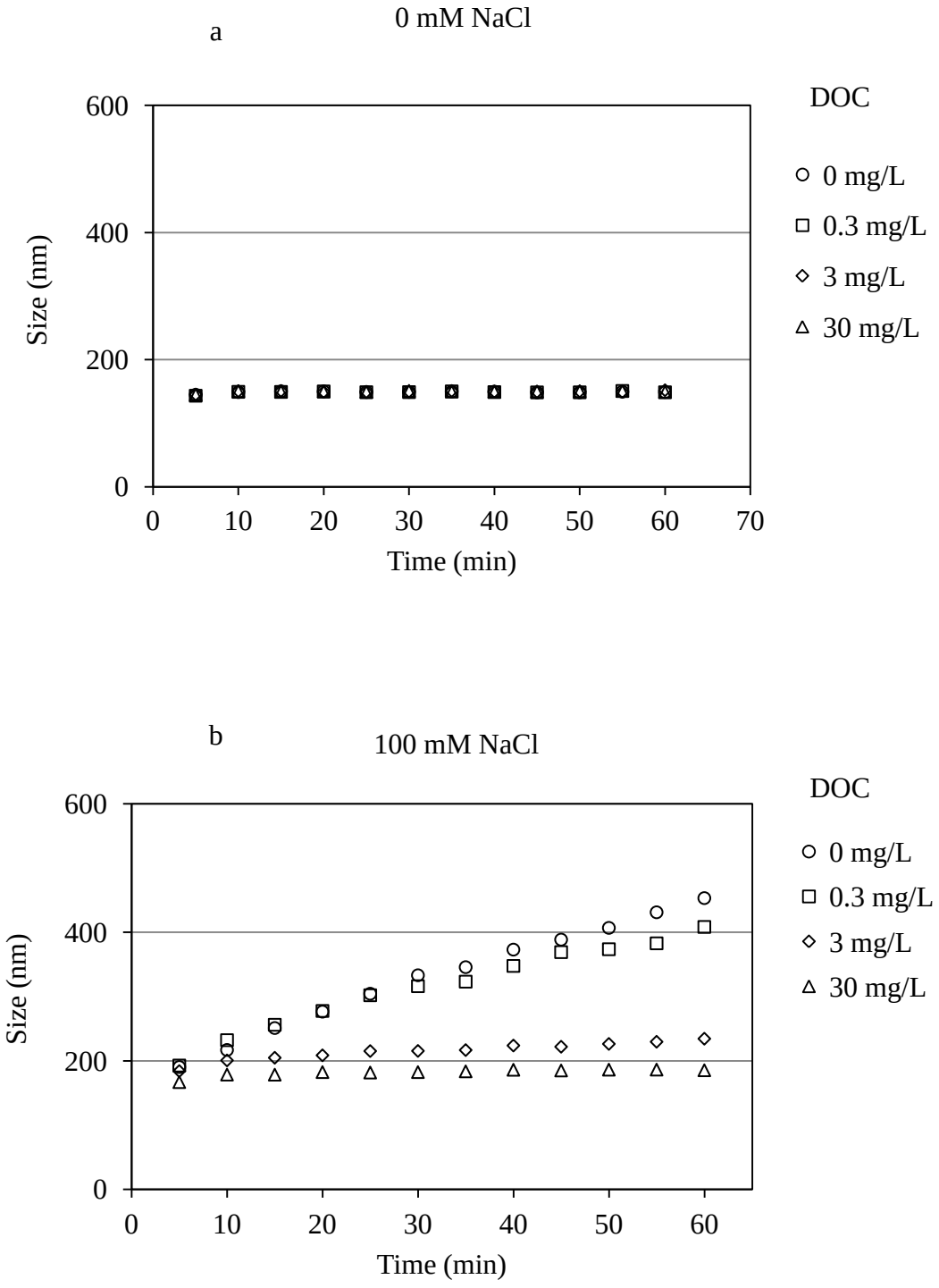

Fig. 4. 1. 11 Aggregation kinetics of nC_{60} with different DOC concentrations (a) without added NaCl and (b) with 100 mM NaCl.

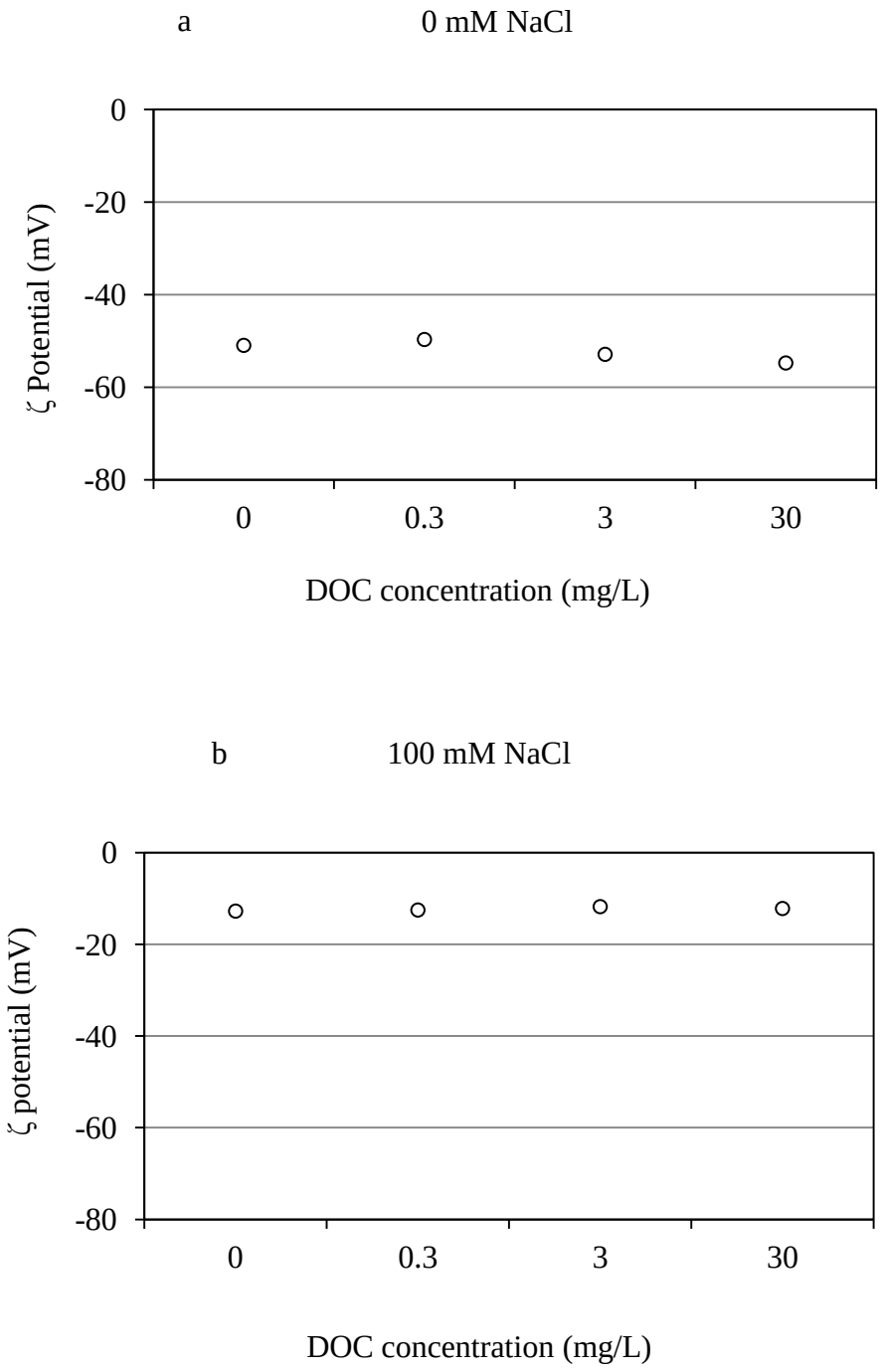

Fig. 4. 1. 12 ζ potential of nC_{60} over time with different DOC concentrations (a) without added NaCl and (b) with 100 mM NaCl.

4.1.4 Conclusions

The size aggregation of nC_{60} in wastewater could affect their fate during the wastewater treatment processes such as the conventional activated sludge treatment and membrane treatment. However, the aggregation behavior of nC_{60} in wastewater is still unclear. To our best knowledge, this study firstly investigated the aggregation behavior of nC_{60} in filtered wastewater. The effects of pH, ionic strength and DOM on nC_{60} aggregation were studied by measuring the size, size distribution and ζ potential. The main conclusions were as follows:

(1) The nC_{60} remained relatively stable up to 24 h under environmentally relevant values of ionic strength and pH. This finding suggested the potential for nC_{60} discharge from wastewater treatment plants in effluent and subsequent long-distance transport in water environment.

(2) At high ionic strength (>100 mM) or under acidic conditions (pH 3), such as the conditions found in seawater or industrial wastewater, the absolute ζ potential of the nC_{60} was reduced to ≲20 mV from an initial ~30 mV, increasing the size of aggregates up to the micrometer scale.

(3) The nC_{60} aggregation behavior varied among wastewater samples. Compared with the aggregation behavior in the filtered secondary effluent and aeration tank liquor, that in the filtered primary effluent was obviously inhibited. The aggregation rate of nC_{60} greatly varied with the DOM amounts in water even at nearly the same ζ potential. This result clearly indicated the steric stabilization on the nC_{60} aggregation due to the DOM isolated from wastewater, in addition to electrostatic effect.

(4) These results showed the aquatic conditions could affect the size and aggregation behavior of nC_{60} in wastewater which might consequently influence their fate during the wastewater treatment process. In addition, the results also suggested the treatment performance of nC_{60} by membrane filtration could be improved by adjustments to pH values.

4.1.5 References

Abdessemed, D., Nezzal, G., 2003. Treatment of primary effluent by coagulation-adsorption-ultrafiltration for reuse. Desalination 152 (1-3), 367–373.

Andrievsky, G.V., Klochkov, V.K., Bordyuh, A.B., Dovbeshko, G.I., 2002. Comparative analysis of two aqueous-colloidal solutions of C_{60} fullerene with help of FTIR reflectance and UV-Vis spectroscopy. Chemical Physics Letters 364 (1-2), 8–17.

Brant, J.A., Labille, J., Bottero, J.Y., Wiesner, M.R., 2006. Characterizing the impact of preparation method on fullerene cluster structure and chemistry. Langmuir 22 (8), 3878–3885.

Brar, S.K., Verma, M., Tyagi, R.D., Surampalli, R.Y., 2010. Engineered nanoparticles in wastewater and wastewater sludge - Evidence and impacts. Waste Management 30 (3), 504–520.

Chen, K.L., Elimelech, M., 2006. Aggregation and deposition kinetics of fullerene (C_{60}) nanoparticles. Langmuir 22 (26), 10994–11001.

Chen, K.L., Elimelech, M., 2007. Influence of humic acid on the aggregation kinetics of fullerene (C_{60}) nanoparticles in monovalent and divalent electrolyte solutions. Journal of Colloid and Interface Science 309 (1), 126–134.

Domingos, R.F., Tufenkji, N., Wilkinson, K.J., 2009. Aggregation of titanium dioxide nanoparticles: role of a fulvic acid. Environmental Science & Technology 43 (5), 1282–1286.

French, R.A., Jacobson, A.R., Kim, B., Isley, S.L., Penn, R.L., Baveye, P.C., 2009. Influence of ionic strength, pH, and cation valence on aggregation kinetics of titanium dioxide nanoparticles. Environmental Science & Technology 43 (5), 1354–1359.

Gomez-Rivera, F., Field, J.A., Brown, D., Sierra-Alvarez, R., 2012. Fate of cerium dioxide (CeO_2) nanoparticles in municipal wastewater during activated sludge treatment. Bioresource Technology 108, 300–304.

Gottschalk, F., Sonderer, T., Scholz, R.W., Nowack, B., 2009. Modeled environmental concentrations of engineered nanomaterials (TiO_2, ZnO, Ag, CNT, Fullerenes) for different regions. Environmental Science & Technology 43 (24), 9216–9222.

Hyung, H., Fortner, J.D., Hughes, J.B., Kim, J.H., 2007. Natural organic matter stabilizes carbon nanotubes in the aqueous phase. Environmental Science & Technology 41 (1), 179–184.

Kim, S.L., Chen, J.P., Ting, Y.P., 2002. Study on feed pretreatment for membrane filtration of secondary effluent. Separation and Purification Technology 29 (2), 171–179.

Kiser, M. a, Ryu, H., Jang, H., Hristovski, K., Westerhoff, P., 2010. Biosorption of nanoparticles to heterotrophic wastewater biomass. Water research 44 (14), 4105–4114.

Kuo, D.H.W., Simmons, F.J., Blair, S., Hart, E., Rose, J.B., Xagoraraki, I., 2010. Assessment of human adenovirus removal in a full-scale membrane bioreactor treating municipal wastewater. Water Research 44 (5), 1520–1530.

Lee, C.W., Bae, S.D., Han, S.W., Kang, L.S., 2007. Application of ultrafiltration hybrid membrane processes for reuse of secondary effluent. Desalination 202 (1-3), 239–246.

Li, K.G., Chen, Y.S., 2012. Effect of natural organic matter on the aggregation kinetics of CeO_2 nanoparticles in KCl and $CaCl_2$ solutions: Measurements and modeling. Journal of Hazardous Materials 209, 264–270.

Li, Q., Xie, B., Hwang, Y.S., Xu, Y., 2009. Kinetics of C_{60} fullerene dispersion in water enhanced by natural organic matter and sunlight. Environmental science & technology 43 (10), 3574–3579.

Murayama, H., Tomonoh, S., Alford, J.M., Karpuk, M.E., 2004. Fullerene production in tons and more: From science to industry. Fullerenes Nanotubes and Carbon Nanostructures 12 (1-2), 1–9.

Qu, X.L., Hwang, Y.S., Alvarez, P.J.J., Bouchard, D., Li, Q.L., 2010. UV irradiation and humic acid mediate aggregation of aqueous fullerene (nC_{60}) nanoparticles. Environmental Science & Technology 44 (20), 7821–7826.

Radjenovic, J., Petrovic, M., Barcelo, D., 2009. Fate and distribution of pharmaceuticals in wastewater and sewage sludge of the conventional activated sludge (CAS) and advanced membrane bioreactor (MBR) treatment. Water Research 43 (3), 831–841.

Thio, B.J.R., Zhou, D.X., Keller, A.A., 2011. Influence of natural organic matter on the aggregation and deposition of titanium dioxide nanoparticles. Journal of Hazardous Materials 189 (1-2), 556–563.

Wang, X.D., Wang, L., Liu, Y., Duan, W.S., 2005. Ozonation pretreatment for ultrafiltration of the secondary effluent. future of urban wastewater systems-Decentralisation and Reuse 529–537.

Zhang, Y., Chen, Y.S., Westerhoff, P., Crittenden, J.C., 2008. Stability and removal of water soluble CdTe quantum dots in water. Environmental Science & Technology 42 (1), 321–325.

4.2 Adsorption behavior of nC_{60} on different wastewater sludges

4.2.1 Introduction

Their growing production and use of fullerene C_{60} will inevitably result in the entry of fullerenes into the environment, raising recent concerns about environmental risks and human health (Oberdorster et al., 2006; Isaacson et al., 2009; Kang et al., 2009). The extremely low solubility (7.96 ng/L) and high hydrophobicity (log K_{ow} 6.67) of C_{60} molecules once assumed little chance of transport into aquatic environments and consequent limited risk to humans (Jafvert and Kulkarni, 2008). However, recent studies showed C_{60} molecules can form stable nanoscale colloidal aggregates (nC_{60}) in water with concentrations at mg/L level via solvent exchange and/or sonication treatment (Deguchi et al., 2001; Fortner et al., 2005; Chen et al., 2008; Qu et al., 2010a), as well as the environmental conditions such as extended mixing (Lyon et al., 2006; Hyung and Kim, 2009; Ma and Bouchard, 2009).

Once the nC_{60} enter into the wastewater during the production and the consumption processes, the wastewater treatment plant would be an important route for their discharge into the water environment. C_{60} has been detected in the commercial cosmetics ranging from 0.04 to 1.1 μg/g (Benn et al., 2011) and <0.005% (w/w) (Chae et al., 2010) which suggesting the potential pathway of C_{60} from consumer products to the wastewater streams. Farre et al. (2010) firstly reported the nC_{60} concentration up to ~20 μg/L in the suspended solids of the wastewater effluents. And the nC_{60} concentration in the treated wastewater was estimated to be several ng/L level based on a probabilistic material flow analysis from a life cycle perspective in the US and Europe (Gottschalk et al., 2009). However, very few studies have examined the fate of nC_{60} during wastewater treatment. It is still not clear about whether the conventional activated sludge process could efficiently removal the nC_{60} or not. No biodegradation was found in either aerobic (Kummerer et al., 2011) or anaerobic systems (Hartmann et al., 2011). Given the low solubility and high hydrophobicity for the nC_{60}, the adsorption on the sludge could play an important role in the fate and removal of nC_{60} during the

wastewater treatment process. Until now, the mechanisms of nC_{60} adsorption on sludge and their influencing factors during the wastewater treatment process are still unclear.

The objective of this part was to investigate the behavior and mechanism of nC_{60} adsorption on different sludges (the primary and activated sludges) in the wastewater treatment process. There were mainly three parts. For the first part, the adsorption kinetics and equilibrium of nC_{60} on the primary sludge were investigated. For the second part, the adsorption kinetics and equilibrium of nC_{60} on the activated sludge were investigated, as well as the effect of mixed liquor suspended solids (MLSS), temperature, pH, and ionic strength. For the third part, six activated sludge samples were collected in the aerobic tank from several wastewater treatment plants which were running under different operational conditions. The adsorption kinetics and equilibrium of nC_{60} on those six types of activated sludges were investigated. The adsorption isotherm and kinetics coefficients were obtained by modeling the experimental data using the associated models. The adsorption mechanisms were evaluated by correlating the adsorption coefficients and the characteristics of activated sludge and nC_{60}. The contents of this part were shown in **Fig. 4.2.1.**

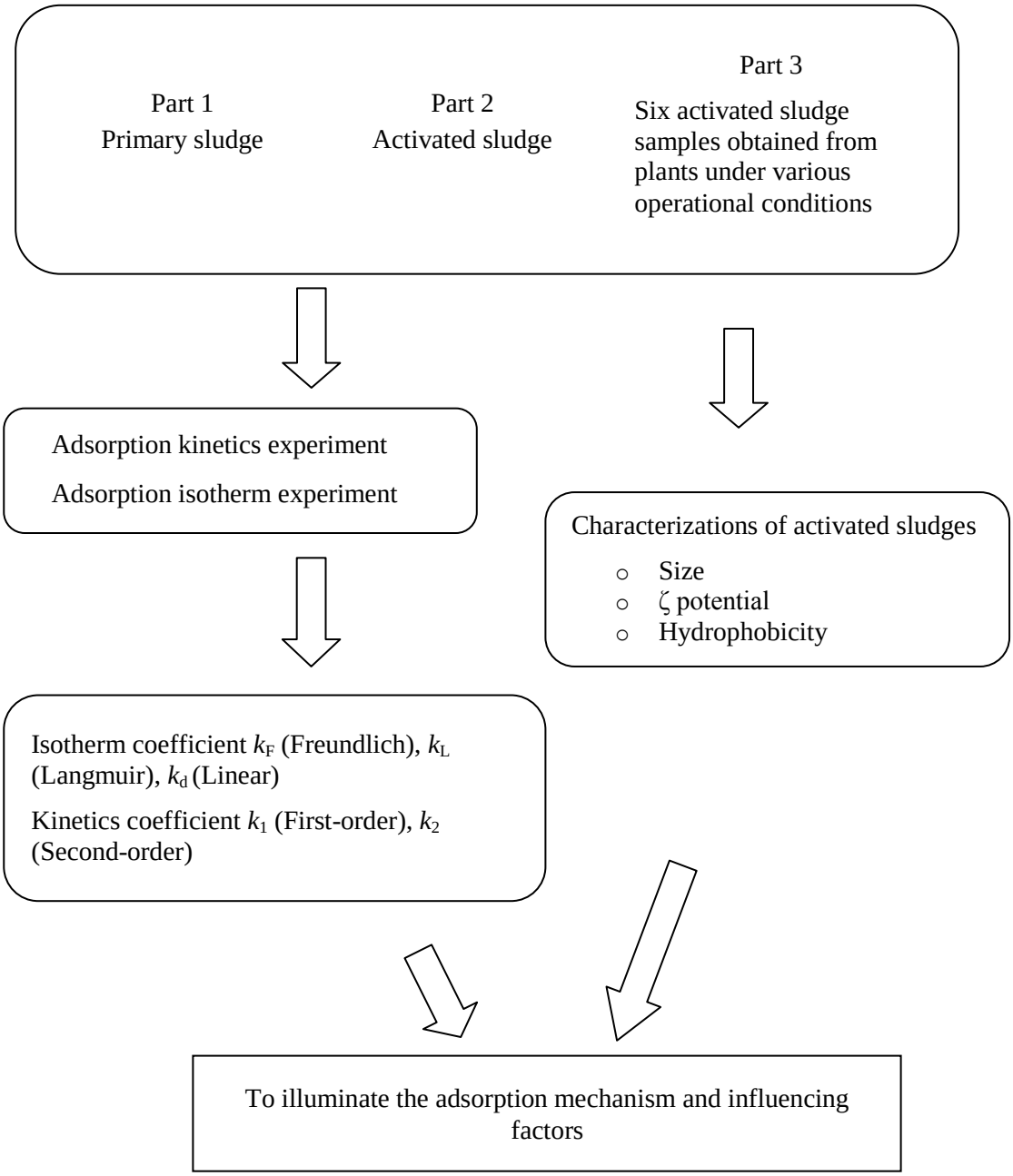

Fig.4. 2. 1 The content structure of this part.

4.2.2 Materials and methods

4.2.2.1 Preparation of nC_{60} aqueous suspension

nC_{60} suspension was prepared according to the toluene-based solvent exchange method. The nC_{60} concentration in prepared suspension was determined by extracting C_{60} into the toluene phase and quantifying it at 332 nm by UV/vis spectrometer. The detailed methods for preparation and quantification were described in Chapter III.

4.2.2.2 Sampling and sample preparation

There were three parts in this study as shown in **Fig. 4.2.1**. For the first and second parts, the primary effluent, primary sludge, and activated sludge were collected from the WWTP A, in Japan as shown in **Table 4.2.1**. The primary effluent was filtered through a glass fiber filter (1.0 μm pore size; GF/B, Whatman, Germany) and adjusted to pH 7 with dilute NaOH or HCl solution. The sludge samples were washed in filtered primary effluent and centrifuged at 2000 ×g for 5 min. The pellet was washed and centrifuged twice more. After the last centrifugation, it was suspended in filtered primary effluent to an MLSS level of 6000 mg/L and stored at 4 °C. The liquid was diluted to the required MLSS level with filtered primary effluent just before the adsorption experiments. The activated sludge was not inactivated, because nC_{60} is not biodegraded (Nyberg et al., 2008; Hartmann et al., 2011; Kummerer et al., 2011).

For the third part, six activated sludge samples were collected in the aeration tank from five WWTPs under different operational conditions in the Kansai area, Japan. The samples were stored and transported in amber glass bottles at temperature of < 4 °C in the cooler box. The key information of operation conditions in five plants were showed in **Table 4.2.1**. Two plants are applying the anaerobic oxic process and anoxic oxic process, respectively, while the others are applying conventional activated sludge treatment process. They had a DO concentration ranged from 2.0 to 5.5 mg/L, SRT from 4.2 to 31.3 days, HRT from 4.9 to 11 h, and MLSS concentration from 870 to 2790 mg/L. In other to reduce the effect of wastewater matrices on the uncertainty of adsorption process, the buffer solution was used in adsorption experiment instead of

filtrated primary effluent for the studies in the first and second parts. The activated sludge was rinsed with buffer solution (2.5 mM NaCl, 0.5 mM $NaHCO_3$, adjusted to pH 7 using dilute HCl and NaOH). After three times of washing, the resulted sludge was suspended in the buffer solution and stored at 4 °C. Before the experiment, the activated sludge suspensions were diluted to determined concentration by the buffer solution.

Table 4. 2. 1 The information of sludge samples and the operational conditions in WWTPs

Sample name	WWTP	Sampling point	Sludge type	Treatment process	Operational conditions				
					Influent (m^3/day)	HRT (h)	SRT (day)	MLSS (mg/L)	DO (mg/L)
A-primary sludge	A	Excess sludge	Primary sludge	–	–	–	–	–	–
A-activated sludge		Aeration tank	Activated sludge	CAS	–	–	–	2570	–
B	B	Aeration tank	Activated sludge	AO[a]	77770	6.3	4.5	1630	5.0
C	C			AO[b]	25864	6.2	7.4	2220	3.6
D	D			CAS	126980	7.6	4.2	616	4.2
A2	A			CAS	19990	5.7	31.3	2790	2.0
E1	E			CAS	39290	10	15	870	3.6
E2				CAS	39190	11	16	1280	4.4

AO[a]: Anaerobic oxic treatment process

AO[b]: Anoxic oxic treatment process

CAS: conventional activated sludge treatment process

–: no data

4.2.2.3 Adsorption kinetics and isotherm experiments

For the kinetics and isotherm studies, 100-mL Erlenmeyer flasks containing 50 mL solution at 1000 mg/L MLSS were agitated on a rotary shaker (125 rpm) at room temperature (25 °C). For the kinetics study, the initial nC_{60} concentrations were 0.100, 0.300, and 0.500 mg/L. Samples were collected at various time intervals and were centrifuged at 2000 ×g for 5 min, and the supernatant was collected (5 mL) for nC_{60} quantification. For the adsorption isotherm experiments, the initial nC_{60} concentrations were 0.050, 0.100, 0.200, 0.350, and 0.500 mg/L. From the results of the kinetics studies, 12 h was chosen as the equilibrium time in the isotherm experiments. After the equilibrium time, the samples were collected and centrifuged as above. The nC_{60} in supernatant was extracted using toluene and then analyzed by a high-performance liquid chromatography (HPLC) system equipped with a UV/vis detector (LC-10AD, Shimadzu, Japan), as described in Chapter III. Reference samples without activated sludge were analyzed so the nC_{60} losses such as by adsorption to glassware could be subtracted. Adsorption to activated sludge was calculated from the mass balance of the nC_{60} concentrations between the experimental and reference samples:

$$q_{\mathrm{t}} = \frac{C_{(ref,\ t)} - C_{(exp,\ t)}}{MLVSS} \qquad (4.2.1)$$

where q_{t} is the nC_{60} adsorbed on the activated sludge at time t (mg/g MLVSS), C(ref, t) is the nC_{60} concentration in the aqueous phase in reference samples at time t (mg/L), C(exp, t) is that in experimental samples at time t (mg/L), and MLVSS is the mixed liquor suspended solids concentration in the flask (g/L). The adsorption data in this study were all normalized into adsorbed amount per gram MLVSS.

4.2.2.4 Factors affecting the adsorption of nC_{60} on activated sludge

Batch experiments were conducted to study the effects of MLSS concentration, temperature, pH, and ionic strength on the adsorption of nC_{60} on the activated sludge. The experimental design was shown in **Table 4.2.2.**

Table 4. 2. 2 Experimental conditions for the studies of influencing factors on nC_{60} adsorption on the activated sludge

Experiments	nC_{60} (mg/L)	Temperature (°C)	MLSS (mg/L)	pH	Added ionic strength (mM NaCl)	Mixture time (h)
MLSS	0.200	25	50–4000	7	not adjusted	1
Temperature		15–35	1000	7	not adjusted	
pH		25	1000	3–11	not adjusted	
Ionic strength		25	1000	7	0–500	

4.2.2.5 nC_{60} quantification in wastewater and other measurements

The nC_{60} in wastewater was extracted using toluene and analyzed using the HPLC-UV/vis system, as described in Chapter III. The dissolved organic carbon concentration in the wastewater was measured with a TOC 5000A analyzer (Shimadzu, Japan). The hydrodynamic diameter and size distribution of nC_{60} were determined by dynamic light scattering at a detection angle of 173° in a Zetasizer Nano ZS size meter equipped with a 633-nm laser (Malvern Instruments, UK). The electrophoretic mobility of nC_{60} and activated sludge were measured with the Zetasizer and used to calculate the zeta (ζ) potential by the Smoluchowski equation (Hunter, 1988). The size of sludges was measured using the SALD-2100 Laser diffraction particle size analyzer (Shimadzu, Japan). The MLVSS, MLSS and SVI of sludge were determined according to the standard method (APHA, 1999). And the relative hydrophobicity of sludge was determined by previously reported method with minor modification (Rosenberg, 1984). In brief, a 5.0 mL sample was placed into a glass test tube and homogenized for 1 min using a vortex mixer and the absorbance at 400 nm (A_0) was measured using the UV-2500 spectrometer (Shimadzu, Japan). And then 2 mL of hexadecane was added to the test tube and the sludge hexadecane mixture was thoroughly agitated for 5 min. and then the hexadecane solvent and aqueous phase were separated by settlement for 30 min.

The absorbance of the aqueous phase at 400 nm was measured (*A*). The relative hydrophobicity (*RH*) of sludge was calculated as follows:

$$RH(\%) = \frac{A_0 - A}{A_0} \quad (4.2.2)$$

4.2.2.6 Model theories

Adsorption kinetics

To understand the mechanism of adsorption, the experimental data were fitted using the pseudo-first-order and pseudo-second-order models.

Pseudo-first-order model

The pseudo-first-order model was suggested by (Lagergren, 1898) and used for the solid/liquid systems in many studies (Chiron et al., 2003; Senthilkumaar et al., 2005; Kumar and Gayathri, 2009). The equation is given as:

$$\frac{\mathrm{d}q_t}{\mathrm{d}t} = \mathrm{k}_1 (q_\mathrm{e} - q_\mathrm{t}) \quad (4.2.3)$$

where q_t (mg/g MLVSS) and q_e (mg/g MLVSS) are the amounts of nC_{60} adsorbed on activated sludge at time *t* (h) and at equilibrium, respectively; and k_1 (1/h) is the rate constant of pseudo-first-order adsorption. Under the boundary condition q_t=0 at *t*=0, Eq.(2) becomes linear:

$$\ln (q_\mathrm{e} - q_\mathrm{t}) = \ln q_\mathrm{e} - \mathrm{k}_1 t \quad (4.2.4)$$

where q_e and k_1 can be determined from the slope and intercept by plotting $\ln(q_\mathrm{e}-q_\mathrm{t})$ versus *t*.

Pseudo-second-order model

The pseudo-second-order model could well fit the adsorption process the dominant sorption mechanism of which is chemisorptions (Ho, 2006). It has been applied for

modeling the adsorption on the activated sludge such as the endocrine disrupting chemicals (Feng et al., 2010) and surfactants (Ren et al., 2011). The pseudo-second-order model is given as (Ho and Mckay, 1998):

$$\frac{\mathrm{d}q_t}{\mathrm{d}t} = \mathrm{k}_2 (q_e - q_t)^2 \qquad (4.2.5)$$

where k_2 (g/(mg·h)) is the rate constant of pseudo-second-order adsorption. After integration, Eq.(4) becomes linear:

$$\frac{t}{q_t} = \frac{1}{\mathrm{k}_2 q_e^{\,2}} + \frac{1}{q_e} t \qquad (4.2.6)$$

where q_e and k_2 can be determined from the slope and intercept by plotting t/q_t versus t.

Adsorption isotherm

The experimental data were analyzed with Langmuir, Freundlich and linear partitioning models, which are most widely used for modeling the adsorption process.

Langmuir model

The Langmuir model assumes that the adsorption occurs on specific sites of the adsorbent surface in a monolayer (Langmuir, 1918). It describes the site-limited sorption on the adsorbents which have homogeneous surface sites and energies for the interacting with adsorbates (Huang et al., 2003). The linear form is given as:

$$\frac{C_e}{q_e} = \frac{1}{\mathrm{k}_L q_m} + \frac{1}{q_m} C_e \qquad (4.2.7)$$

where q_m (mg/g MLVSS) is the maximum adsorption capacity of nC_{60} on activated sludge, C_e (mg/L) is the nC_{60} concentration in the aqueous phase at equilibrium, and k_L is the Langmuir constant (L/mg). The values of k_L and q_m can be determined from the intercept and slope by plotting C_e/q_e versus C_e.

Freundlich model

The Freundlich model is an empirical relationship assuming that the adsorption process on the heterogeneous surface (Freundlich, 1906). The adsorption process occurs on the multilayer of adsorbents and these adsorption sites have different adsorption energies. The linear form is given as:

$$\ln q_e = \ln k_F + \frac{1}{n} \ln C_e \tag{4.2.8}$$

where k_F and n are Freundlich constants. And they can be determined from the intercept and slope by plotting ln q_e versus ln C_e.

Linear partitioning model

The linear partitioning model is based on the assumption that there is no limitation f adsorption sites or spaces to accommodate the adsorbates as the concentration of adsorbate increases (Chlou et al., 1983; Huang et al., 2003). The equation is given as,

$$q_e = k_d C_e \tag{4.2.9}$$

where k_d is the partitioning coefficients for adsorption on sludges. And it can be determined from the slopes by plotting q_e versus C_e.

4.2.3 Results and discussions

The results were discussed by two separate parts. The first one was to discuss the nC_{60} adsorption behavior on the primary and activated sludges according to the results from the first and second studies. And the second part was to discuss the adsorption mechanism on activated sludges according to the results from the third study.

4.2.3.1 nC_{60} adsorption behavior on the primary and activated sludge

Characterization of nC_{60} aqueous suspension and sludge samples

The nC_{60} had a negative charge in the range of pH studied. And the absolute values of ζ potential decreased with the decrease in pH from 11 to 1, with an isoelectric point around pH 1. Detailed information was shown in Chapter III.

The properties of primary and activated sludge used were shown in **Table 4.2.3**. By comparison, the primary sludge has higher absolute ζ potential, smaller size, and lower hydrophobicity than those of the activated sludge.

Table 4. 2. 3 Properties of primary and activated sludge used in this study

Sample	ζ potential (mV)	Size (μm)	Relative hydrophobicity (%)	MLVSS/MLSS (%)
A-primary sludge	-18.2±0.9	111.3±7.6	33.2±6.1	88.4±4.9
A-activated sludge	-12.5±1.7	139.0±17.0	74.6±5.6	75.3±0.1

Time profile of nC_{60} adsorption on the primary and activated sludge

At a lower initial nC_{60} concentration, the adsorption of nC_{60} on both the primary and activated sludge reached equilibrium sooner (**Fig. 4.2.2**) because of the relative abundance of adsorption sites available (Hanafiah et al., 2006). At all initial concentrations tested, the adsorption reached equilibrium after 12 h, so 12 h was used as the equilibrium time in the following adsorption isotherm experiments.

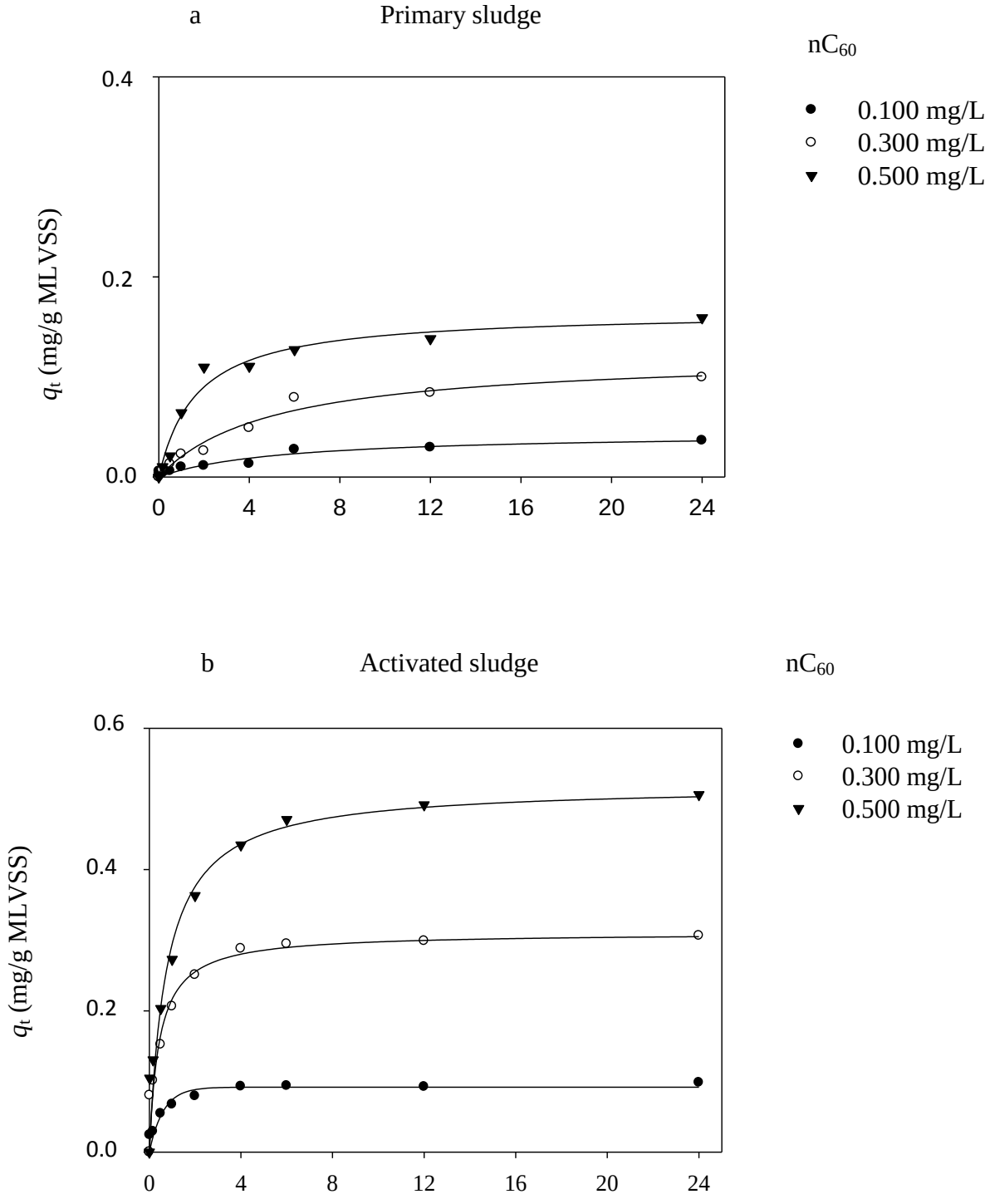

Fig.4. 2. 2 Time profile of nC_{60} adsorption on primary (a) and activated (b) sludge. The adsorbed amounts were normalized by the MLVSS concentration.

Adsorption kinetics

The adsorption kinetics at different initial concentrations on the primary sludge was fitted to pseudo-first-order and pseudo-second-order model (**Fig. 4.2.3**). Although no significant difference in correlation coefficients between the two models (**Table 4.2.4**), the calculated ($q_{e(cal)}$) values by the second-order model were very close to the observed ($q_{e(obs)}$) values indicating the nC_{60} adsorption on primary sludge better followed the second-order model. On the other hand, the data of nC_{60} adsorption on the activated sludge also fitted the second-order model much better than the first-order model based on the high correlation coefficient (> 0.99) and calculated ($q_{e(cal)}$) values (**Fig. 4.2.4 and Table 4.2.4**). It indicated the chemical adsorption played an important role in adsorption of nC_{60} on the wastewater sludges (Ho, 2006; Kililç et al., 2009). An interaction between the :OH on the surface of the nC_{60} aggregate (Andrievsky et al., 2002) and the functional groups on the wastewater sludge might contribute to the adsorption process by forming hydrogen bonds, which are intermediate in strength between van der Waals bonds and covalent bonds (Chang, 2000).

By comparison, the k_2 values (kinetic constant for pseudo second-order model) for the activated sludge was around two times as high as that for the primary sludge suggesting the adsorption rate on activated sludge was much faster than that on primary sludge.

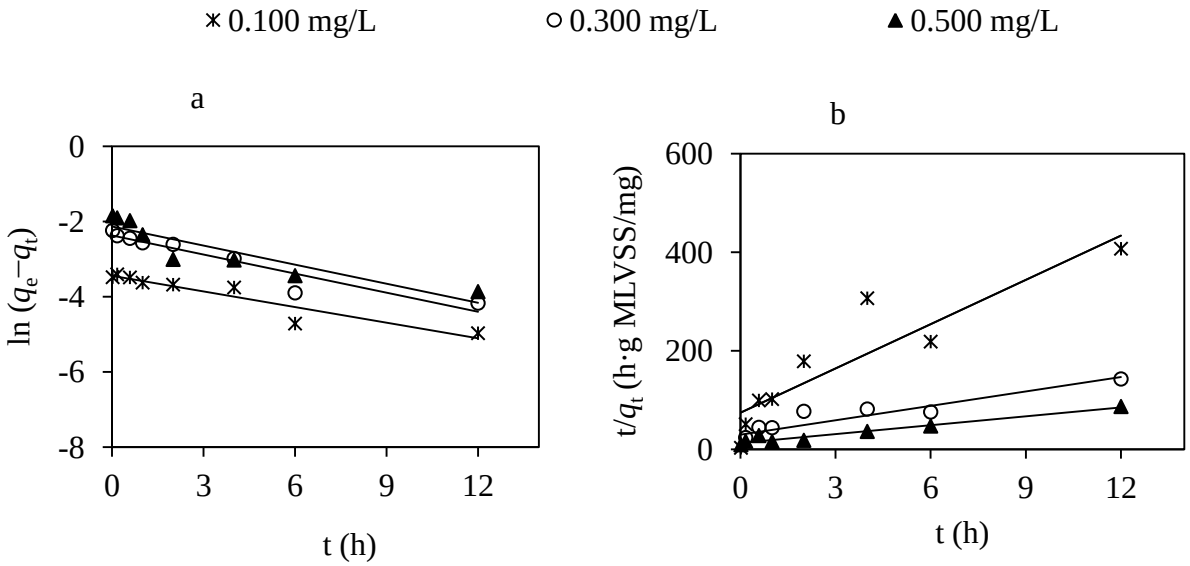

Fig.4. 2. 3 Adsorption kinetics of nC_{60} on primary sludge by (a) pseudo-first-order and (b) pseudo-second-order models.

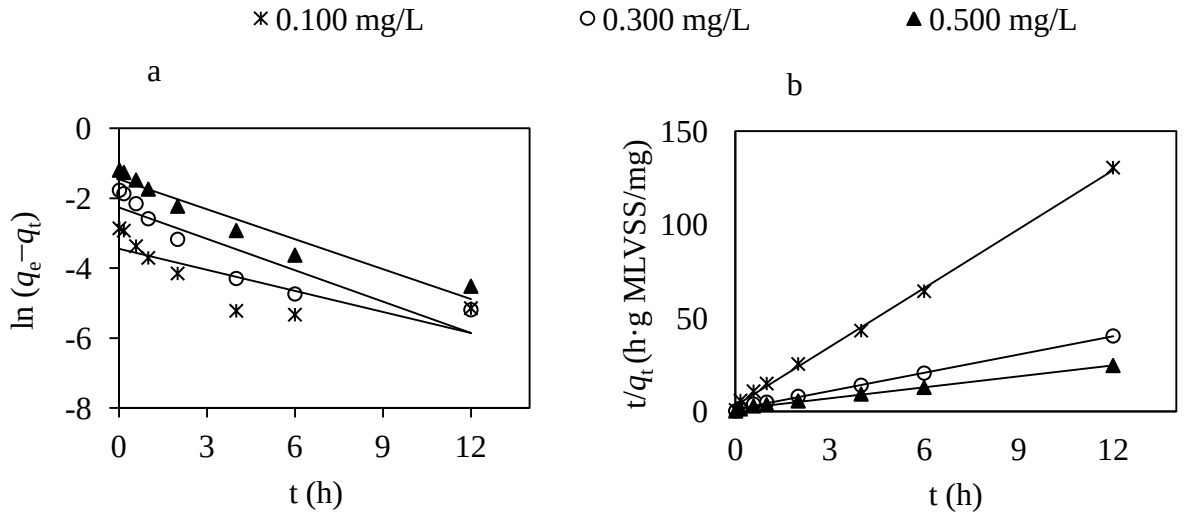

Fig.4. 2. 4 Adsorption kinetics of nC_{60} on activated sludge by (a) pseudo-first-order and (b) pseudo-second-order models.

Table 4. 2. 4 Calculated parameters of adsorption kinetics models

Sludge	Conc. of nC_{60} (mg/L)	$q_{e(obs)}$ (mg/g)	Pseudo-first-order model			Pseudo-second-order model		
			k_1 (1/h)	$q_{e(cal)}$ (mg/g)	R^2	k_2 (g/(mg·h))	$q_{e(cal)}$ (mg/g)	R^2
A-primary sludge	0.100	0.036	0.138	0.032	0.890	12.131	0.033	0.824
	0.300	0.100	0.169	0.094	0.906	3.226	0.102	0.829
	0.500	0.159	0.169	0.118	0.823	2.830	0.166	0.952
A-activated sludge	0.100	0.100	0.224	0.040	0.639	27.174	0.096	0.998
	0.300	0.305	0.298	0.139	0.826	6.700	0.309	0.998
	0.500	0.504	0.287	0.311	0.938	2.319	0.515	0.995

Adsorption isotherm

The experimental data were fitted by Langmuir, Freundlich and linear partitioning models on the primary and activated sludge, as shown in **Fig. 4.2.5** and **4.2.6,** respectively. The adsorption isotherm fitting showed the nC_{60} adsorption could better described by the Freundlich and linear partitioning models than the Langmuir model. Based on the correlation coefficients of three models in **Table 4.2.5,** the Freundlich model best fitted the adsorption process with highest R^2 values. The best fit might be due to the nC_{60} adsorption occurring at multi-layer and on the heterogeneous surface of the activated sludge, following the assumption of the Freundlich model. It also indicated the adsorption process was not only controlled by the chemical adsorption which generally occurred at the monolayer of the adsorbents.

According to the analysis of Freundlich model, the k_F value for the activated sludge was much higher than that for the primary sludge confirming the higher

adsorption capacity of nC_{60} on the activated sludge. By analyzing the surface properties of both sludge samples (**Table 4.2.3)**, the higher adsorption capacity by activated sludge might be attributed to their lower absolute ζ potential and higher hydrophobicity. Both the nC_{60} and activated sludge had the negative charge which could result in the electrostatic repulsion to prevent the adsorption interaction. The lower absolute negative charge on the activated sludge might contribute to the higher nC_{60} adsorption. Although the nC_{60} could be suspended in water for a long time by certain techniques, the nC_{60} are still relative hydrophobic (Brant et al., 2005). Therefore, the nC_{60} adsorption could also be improved by the increased hydrophobic interaction between the nC_{60} and activated sludge which had a higher hydrophobicity.

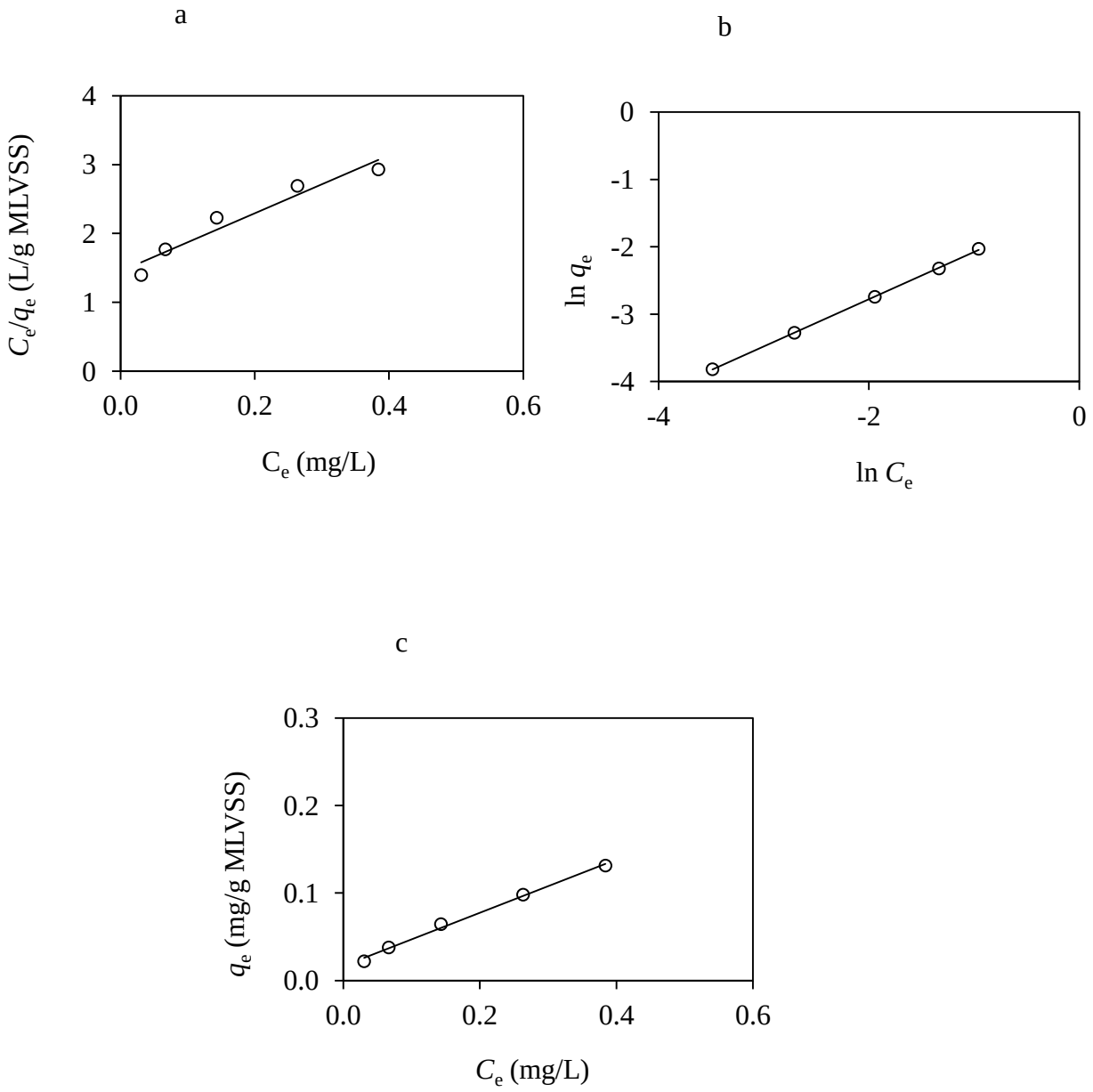

Fig. 4. 2. 5 (a) Langmuir, (b) Freundlich and (c) linear partitioning isotherms of nC_{60} on primary sludge. 12 h was used as the equilibrium time.

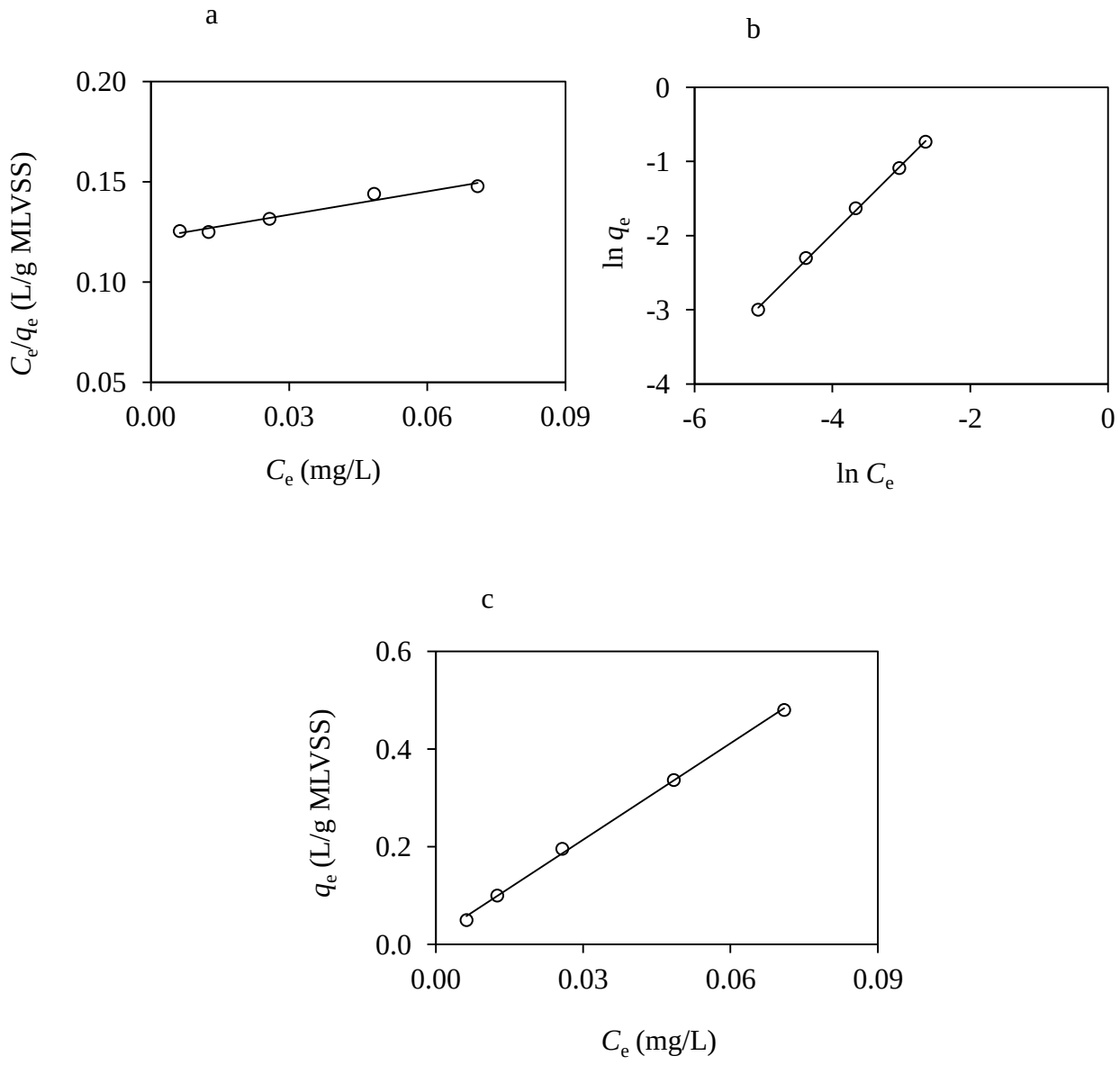

Fig. 4. 2. 6 (a) Langmuir, (b) Freundlich and (c) linear partitioning isotherms of nC_{60} on activated sludge. 12 h was used as the equilibrium time.

Table 4. 2. 5 Calculated parameters of adsorption isotherm models

Sample	Langmuir			Freundlich			linear partitioning	
	k_L (L/mg)	q_m (mg/g MLVSS)	R^2	k_F	n	R^2	k_d	R^2
A-primary sludge	2.892	0.238	0.936	0.254	1.422	0.999	0.304	0.994
A-activated sludge	3.172	2.584	0.960	5.623	1.081	0.999	6.583	0.998

Factors affecting the adsorption behavior of nC_{60} on activated sludge

Effect of MLSS concentration

The nC_{60} concentration in the aqueous phase decreased as the MLSS increased from 50 to 4000 mg/L (**Fig. 4.2.7**). The decrease in concentration can be partially attributed to the increased surface area and availability of more adsorption sites, as seen in the adsorption of dye on activated sludge (Wang et al., 2006). At MLSS concentrations of 1000 and 2000 mg/L, which are common in conventional activated sludge process, the reduction of nC_{60} in the aqueous phase after 1 h of mixture reached up to 48 and 74%, respectively, indicating that adsorption on activated sludge played an important role in the removal of nC_{60} during activated sludge treatment.

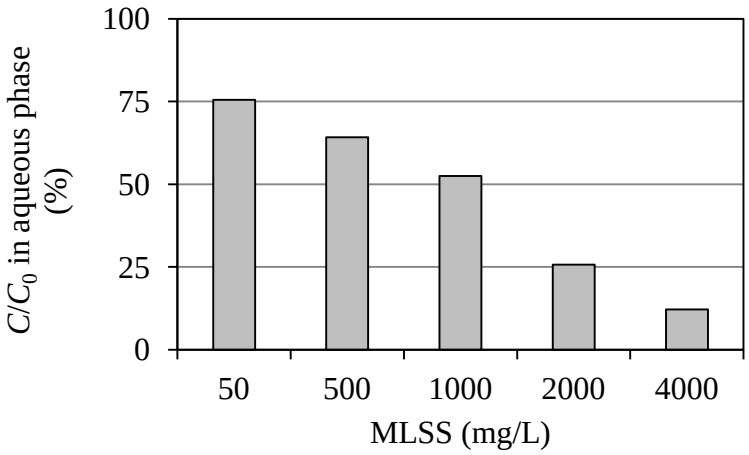

Fig. 4. 2. 7 nC_{60} adsorption on activated sludge as a function of MLSS.

Effect of Temperature

The nC_{60} adsorption slightly increased from 46 to 60% with increasing temperature from 15 to 35 °C (**Fig. 4.2.8**). However the increase was not significant according to the Analysis of Variance ($p > 0.05$) which indicated there was no obvious effect of temperature on the nC_{60} adsorption.

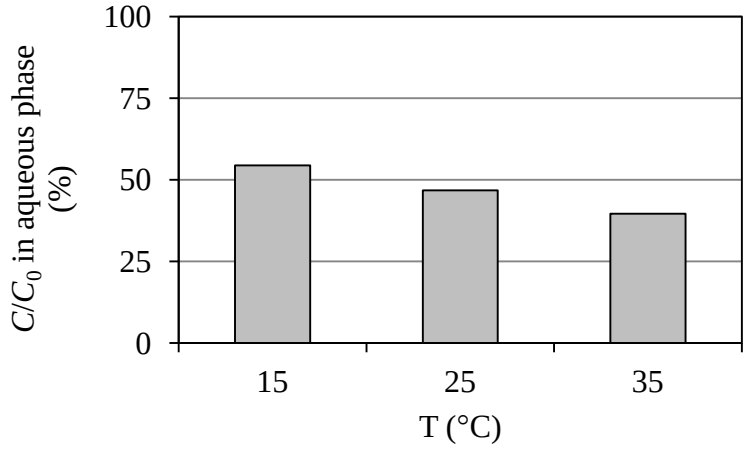

Fig. 4. 2. 8 nC_{60} adsorption on activated sludge as a function of temperature.

Effect of pH

nC_{60} adsorption on activated sludge was highly dependent on pH, increasing as the pH decreased (**Fig. 4.2.9**). pH could affect both the adsorbate and the adsorbent through its effects on surface charge, protonation, and speciation (Reddad et al., 2002). The ζ potential of activated sludge in primary effluent was negative within the pH range studied, and the absolute values decreased as the pH decreased (**Fig. 4.2.10**). Previous section (Section 4.1.3.4) showed the change in ζ potential of nC_{60} in primary effluent as a function of pH was consistent with that of the activated sludge (**Fig. 4.1.10**). At lower pH, proton neutralization could decrease the surface charge of nC_{60} and activated sludge, decreasing electrostatic repulsion and consequently increasing nC_{60} adsorption on activated sludge. The results here indicated the role of electrostatic effect in the nC_{60} adsorption on activated sludge. Similar behavior was also observed on the adsorption of negative-charged perfluorooctane sulfonate on activated sludge (Zhou et al., 2010).

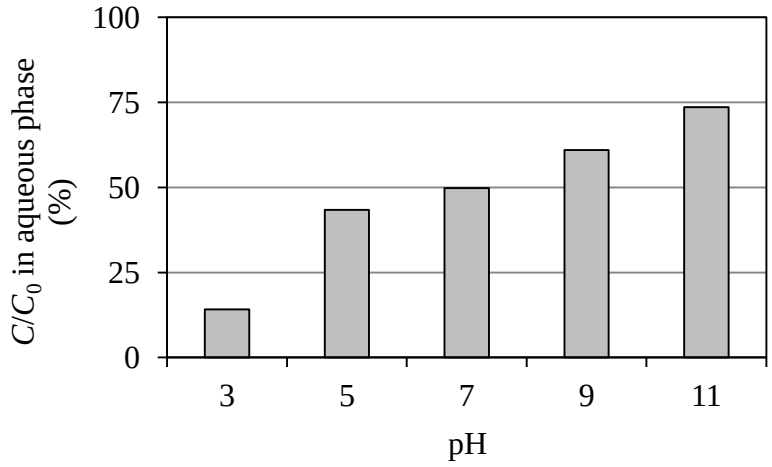

Fig. 4. 2. 9 nC_{60} adsorption on activated sludge as a function of pH.

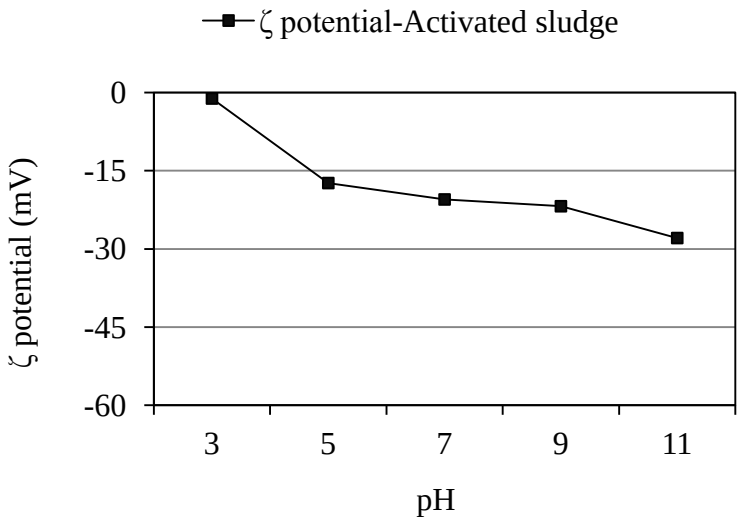

Fig. 4. 2. 10 ζ potential of activated sludge in filtered primary effluent as a function of pH.

Effect of ionic strength

At an added ionic strength of ≤10 mM–in the range of common surface waters, domestic wastewater, and groundwaters–there was no significant effect on nC_{60} adsorption (**Fig. 4.2.11**). However, adsorption was decreased at 50 and 500 mM NaCl, levels of some industrial wastewaters or wastewater mixed with seawater. This result is opposite to the hypothesis that an increase in ionic strength would decrease the surface charge of nC_{60} and activated sludge and thus increase the adsorption on activated sludge. A higher ionic strength indeed decreased the negative charge of activated sludge (**Fig. 4.2.12**), along with that of nC_{60} shown in the section 4.1.3.4 (**Fig. 4.1.7**). However, the increasing ionic strength also increased the concentration of dissolved organic carbon (DOC) in the supernatant (**Fig. 4.2.12**). This result indicates that the nC_{60} remained stable in solution and was prevented from adsorbing to activated sludge by coexisting dissolved organic matter even with very low electrostatic repulsion at high ionic strength. It may be explained that the stability of nC_{60} in solution was enhanced by

steric repulsion due to the increase in the dissolved organic matter in water, as discussed in the previous section (section 4.1.3.4). Thus in addition to the electrostatic effect, the results here showed the steric interaction could also affect the nC_{60} adsorption behavior on activated sludge.

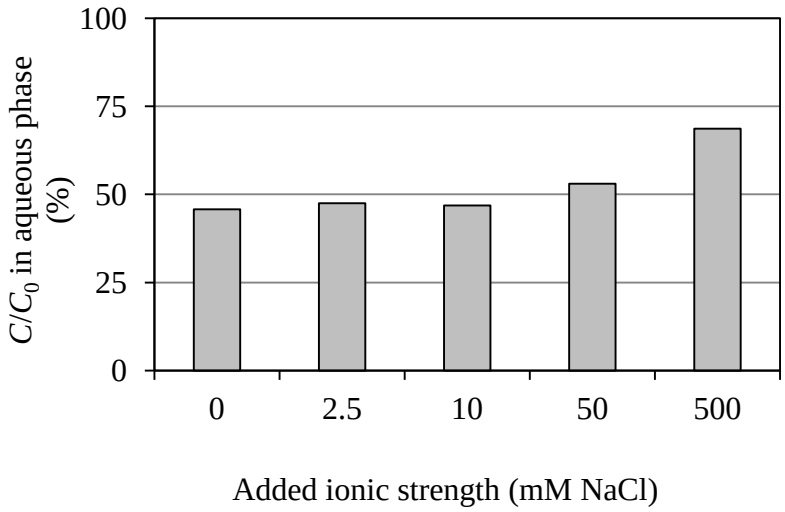

Fig. 4. 2. 11 nC_{60} adsorption on activated sludge as a function of ionic strength.

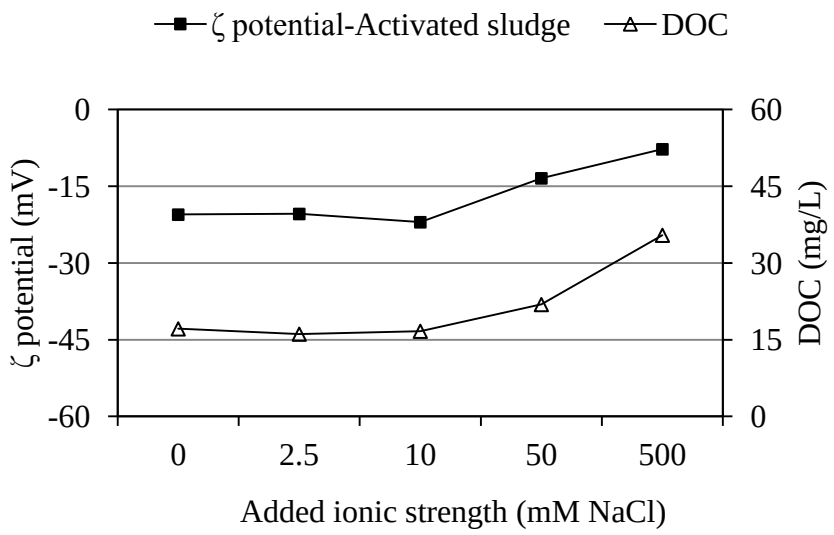

Fig. 4. 2. 12 ζ potential of activated sludge in filtered primary effluent and concentration of dissolved organic carbon (DOC) in supernatant of the mixture of activated sludge and filtrated primary effluent (without nC_{60}) as a function of ionic strength.

4.2.3.2 nC_{60} adsorption behavior on the different activated sludges and related adsorption mechanism

Characterizations of activated sludge from the wastewater treatment plants under different operational conditions

The main characteristics of the activated sludge samples used in this study were listed in **Table 4.2.6.** The activated sludge samples had the particle size ranged from 59 μm (sample C) to 216 μm (sample B). The absolute ζ potential were lower for the sample C and A2 than those of other activated sludges. And the sample B has the lowest hydrophicitiy while the sample C has the highest one.

Table 4. 2. 6 Main characteristics of activated sludge samples

Sample	ζ potential (mV)	Size (μm)	Relative hydrophobicity (%)	MLVSS/MLSS (%)
B	–30.0±2.1	216.3±2.5	55.7±5.6	84.3±0.4
C	–20.9±1.0	59.0±1.0	84.9±2.1	75.3±0.1
D	–30.5±0.9	131.7±2.1	67.6±7.0	85.9±2.5
A2	–20.6±2.3	128.0±8.6	72.8±3.6	72.0±2.3
E1	–29.7±1.0	175.7±28.0	72.6±5.5	86.0±0.3
E2	–25.4±2.1	124.0±20.8	68.0±5.8	85.9±0.4

The data were shown as the mean ± SD

The properties of activated sludge could be affected by a number of operational conditions such as the HRT, SRT and DO (Liu and Fang, 2010). The correlation was investigated between the operational conditions and the properties of activated sludge in **Fig. 4.2.13**, and the correlation coefficients were summarized in **Table 4.2.7**. Here although no significant relationship (all p values > 0.05) was found between the operational parameter and sludge properties, the DO could greatly affected the surface properties of activated sludge compared to the HRT and SRT. The low correlations might be due to the combined effects of the operational parameters as well as the nutrient levels such as the C:N ratio (Wilen et al., 2003).

a

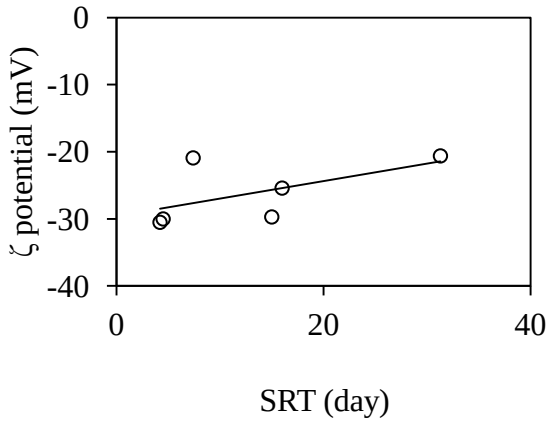
ζ potential × SRT
0
-10
-20
-30
-40
ζ potential (mV)
0
20
40
SRT (day)

b

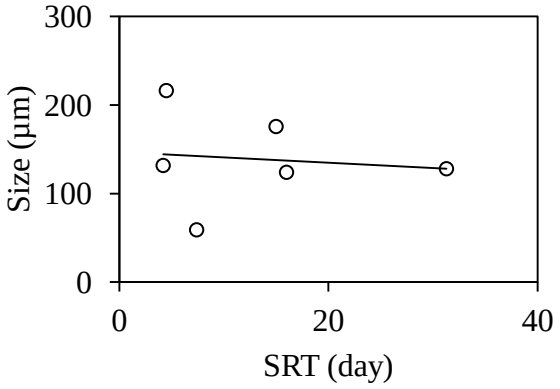
Size× SRT
300
200
100
0
Size (µm)
0
20
40
SRT (day)

a

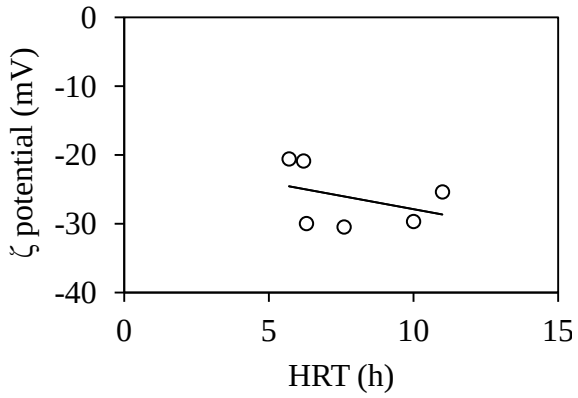
ζ potential × HRT
0
-10
-20
-30
-40
ζ potential (mV)
0
5
10
15
HRT (h)

b

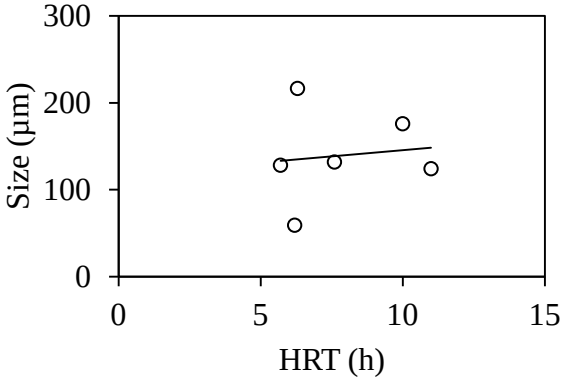
Size× HRT
300
200
100
0
Size (µm)
0
5
10
15
HRT (h)

a

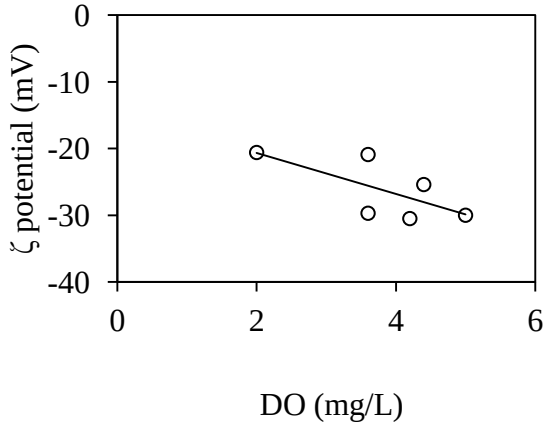
ζ potential × DO
0
-10
-20
-30
-40
ζ potential (mV)
0
2
4
6
DO (mg/L)

b

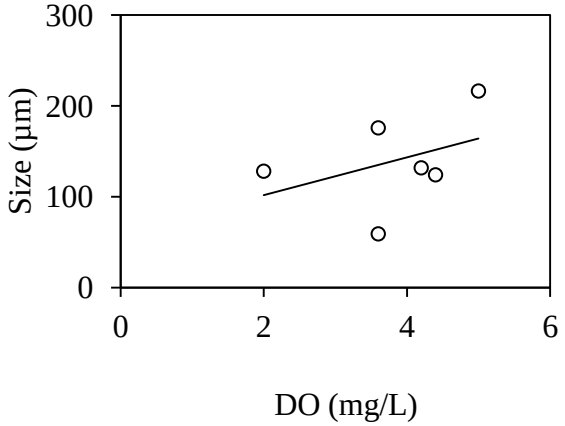
Size × DO
300
200
100
0
Size (µm)
0
2
4
6
DO (mg/L)

c

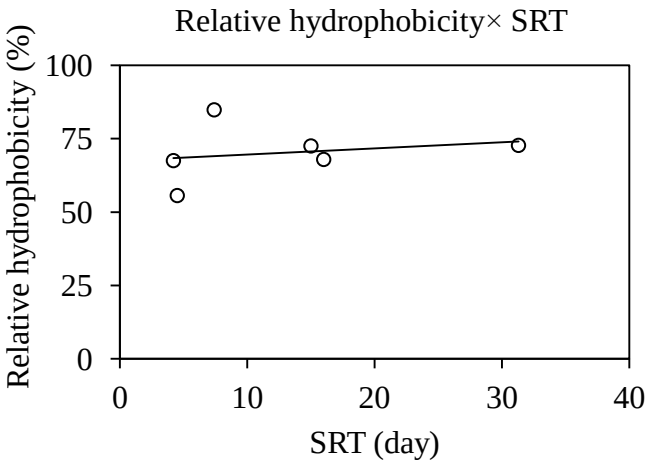

c

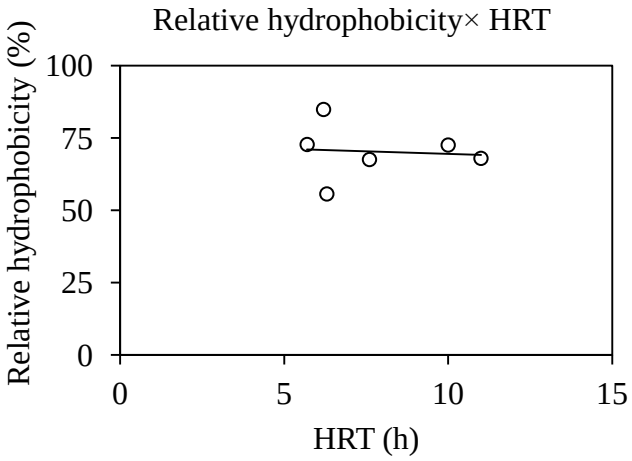

c

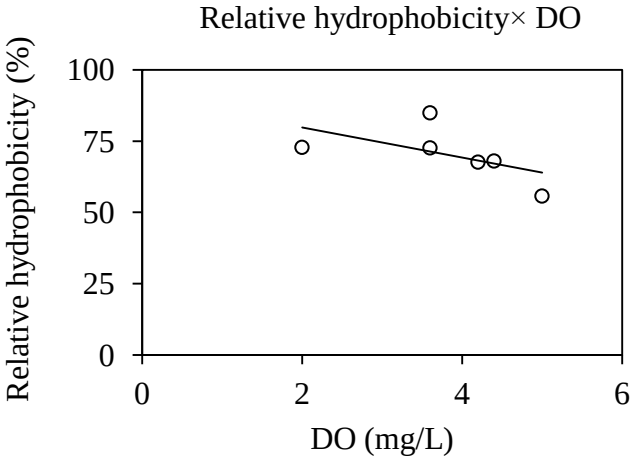

Fig. 4. 2. 13 ζ potential (a), size (b) and relative hydrophobicity (c) of the activated sludge as a function of SRT, HRT and DO.

Table 4. 2. 7 Correlation between the operational condition and surface properties of activated sludge

Operational conditions	ζ potential		Size		Relative hydrophobicity	
	R^2	p	R^2	p	R^2	p
SRT	0.343	0.221	0.014	0.826	0.050	0.669
HRT	0.138	0.468	0.013	0.823	0.006	0.879
DO	0.474	0.130	0.160	0.423	0.326	0.236

Adsorption kinetics

Fig. 4.2.14 showed the adsorption kinetics of nC_{60} after spiking 0.200 mg/L nC_{60} on different activated sludge samples. All the adsorption process could reach equilibrium after 12 h, so 12 h was used as the equilibrium time in the following adsorption isotherm experiments. The adsorption kinetics on different sludge samples were fitted to the first-order and second-order equations (**Fig. 4.2.15**) and calculated coefficients were listed in **Table 4.2.8**. The second-order model's correlation coefficient was > 0.95 and the calculated ($q_{e(cal)}$) values were very close to the observed ($q_{e(obs)}$) values (**Table 4.2.8**). Both facts indicate that the adsorption of nC_{60} on activated sludge followed the second-order model, which is consistent with the results of adsorption on the primary and activated sludge above.

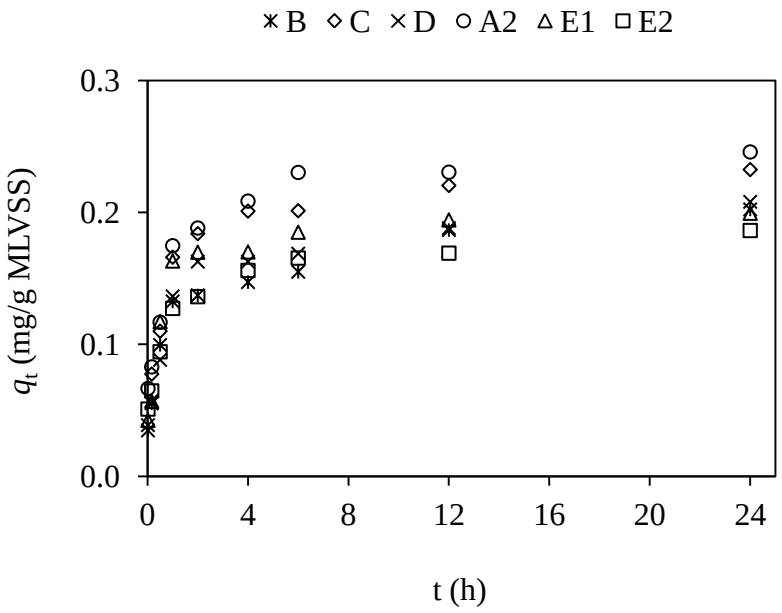

Fig. 4. 2. 14 Time profile of nC_{60} adsorption on different activated sludges.

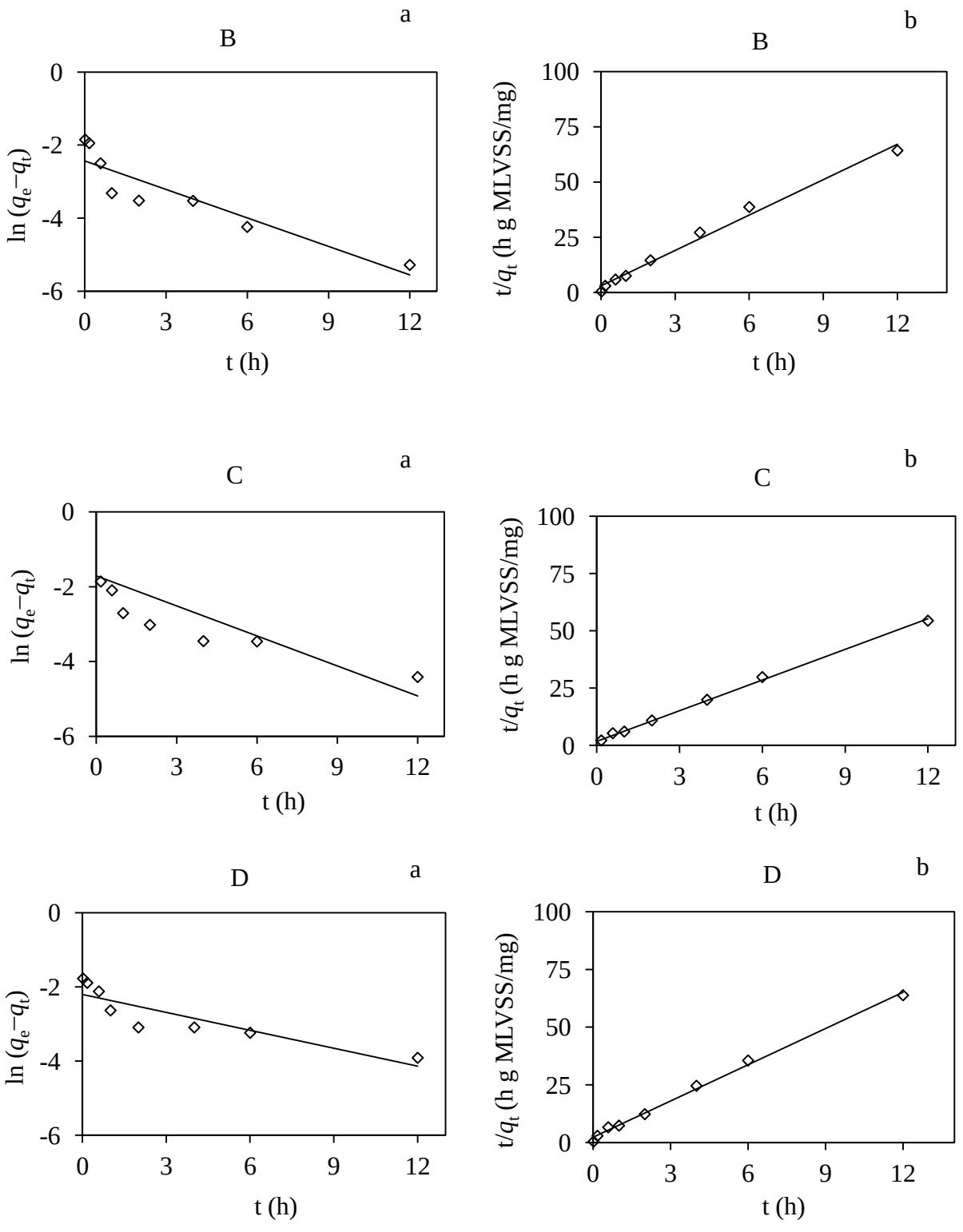
a
B
0
-2
-4
-6
ln (q_e−q_t)
0
3
6
9
12
t (h)
b
B
100
75
50
25
0
t/q_t (h g MLVSS/mg)
0
3
6
9
12
t (h)
a
C
0
-2
-4
-6
ln (q_e−q_t)
0
3
6
9
12
t (h)
b
C
100
75
50
25
0
t/q_t (h g MLVSS/mg)
0
3
6
9
12
t (h)
a
D
0
-2
-4
-6
ln (q_e−q_t)
0
3
6
9
12
t (h)
b
D
100
75
50
25
0
t/q_t (h g MLVSS/mg)
0
3
6
9
12
t (h)

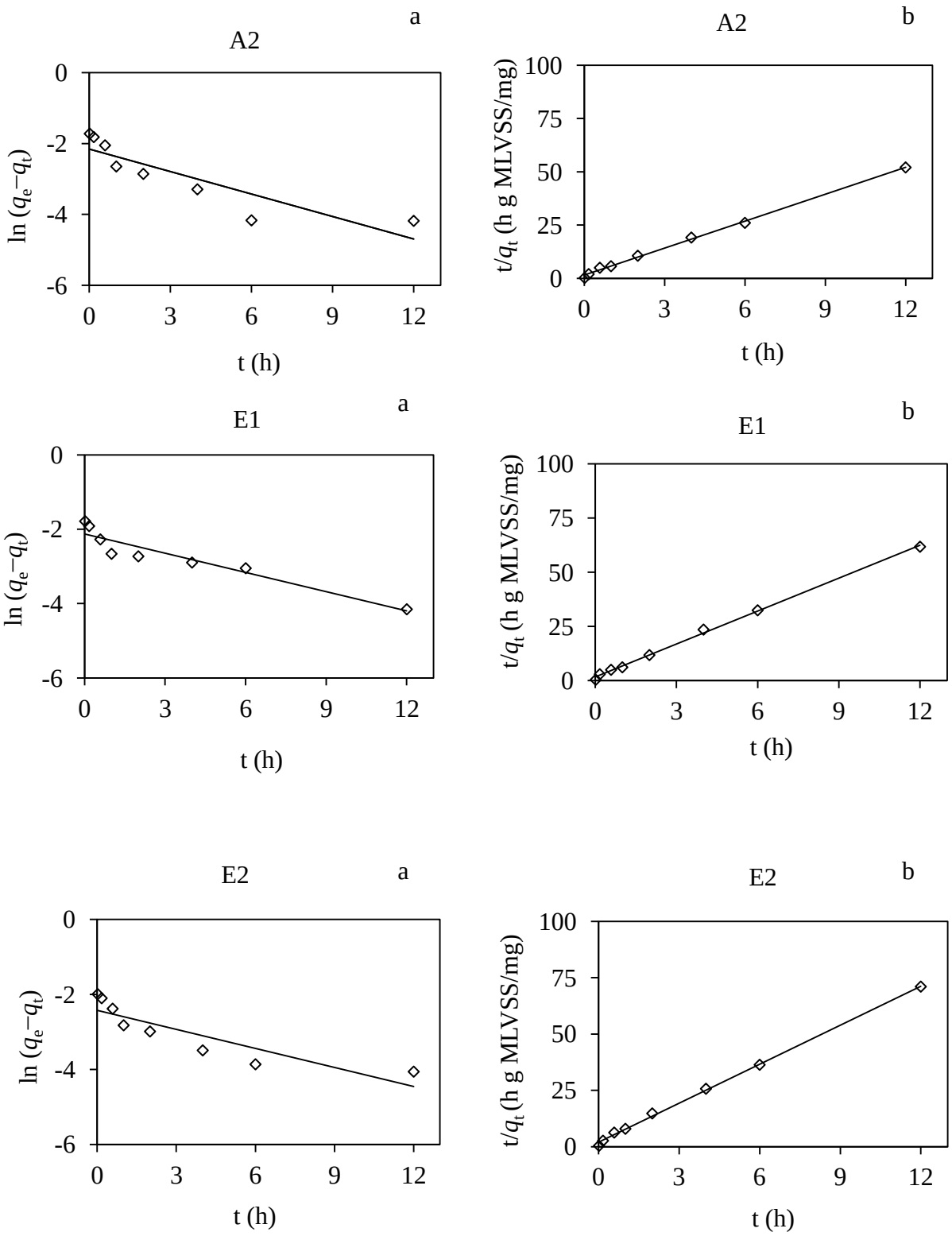

Fig. 4. 2. 15 Adsorption kinetics of nC_{60} on different activated sludges by (a) pseudo-first-order and (b) pseudo-second-order models.

Table 4. 2. 8 Calculated parameters of adsorption kinetics models

Sample	Conc. of nC_{60} (mg/L)	$q_{e(obs)}$ (mg/g)	Pseudo-first-order model			Pseudo- second-order model		
			k_1 (1/h)	$q_{e(cal)}$ (mg/g)	R^2	k_2 (g/(mg·h))	$q_{e(cal)}$ (mg/g)	R^2
B	0.200	0.202	0.260	0.088	0.843	9.516	0.187	0.988
C		0.232	0.267	0.181	0.558	12.002	0.224	0.997
D		0.208	0.161	0.111	0.784	11.680	0.191	0.966
A2		0.246	0.211	0.116	0.786	11.470	0.237	0.997
E1		0.200	0.172	0.119	0.898	15.207	0.198	0.998
E2		0.186	0.169	0.089	0.787	16.840	0.173	0.998

Adsorption isotherm

The Langmuir, Freundlich and linear partitioning models were used to fit the experimental data. The isotherms were shown in **Fig. 4.2.16, 4.2.17,** and **4.2.18**, and the calculated parameters were summarized in **Table 4.2.9**. The Freundlich and linear partitioning models better described the adsorption process based on the high correlation coefficient (>90%). Moreover, the much better fit was observed by the Freundlich model, consistent with the results on the nC_{60} adsorption on the primary and activated sludges. The good modeling by the linear partitioning model indicated the partitioning might play an important role in the adsorption interaction between the nC_{60} and activated sludge such as the hydrophobic-hydrophobic interactions (Zhao et al., 2008).

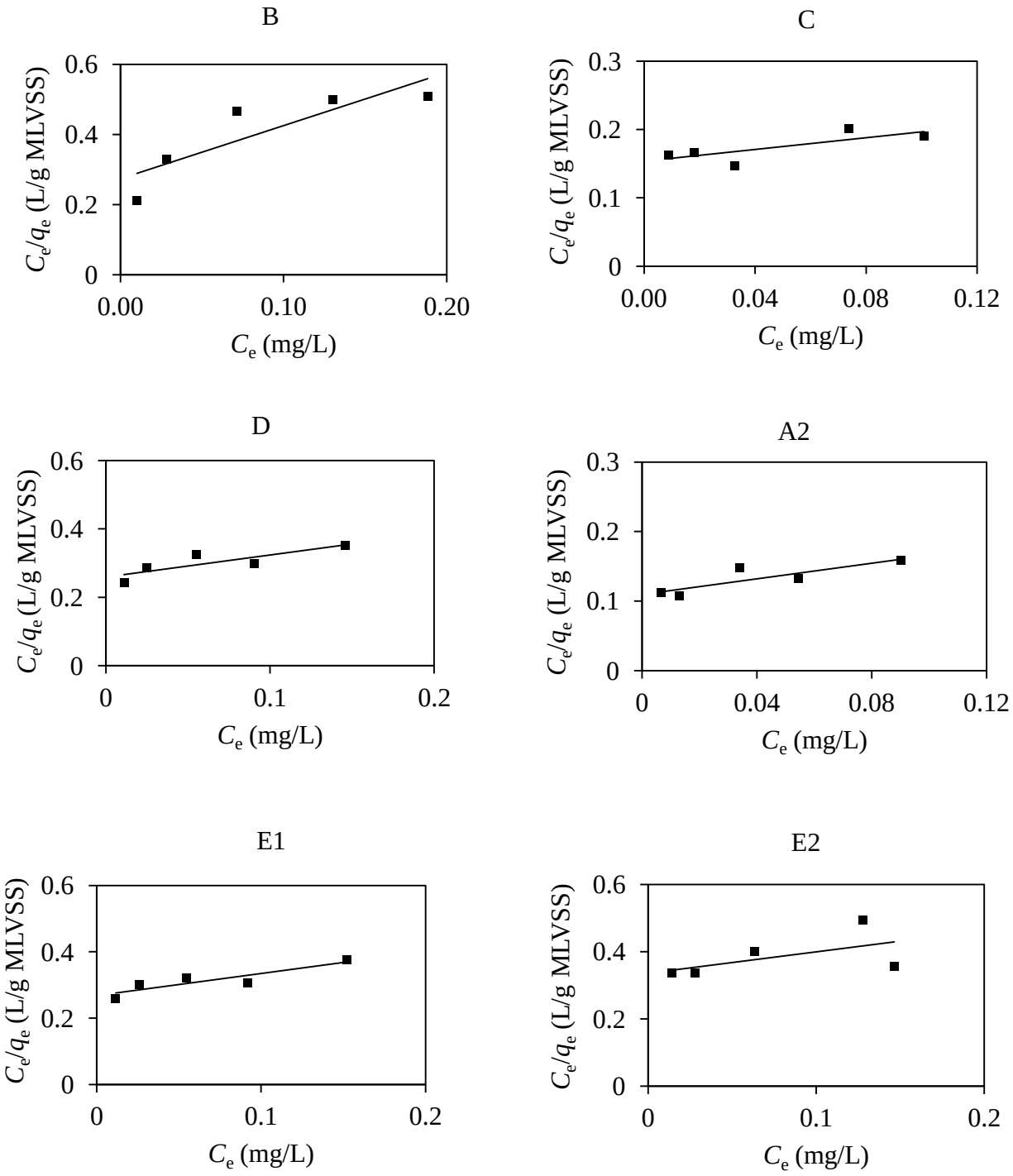

Fig. 4. 2. 16 Langmuir adsorption isotherm of nC_{60} on different activated sludges.

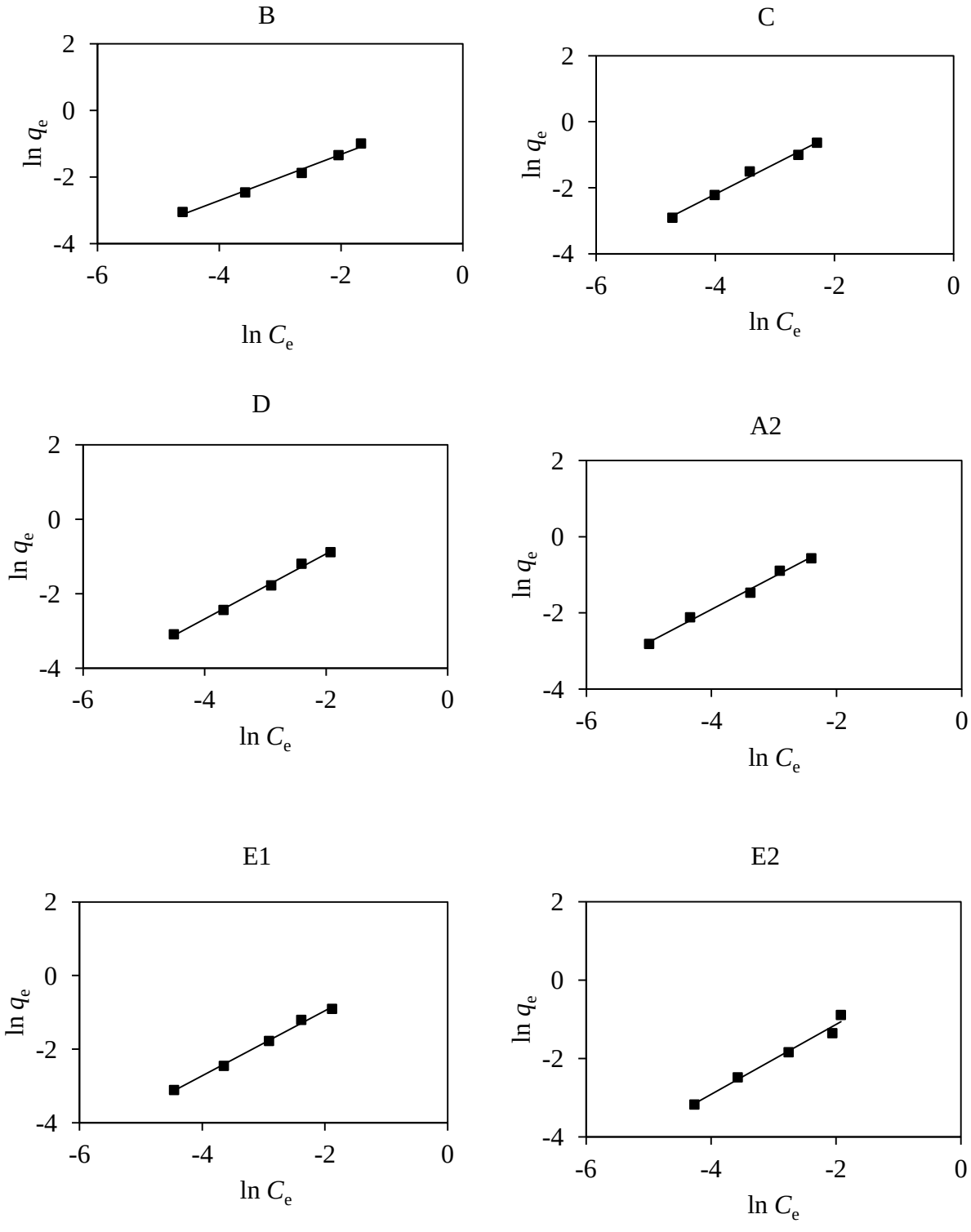

Fig. 4. 2. 17 Freundlich adsorption isotherm of nC_{60} on different activated sludges.

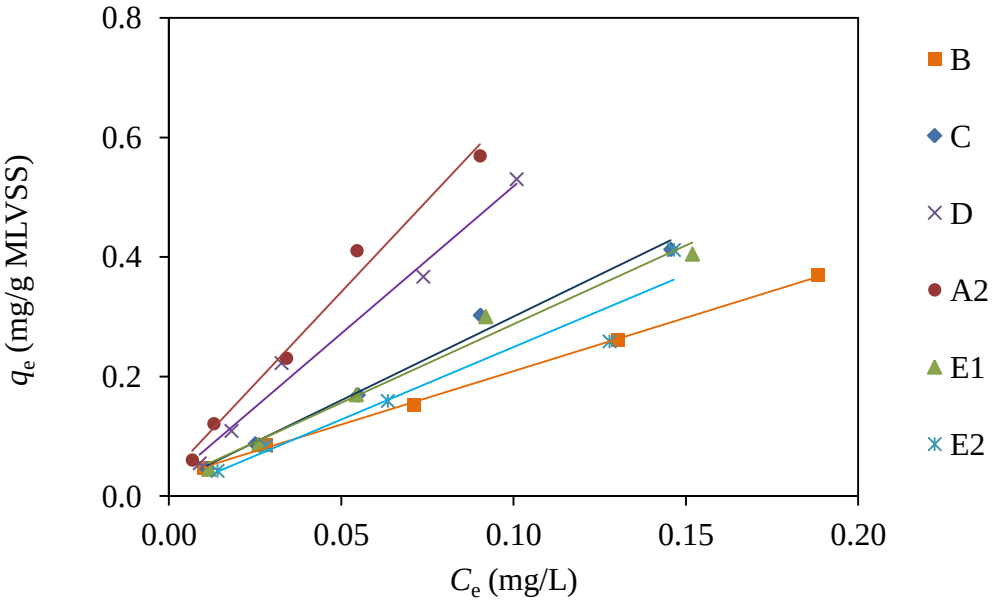

Fig. 4. 2. 18 Linear partitioning isotherm of nC_{60} on different activated sludges.

Table 4. 2. 9 Calculated parameters of Langmuir, Freundlich and linear partitioning models

Samples	Langmuir			Freundlich			linear partitioning	
	k_L (L/mg)	q_m (mg/g MLVSS)	R^2	k_F	n	R^2	k_d	R^2
B	5.549	0.660	0.752	1.070	1.443	0.989	1.788	0.999
C	2.804	2.331	0.588	4.367	1.091	0.989	4.932	0.986
D	2.483	1.555	0.719	2.280	1.443	0.996	2.798	0.987
A2	5.101	1.800	0.736	4.623	1.164	0.992	6.148	0.985
E1	2.491	1.504	0.798	2.246	1.134	0.995	2.632	0.981
E2	1.884	1.580	0.314	1.943	1.116	0.980	2.426	0.932

Effect of sludge properties on the nC_{60} adsorption

The effects of sludge properties on adsorption were investigated by correlating the sludge properties with the coefficients (the Langmuir (k_L), Freundlich (k_F) and linear partitioning coefficient (k_d) obtained from different activated sludge samples, as shown in **Fig. 4.2.19, 4.2.20,** and **4.2.21.** The calculated correlation coefficients were summarized in **Table 4.2.10**. The k_L values were not correlated with the surface properties of activated sludge according to the low correlation coefficients indicating the Langmuir model is not appropriate for nC_{60} adsorption on activated sludge. On the other hand, the k_F and k_d showed consistent correlations with the surface properties: positive correlation with relative hydrophobicity and ζ potential, negative with sludge size. According to the regression analysis, the correlations reached significant ($p < 0.05$) between the k_F and ζ potential, and relative hydrophobicity. The attractive interactions between particles and activated sludge in general include the van der Waals, electrostatic and hydrophobic forces (Song et al., 2011). The negative surface charges for both nC_{60} and activated sludge could only showed potential electrostatic repulsions. Therefore, the lower value of absolute ζ potential on sludge samples reduced the repulsive electrostatic between the nC_{60} and activated sludge and therefore resulted in the increase in the adsorbed amounts. The negative correlation between the size and adsorption coefficients indicated the activated sludge with small size had higher the nC_{60} adsorption capacity. It might be due to the increase in the adsorption surface area and adsorption sites along with the smaller sludge in size. The high K_{ow} value of 3.08 for the nC_{60} showed their hydrophobic surfaces (Xiao and Wiesner, 2012). The higher hydrophobicity of activated sludge helped the adsorption interaction by increasing the hydrophobic-hydrophobic forces between the nC_{60} and sludges.

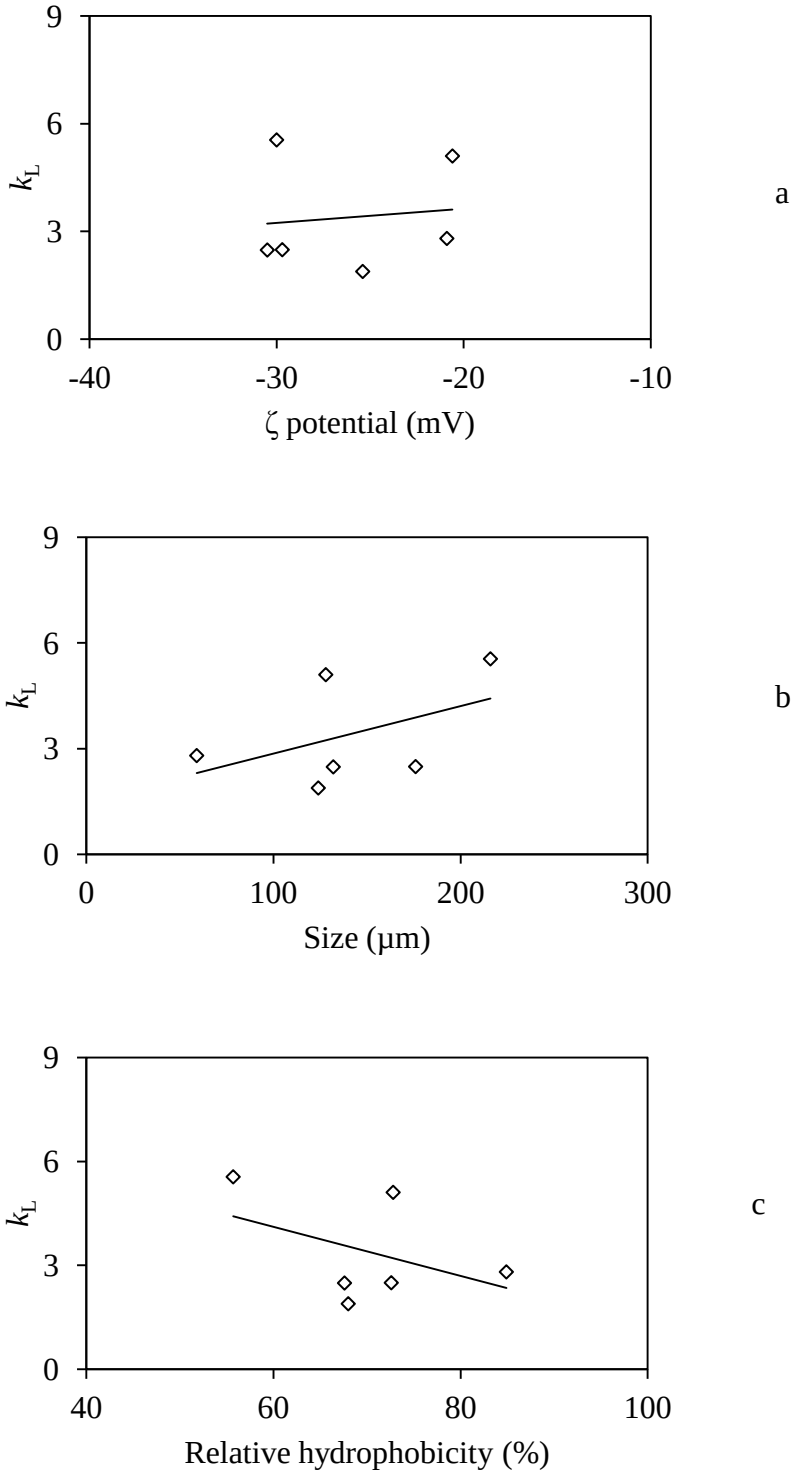

Fig. 4. 2. 19 Correlation of Langmuir coefficient (k_L) and surface properties of activated sludge: (a) ζ potential, (b) size, and (c) relative hydrophobicity.

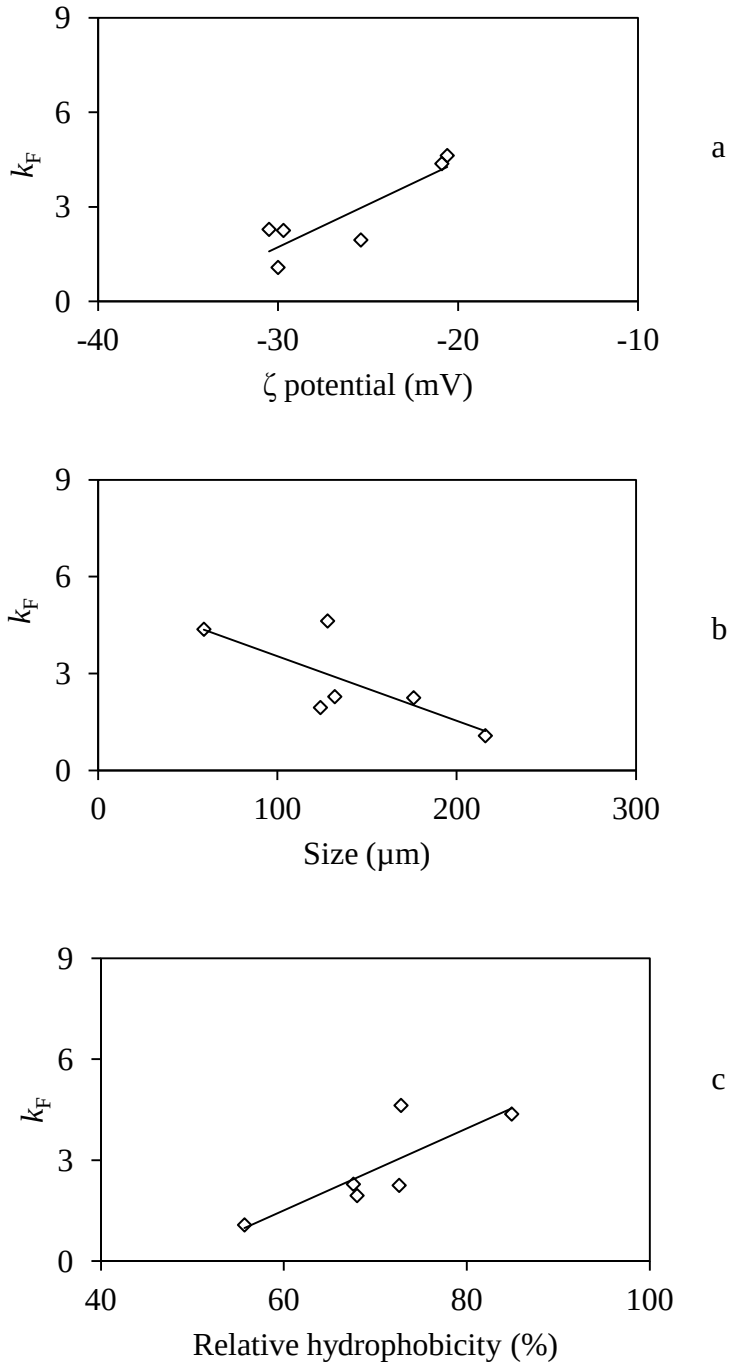

Fig. 4. 2. 20 Correlation of Freundlich coefficient (k_F) and surface properties of activated sludge: (a) ζ potential, (b) size, and (c) relative hydrophobicity.

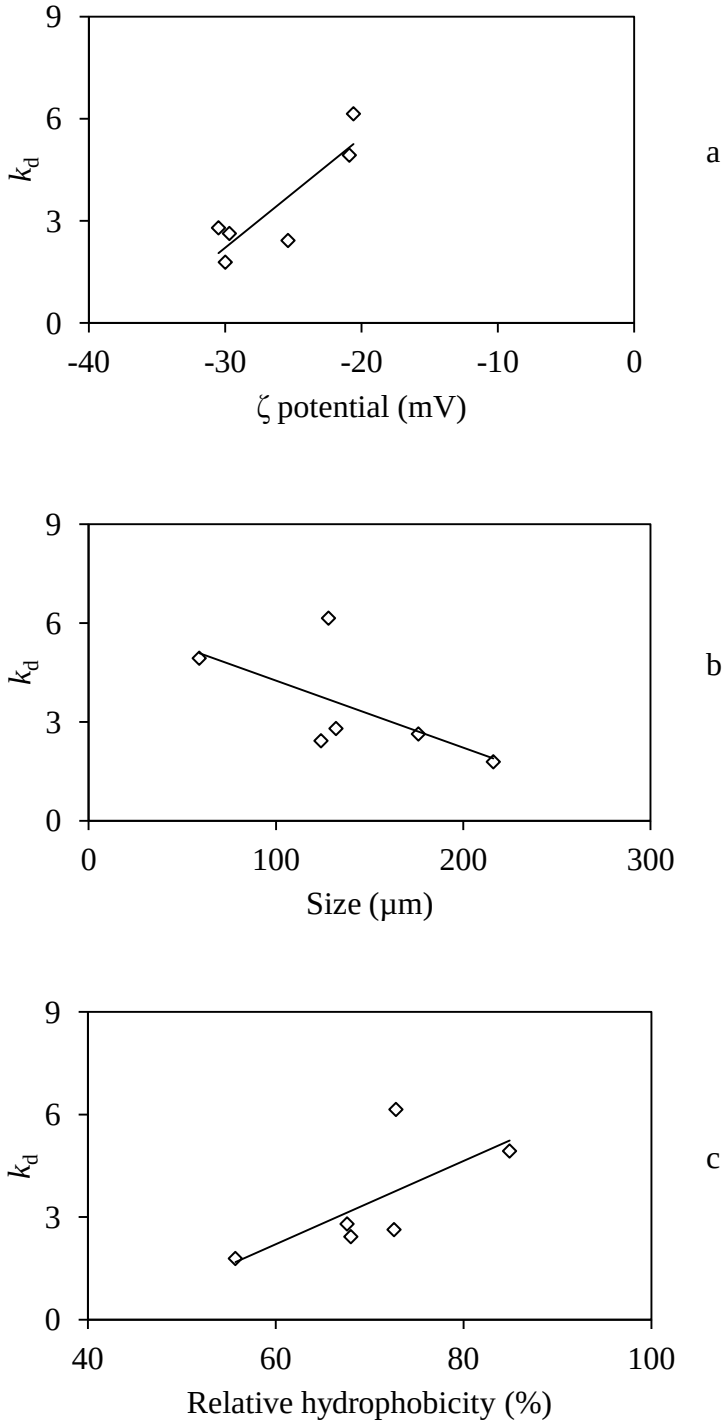

Fig. 4. 2. 21 Correlation of linear partitioning coefficient (k_d) and surface properties of activated sludge: (a) ζ potential, (b) size, and (c) relative hydrophobicity.

Table 4. 2. 10 Calculated correlation coefficient and *p* values between the surface properties of activated sludge and adsorption isotherm coefficients

Coefficient	ζ potential		Sludge size		Relative hydrophobicity	
	R	*p*	*R*	*p*	*R*	*p*
k_L	0.114	0.826	0.465	0.352	–0.437	0.385
k_F	0.877	0.021	–0.750	0.086	0.661	0.049
k_d	0.877	0.022	–0.634	0.174	0.682	0.135

4.2.4 Conclusions

The rapid increase in the application and use of nC_{60} would result in their discharge into the water environment if no efficient treatment. Until now, it is still unclear whether the conventional activate sludge process could remove the nC_{60} from the wastewater or not. The nC_{60} adsorption on activated sludge was considered to be an important process due to the hydrophobic properties of nC_{60}. However, very few information was available on the adsorption behavior (the equilibrium and kinetics), the influencing factors (the type of wastewater sludge and wastewater conditions) and the adsorption mechanism. This part investigated the adsorption behavior of nC_{60} on the different sludge samples. And the adsorption mechanism was explained by modeling the adsorption isotherm and kinetics, analyzing the correlation of nC_{60} adsorption coefficients and surface properties of sludge samples, as well as the effect of influencing factors on the adsorption on sludge.

It mainly included three parts. The first one investigated the adsorption kinetics and equilibrium of nC_{60} on the primary sludge. For the second part, the adsorption kinetics and equilibrium of nC_{60} on the activated sludge were investigated, as well as the effect of mixed liquor suspended solids (MLSS), temperature, pH, and ionic strength. For the third part, six activated sludge samples were collected in the aerobic tank from several wastewater treatment plants which were running under different operational conditions. The adsorption kinetics and equilibrium of nC_{60} on different activated sludges were conducted and the adsorption coefficients were used to eliminate the adsorption mechanisms. The main conclusion as follows:

(1) The adsorption reached equilibrium after 12 h at an MLSS level of 1000 mg/L for both the primary sludge and activated sludge. The process well followed the Freundlich isotherm model indicating the nC_{60} adsorption occurred at multi-layer and on the heterogeneous surface of the activated sludge. The high correlation with linear partitioning model suggested the partitioning process played an important role in the adsorption process on the sludge such as the hydrophobic-hydrophobic interactions.

(2) The activated sludge had a much higher Freundlich coefficient (k_F) and linear partitioning coefficient (k_d) than those for the primary sludge indicating their higher adsorption capacity. It could be attributed to the higher hydrophobicity and lower absolute ζ potential which could contribute to the adsorption of nC_{60} by increasing the attractive force and reducing the repulsive forces, respectively.

(3) The pH values greatly affected the adsorption process, decreasing the adsorption of nC_{60} from 86% at pH 3 to 26% at pH 11 after 1 h of mixture. At an ionic strength of 0 to10 mM, there was no significant effect on nC_{60} adsorption. At MLSS concentrations of 1000 and 2000 mg/L, which are common in conventional activated sludge treatment, the reduction of nC_{60} in the aqueous phase after 1 h of mixture reached up to 48 and 74%, respectively, demonstrating high removal efficiency.

(4) The adsorption mechanism was further investigated by analyzing the correlation between the adsorption coefficient and the surface properties of activated sludge samples. The Freundlich coefficient (k_F) and linear partitioning coefficient (k_d) showed consistent correlations with the surface properties: positive correlation with relative hydrophobicity and ζ potential, negative with sludge size. The lower value of absolute ζ potential on sludge samples reduced the repulsive electrostatic between the nC_{60} and activated sludge and therefore resulted in the increase in the adsorbed amounts. The higher hydrophobicity of activated sludge helped the adsorption interaction by increasing the hydrophobic-hydrophobic forces between the nC_{60} and sludges. In addition, the size of activated sludge could also affect the adsorption might due to the effect on the adsorption sites and surface area. The results showed both the electrostatic repulsions and hydrophobic attractions were involved in the nC_{60} adsorption on activated sludge.

4.2.5 References

Benn, T.M., Westerhoff, P., Herckes, P., 2011. Detection of fullerenes (C_{60} and C_{70}) in commercial cosmetics. Environmental Pollution 159 (5), 1334–1342.

Chae, S.R., Hotze, E.M., Xiao, Y., Rose, J., Wiesner, M.R., 2010. Comparison of methods for fullerene detection and measurements of reactive oxygen production in cosmetic products. Environmental Engineering Science 27 (9), 797–804.

Chen, K.L., Elimelech, M., 2007. Influence of humic acid on the aggregation kinetics of fullerene (C_{60}) nanoparticles in monovalent and divalent electrolyte solutions. Journal of Colloid and Interface Science 309 (1), 126–134.

Chen, Z., Westerhoff, P., Herckes, P., 2008. Quantification of C_{60} fullerene concentrations in water. Environmental Toxicology and Chemistry 27 (9), 1852–1859.

Chiron, N., Guilet, R., Deydier, E., 2003. Adsorption of Cu(II) and Pb(II) onto a grafted silica: isotherms and kinetic models. Water Research 37 (13), 3079–3086.

Chlou, C.T., Porter, P.E., Schmeddlng, D.W., 1983. Partition equilibria of nonionic organic compounds between soil organic matter and water. Environmental Science & Technology 1983, 17 (4), 227–231.

Deguchi, S., Alargova, R.G., Tsujii, K., 2001. Stable dispersions of fullerenes, C_{60} and C_{70}, in water. Preparation and characterization. Langmuir 17 (19), 6013–6017.

Farre, M., Perez, S., Gajda-Schrantz, K., Osorio, V., Kantiani, L., Ginebreda, A., Barcelo, D., 2010. First determination of C_{60} and C_{70} fullerenes and N-methylfulleropyrrolidine C_{60} on the suspended material of wastewater effluents by liquid chromatography hybrid quadrupole linear ion trap tandem mass spectrometry. Journal of Hydrology 383 (1-2), 44–51.

Feng, Y., Zhang, Z., Gao, P., Su, H., Yu, Y., Ren, N., 2010. Adsorption behavior of EE2 (17 alpha-ethinylestradiol) onto the inactivated sewage sludge: kinetics, thermodynamics and influence factors. Journal of Hazardous Materials 175 (1-3), 970–976.

Fortner, J.D., Lyon, D.Y., Sayes, C.M., Boyd, a M., Falkner, J.C., Hotze, E.M., Alemany, L.B., Tao, Y.J., Guo, W., Ausman, K.D., Colvin, V.L., Hughes, J.B.,

2005. C_{60} in water: nanocrystal formation and microbial response. Environmental Science & Technology 39 (11), 4307–4316.

Freundlich, H., 1906. Concerning adsorption in solutions. Zeitschrift Fur Physikalische Chemie-Stochiometrie Und Verwandtschaftslehre 57 (4), 385–470.

Hanafiah, M.A.K.M., Shafiei, S., Harun, M.K., Yahya, M.Z.A., 2006. Kinetic and thermodynamic study of Cd^{2+} adsorption onto rubber tree (Hevea Brasiliensis) leaf powder. Functional Materials and Devices 517, 217–221.

Hartmann, N.B., Buendia, I.M., Bak, J., Baun, A., 2011. Degradability of aged aquatic suspensions of C_{60} nanoparticles. Environmental Pollution 159 (10), 3134–3137.

Ho, Y.-S., 2006. Review of second-order models for adsorption systems. Journal of Hazardous Materials 136 (3), 681–689.

Ho, Y.S., Mckay, G., 1998. A comparison of chemisorption kinetic models applied to pollutant removal on various Sorbents. Process Safety and Environmental Protection, 76, 332–340.

Huang, W., Yu, Z., Fu, J., 2003. Effects of organic matter heterogeneity on sorption and desorption of organic contaminants by soils and sediments. Applied Geochemistry 18 (7), 955–972.

Hyung, H., Kim, J.H., 2009. Dispersion of C_{60} in natural water and removal by conventional drinking water treatment processes. Water Research 43 (9), 2463–2470.

Isaacson, C.W., Kleber, M., Field, J.A., 2009. Quantitative analysis of fullerene nanomaterials in environmental systems: a critical review. Environmental Science & Technology 43 (17), 6463–6474.

Jafvert, C.T., Kulkarni, P.P., 2008. Buckminsterfullerene's (C_{60}) octanol-water partition coefficient (K_{ow}) and aqueous solubility. Environmental Science & Technology 42 (16), 5945–5950.

Kang, S., Mauter, M.S., Elimelech, M., 2009. Microbial cytotoxicity of carbon-based nanomaterials: implications for river water and wastewater effluent. Environmental Science & Technology 43 (7), 2648–2653.

Kililç, M., Yazilcil, H., Solak, M., 2009. A comprehensive study on removal and recovery of copper(II) from aqueous solutions by NaOH-pretreated Marrubium

globosum ssp. globosum leaves powder: potential for utilizing the copper(II) condensed desorption solutions in agricultural applications. Bioresource Technology 100 (7), 2130–2137.

Kumar, P.S., Gayathri, R., 2009. Adsorption of Pb^{2+} ions from aqueous solutions onto Bael tree leaf powder: isotherms, kinetics and thermodynamics. Journal of Engineering Science and Technology, 4(4), 381–399.

Kummerer, K., Menz, J., Schubert, T., Thielemans, W., 2011. Biodegradability of organic nanoparticles in the aqueous environment. Chemosphere 82 (10), 1387–1392.

Langmuir, I., 1918. The adsorption of gases on pane surfaces of glass, mica and platinum. Journal of the American Chemical Society 40, 1361–1403.

Li, Q., Xie, B., Hwang, Y.S., Xu, Y., 2009. Kinetics of C_{60} fullerene dispersion in water enhanced by natural organic matter and sunlight. Environmental Science & Technology 43 (10), 3574–3579.

Liu, X.Y., Wazne, M., Chou, T.M., Xiao, R., Xu, S.Y., 2011. Influence of Ca^{2+} and suwannee river humic acid on aggregation of silicon nanoparticles in aqueous media. Water Research 45 (1), 105–112.

Liu, Y., Fang, H.H.P., 2003. Influences of extracellular polymeric substances (EPS) on flocculation, settling, and dewatering of activated sludge. Critical Reviews in Environmental Science and Technology 33, 237–273.

Lyon, D.Y., Adams, L.K., Falkner, J.C., Alvarez, P.J.J., 2006. Antibacterial activity of fullerene water suspensions: effects of preparation method and particle size. Environmental Science & Technology 40 (14), 4360–4366.

Ma, X., Bouchard, D., 2009. Formation of aqueous suspensions of fullerenes. Environmental Science & Technology 43 (2), 330–336.

Nyberg, L., Turco, R.F., Nies, L., 2008. Assessing the impact of nanomaterials on anaerobic microbial communities. Environmental Science & Technology 42 (6), 1938–1943.

Oberdorster, E., Zhu, S.Q., Blickley, T.M., McClellan-Green, P., Haasch, M.L., 2006. Ecotoxicology of carbon-based engineered nanoparticles: effects of fullerene (C_{60}) on aquatic organisms. Carbon 44 (6), 1112–1120.

Qu, X.L., Hwang, Y.S., Alvarez, P.J.J., Bouchard, D., Li, Q.L., 2010a. UV irradiation and humic acid mediate aggregation of aqueous fullerene (nC_{60}) nanoparticles. Environmental Science & Technology 44 (20), 7821–7826.

Qu, X.L., Hwang, Y.S., Alvarez, P.J.J., Bouchard, D., Li, Q.L., 2010b. UV irradiation and humic acid mediate aggregation of aqueous fullerene (nC_{60}) nanoparticles. Environmental Science & Technology 44 (20), 7821–7826.

Reddad, Z., Gerente, C., Andres, Y., Le Cloirec, P., 2002. Adsorption of several metal ions onto a low-cost biosorbent: kinetic and equilibrium studies. Environmental Science & Technology 36 (9), 2067–2073.

Ren, R., Li, K., Zhang, C., Liu, D., Sun, J., 2011. Biosorption of tetradecyl benzyl dimethyl ammonium chloride on activated sludge: kinetic, thermodynamic and reaction mechanisms. Bioresource Technology 102 (4), 3799–3804.

Rosenberg, M., 1984. Bacterial adherence to hydrocarbons - a useful technique for studying cell-surface hydrophobicity. FEMS Microbiology Letters 22 (3), 289–295.

Senthilkumaar, S., Varadarajan, P.R., Porkodi, K., Subbhuraam, C.V., 2005. Adsorption of methylene blue onto jute fiber carbon: kinetics and equilibrium studies. Journal of Colloid and Interface Science 284 (1), 78–82.

Wang, Y., Mu, Y., Zhao, Q.B., Yu, H.Q., 2006. Isotherms, kinetics and thermodynamics of dye biosorption by anaerobic sludge. Separation and Purification Technology 50 (1), 1–7.

Zhou, Q., Deng, S.B., Zhang, Q.Y., Fan, Q., Huang, J., Yu, G., 2010. Sorption of perfluorooctane sulfonate and perfluorooctanoate on activated sludge. Chemosphere 81 (4), 453–458.

CHAPTER V

EFFECT OF nC_{60} ON THE ACTIVATED SLUDGE PROCESS

5.1 Introduction

C_{60} have displayed antibacterial effects in recent studies. Lyon et al. (2005) reported the minimal inhibitory concentration of 0.5 to 1 mg/L, and 1.5 to 3 mg/L for nC_{60} against the Gram-negative *Escherichia coli* and Gram-positive *Bacillus subtilis*. And the smaller fraction of nC_{60} had greater antibacterial activity on *Bacillus subtilis* (Lyon et al., 2006; Lyon et al., 2005). The bacteria of *Peseudomona Putida* showed the response in lipid composition and membrane phase behavior after exposure of nC_{60} (Fang et al., 2007). Although the toxicity mechanism is still not clear, the most published is due to the oxidative stress via reactive oxygen species (ROS) dependent (Sayes et al., 2004) or independent (Lyon et al., 2008). The toxicities on the bacteria suggested the potential of adverse effect of C_{60} on the activated sludge which is important for the removal of organic matters and nutrient compounds in wastewater. Recent studies have pointed out the toxicity of metal nanoparticles (silver (Liang et al., 2010; Radniecki et al., 2011), copper (Ganesh et al., 2010), zinc oxide and titanium dioxide (Mu et al., 2011)), on the aerobic/anaerobic activated sludge. However, very limited studies studied on C_{60} toxicity on the activated sludge.

The objective of this study is to assess the effect of nC_{60} on the treatment performance of activated sludge process and the potential toxicity to the activated sludge. The aqu/nC_{60} was prepared by the extended stirring in order to represent the likely transition of C_{60} to water environment during the C_{60}' production and consumption. And the tol/nC_{60} by the toluene exchange method was also used to investigate the effect of preparation methods on nC_{60} toxicity. The sequencing batch reactor (SBR) was run to investigate the effect of nC_{60} on activated sludge process. Nitrification inhibition test was chosen to evaluate the toxicity on sludge because of the high sensitivity of nitrifying bacteria to the pollutants. Moreover, the effect of nC_{60} on

these nitrifying organisms would directly affect the removal of NH_4^+–N in wastewater. In addition, the Microtox® test was also conducted as a standardized screening test. The content structure of this chapter was shown in **Fig. 5.1.**

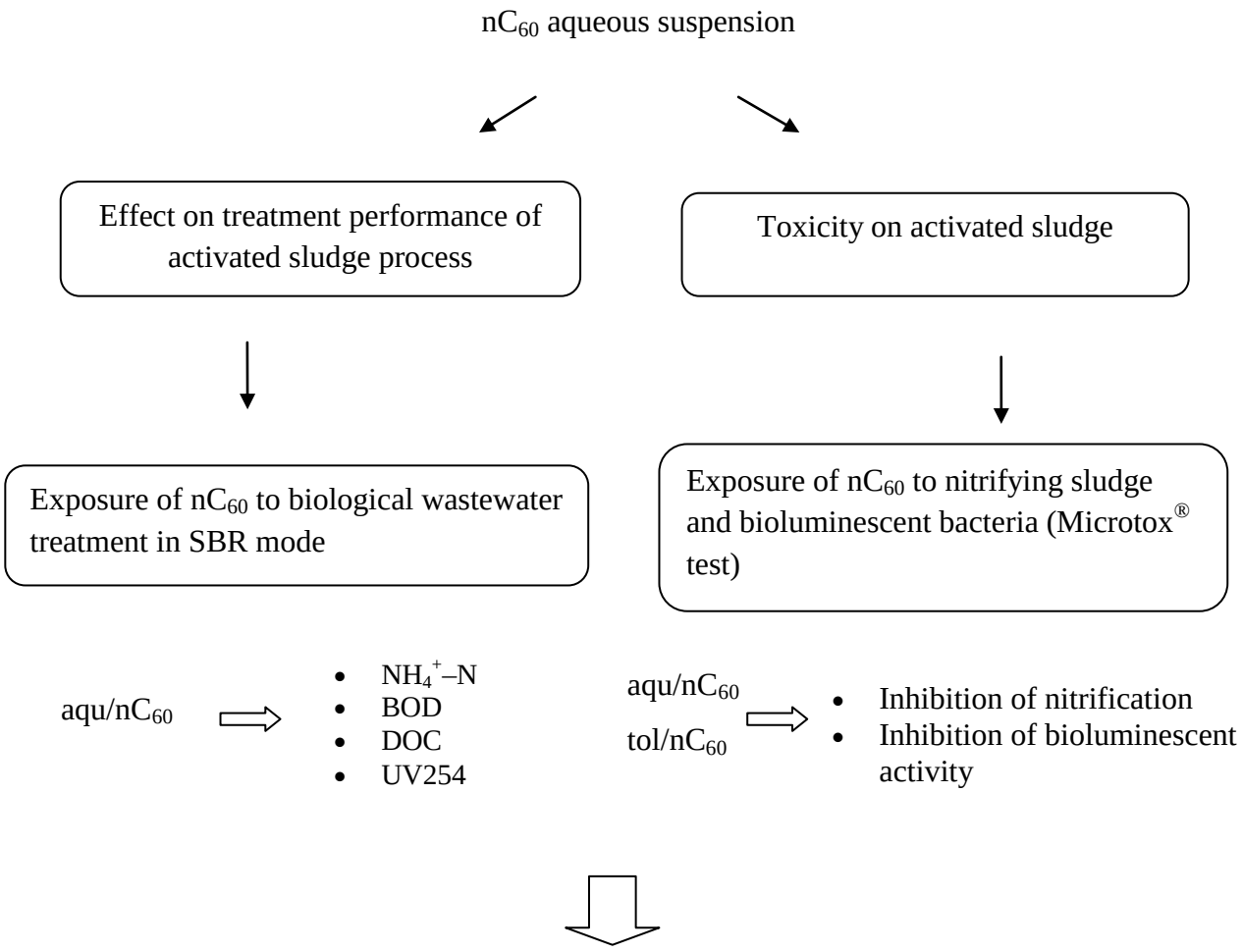

Fig. 5. 1 The content structure of this chapter.

5.2 Materials and methods

5.2.1 Preparation of nC_{60} aqueous suspensions

Two types of nC_{60} aqueous suspensions were prepared using the extended mixing of powder C_{60} in water (aqu/nC_{60}) and the toluene-involved solvent exchange method (tol/nC_{60}). The procedures were detailed in Chapter III.

5.2.2 Sequencing batch reactor operation and nC_{60} exposure

The effect of aqu/nC_{60} on activated sludge process was investigated using three same sequencing batch reactors (SBR). The reactors had a working volume of 800 mL. They were inoculated with ~ 2000 mg/L of mixed liquor suspended solids collected from a conventional activated sludge treatment plant. The DO concentration was kept at the level of 2.5 to 5.0 mg/L by passing the CO_2-free air produced using an B4000 air compressor (Nisso, Japan) connected with two washing bottles (0.1 N NaOH and Milli-Q water). The liquor in reactors was mechanically mixed at 120 rpm using a NZ-1300 motor (EYELA, Japan). The feed solution was the primary effluent collected from the same wastewater treatment plant as the activated sludge. It had a BOD of ~88 mg/L and NH_4^+–N of ~14 mg/L. The SBR rectors were worked at 25 °C with an operational condition as follows: the hydraulic residence time (HRT) was 12 h including the 10 h of aeration time, 1.5 h for settlement, 0.25 h for the refill and 0.25 h for the decant. At each cycle, after the settlement 560 mL supernatant was decant from the reactor followed by refilling with equal fresh primary effluent. The reactors' state was monitored by measuring the NH_4^+–N, BOD, DOC, and UV 254 in the treated effluent as well as the MLSS concentration. During the acclimation period, 80 mL of mixed suspended solid was collected from the reactors for the MLSS measurement every two days. After reaching the steady state, the reactors were exposed to the nC_{60} by spiking them into the feed solution for each cycle. Three SBR reactors were run at two exposure levels of nC_{60} (0.100 and 0.500 mg/L) and a blank control.

5.2.3 Cultivation of nitrifying activated sludge

The seed activated sludge was collected from the nitrification tank of an activated sludge treatment plant. The nitrifying activated sludge was obtained by cultivating the seed sludge at 30 °C in a 3 L water-jacketed glass reactor. The reactor was operated at fill and draw mode at a HRT of 12 h and SRT of 20 days in the dark. The dissolved oxygen (DO) was kept at above 1.0 mg/L by introducing the filtered compressed air via diffusers and the pH was maintained at 7.5 ± 0.1 with the automatic addition of 1 M Na_2CO_3. The feed solution only consisted of the inorganic medium (25 mM $(NH_4)_2SO_4$). The other nutrient composition, data acquisition and process control were described in the previous study (Ghosh et al., 2009). After reaching the steady state by checking the NH_4^+ removal efficiency, the mixed liquor in the reactor was collected and washed three times using 40 mM KH_2PO_4 buffer (pH 7.8) by centrifugation (2000 *g*×5 min).

5.2.4 Nitrification inhibition experiment

The nitrification inhibition studies were conducted in accordance with the ISO 9509 test guideline (ISO 9509, 2006). Batch experiments were carried out by agitating 100−mL Erlenmeyer flasks containing 50 mL medium solution (2 mM $(NH_4)_2SO_4$, 6 mM ($NaHCO_3$) and 2 mM KH_2PO_4 buffer), determined nitrifying activated sludge and different amounts of nC_{60} at controlled room temperature (25 °C). The experimental conditions, the incubating time of 3 h and MLSS of 40 mg/L, were determined to ensure about 50% of initial NH_4^+−N was left at the end of incubating time to avoid rate-limiting (ISO 9509, 2006). The DO was kept at above 4 mg/L by the shaking (150 rpm) on a rotary shaker. The nitrification inhibition (*I*) was calculated by the difference of oxidized N formation (NO_3^- and NO_2^-) between the control and the nC_{60} exposure test after 3 h. The equation is given as,

$$I\ (\%) = (N_c - N_f)/(N_c - N_i) \times 100 \qquad (5.1)$$

where N_c (mg–N/L) is the concentration of oxidized N in the control flask after 3 h, N_f (mg−N /L) is the concentration of oxidized N in the flask containing nC_{60} after 3 h, N_i (mg−N /L) is the concentration of oxidized N in the flask containing the reference inhibitor of *N*-allylthiourea (ATU). The EC_{20}, nC_{60} concentration with a

reduction of oxidized N formation by 20%, was calculated using the SPSS probit regression analysis (SPSS, USA).

5.2.5 Microtox® test

The *V. fischeri* bioassay is also used for assessing the toxicity of compounds on the activated sludge (Dalzell et al., 2002; Ren, 2004) which is based on the decrease in bioluminescence from the bacterium due to the exposure to the toxicants. The experiment was carried out using a Model 500 luminometer (Azur Environmental, USA) in accordance with the Microtox® acute toxicity procedure (Azur, 1995). The reagent (freeze-dried *V. fischeri*) and the solutions (diluent, reconstitution and osmotic adjusting solution) were purchased from Strategic Diagnostics Inc., USA. The EC_{20}, nC_{60} concentration with a reduction of bioluminescence by 20%, was calculated at each test with different exposure periods (5, 15 and 30 min) using the Microtox® Omni Software (Strategic Diagnostics, USA). The phenol was used for the quality control of this test.

5.2.6 nC_{60} aggregation in the incubation medium for the toxicity test

The aggregation of nC_{60} as a function of incubation time was determined using the same medium of the toxicity tests. For the studies on the effect on SBR process, the size of nC_{60} was measured in the filtrated primary effluent up to 24 h. For the nitrification inhibition test, the nC_{60} size in medium (2 mM $(NH_4)_2SO_4$, 6 mM ($NaHCO_3$) and 2 mM KH_2PO_4 buffer) was measured after 5 min (minimum time for one measurement) and 3 h. And for the Microtox® test, the nC_{60} size in 2% NaCl solution was measured after 5, 15 and 30 min.

5.2.7 Analysis

The MLSS, SVI, BOD, DOC, UV 254, NH_4^+–N, NO_3^-–N and NO_2^-–N concentrations were determined based on the standard methods (APHA, 1999). The UV absorbance of the stock C_{60} toluene solution and nC_{60} suspension in water was measured using a UV-2500 spectrophotometer (Shimadzu, Japan). nC_{60} size was determined by the dynamic light scattering using a Zetasizer Nano ZS equipped with

a 633 nm laser source and a detection angle of 173 °C (Malvern Instruments, UK). The nC_{60} in the wastewater was quantified using HPLC-UV/vis system (LC-10AD, Shimadzu, Japan), detailed in Chapter III.

5. 3 Results and discussions

5.3.1 Characterization of prepared nC_{60}

The characteristics of prepared nC_{60} were described in Chapter III. In brief, two types of nC_{60} demonstrated very similar size distribution with an average size of 154 and 144 nm for aqu/nC_{60} and tol/nC_{60}, respectively. Both nC_{60} were negatively charged at pH 5.6. However, the ratio of UV absorbance at 260, 350 and 450 nm varied with the nC_{60} types suggesting the difference in the structure and composition of nC_{60}.

5.3.2 Effect of nC_{60} on treatment performance of the activated sludge process

5.3.2.1 Acclimation of activated sludge in SBR process

The average MLSS concentration of three reactors decreased with time during the acclimation period (**Fig. 5.2**). The reactors reached steady state after approximate three weeks and the MLSS concentration kept at ~900 mg/L from the initial 1738 mg/L. And the removal efficiencies of DOC, BOD, and UV 254 in wastewater by SBR reached up to around 85, 98 and 63%, respectively. And the concentrations in the treated wastewater were around 5 mg/L, 2 mg/L and 0.1 cm^{-1} for the DOC, BOD, and UV 254, respectively (**Fig. 5.3**). No NH_4^+–N was detected in treated wastewater after three weeks.

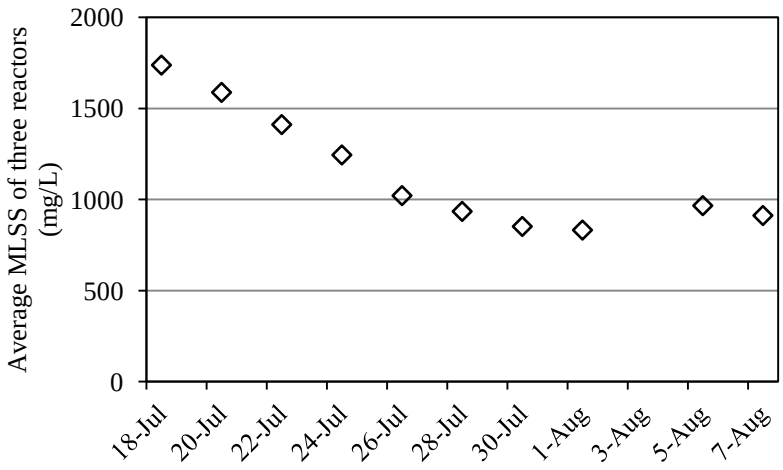

Fig. 5. 2 Change in average MLSS concentration in three reactors over time during the acclimation period.

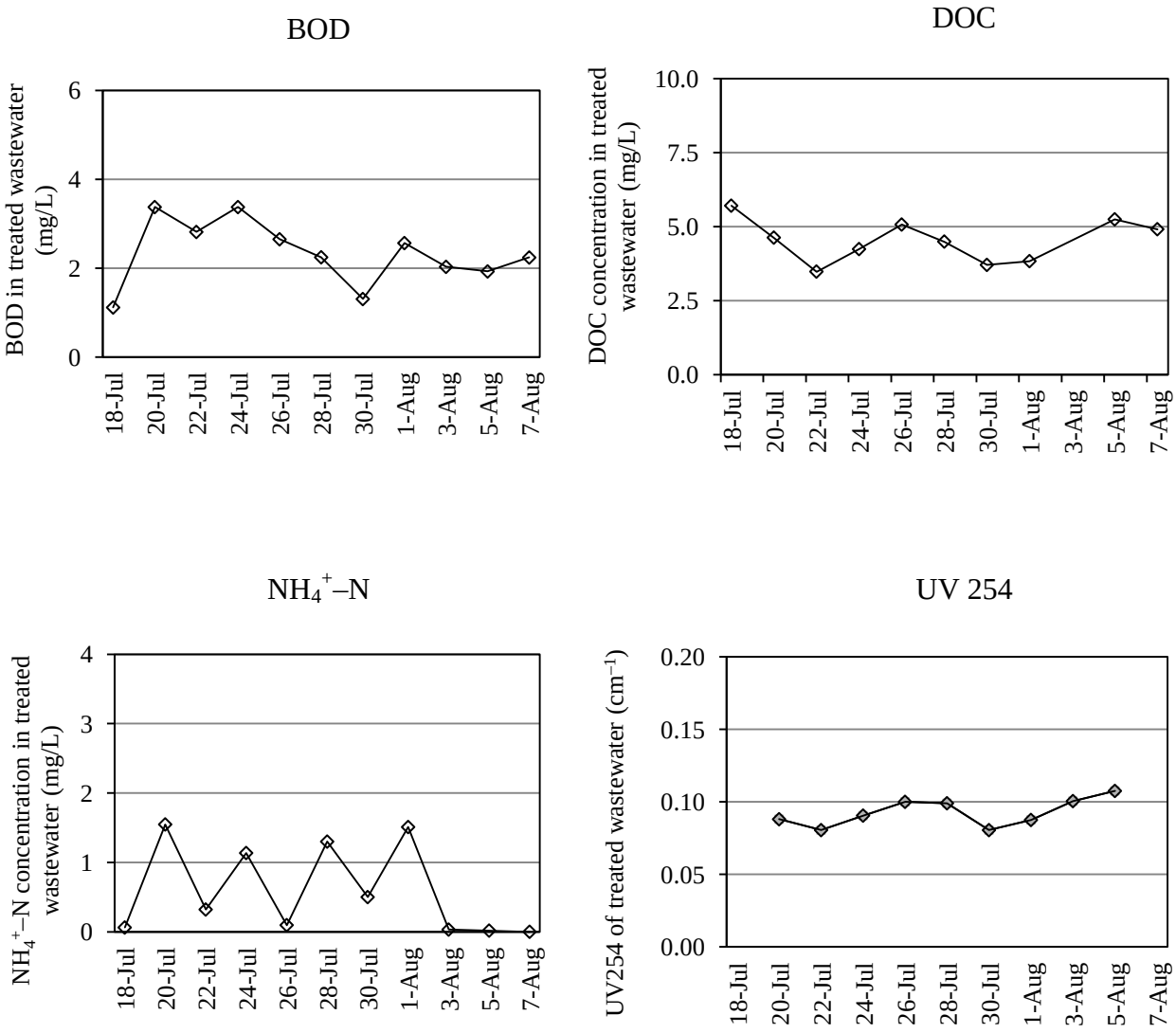

Fig. 5. 3 Water quality of treated wastewater from SBR reactors during the acclimation period.

5.3.2.2 Effect of nC_{60} on treatment performance

The nC_{60} exposure started after the reactor reached the steady state. The average BOD in treated wastewater during the 10-day nC_{60} exposure period were calculated to be 2.303, 2.195 and 2.211 mg/L in the Blank, 0.100 mg/L- and 0.500 mg/L-exposure reactors, respectively (**Fig. 5.4**). The average values of UV 254 were 0.093, 0.094 and 0.092 cm^{-1} for three reactors. And the values for DOC were 3.712, 3.612 and 3.636 mg/L. No NH_4^+–N in treated wastewater was detected from three reactors. According to one-way analysis of variance, there was no significant difference for BOD, UV 254, and DOC between the nC_{60} exposure- and blank-reactors. Therefore under the conditions (exposure concentration and contact time) studied, no negative effect of nC_{60} was found on the treatment performance for the organic matter in wastewater.

Although the recent studies showed the antibacterial properties of nC_{60}, it is still under debate on the toxicity mechanism and the effect of introduced impurity during the nC_{60} preparation (Li et al., 2008). The results here presented the low toxicity of nC_{60} prepared by extended mixture technique. Lyon et al. (2006) found the toxicity of nC_{60} strongly depended on preparation methods and the aqu/nC_{60} had an obvious lower toxicity on the bacteria compared to that prepared by the tetrahydrofuran exchange method. Zhu et al. (2006) found the EC_{50} (48 h) of aqu/nC_{60} on *Daphnia magna* was higher than 35 mg/L. In addition, the extracellular polymeric substances (EPS) could protect the microorganisms from the toxicity of nanoparticles by adsorption (Comte et al., 2008; Liang et al., 2010). The no effect concentration of nC_{60} on the activated sludge might be obviously higher than the reported values based on the pure bacteria. Previous report found no significant impact was identified on the complex microorganisms community such as the microbial community structure in aerobic soil (Tong et al., 2007) and anaerobic sludge (Nyberg et al., 2008).

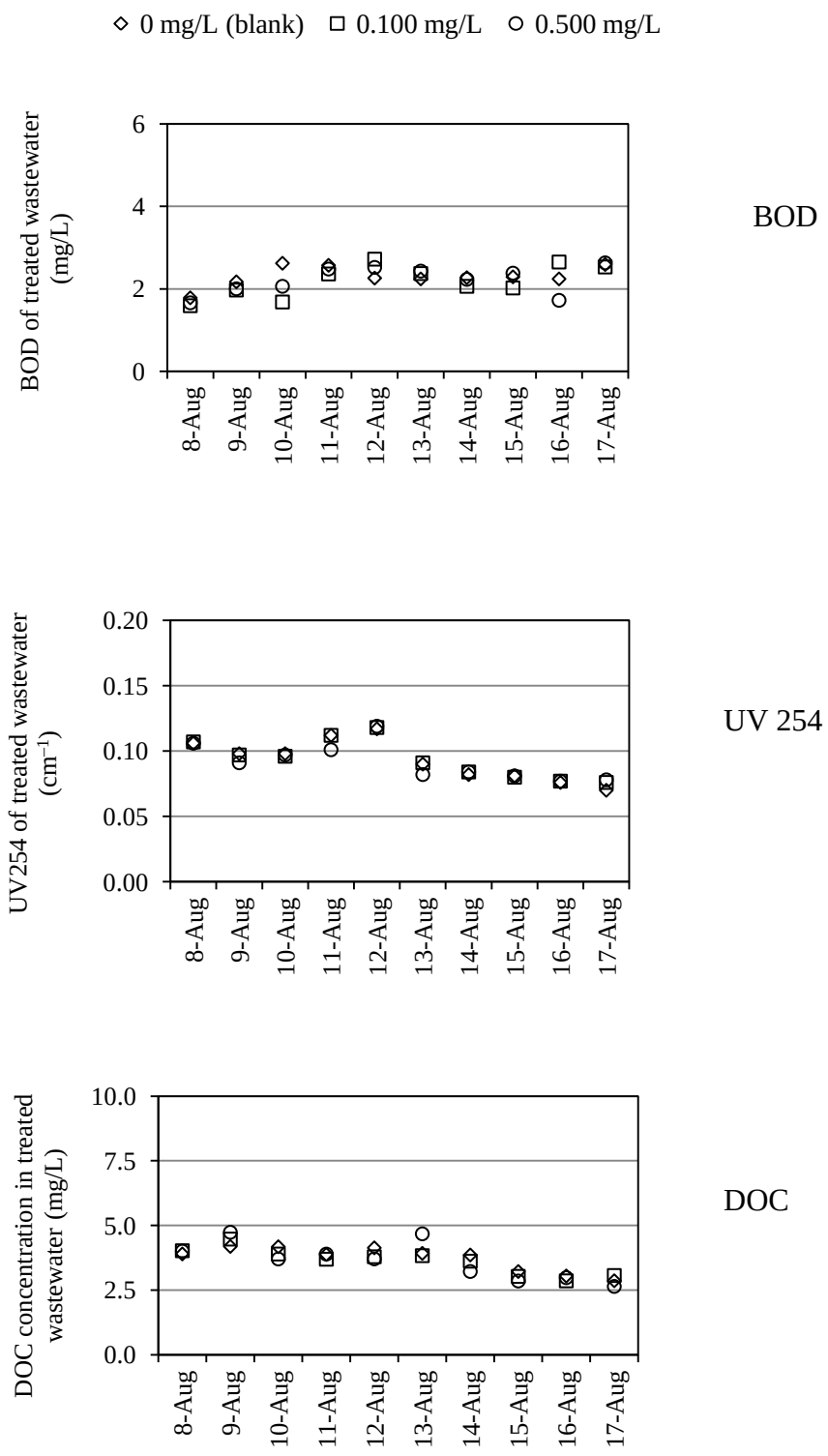

Fig. 5. 4 Water quality of treated wastewater from SBR reactors during nC_{60}-exposure period.

5.3.2.3 Effect of nC_{60} on activated sludge in SBR process

The effect of nC_{60} on sludge growth was checked by calculating the percentage of growth in MLSS concentration after 10-day exposure of nC_{60}. And the effect of nC_{60} on settlement property of sludge was checked by measuring the SVI value. As shown in **Fig. 5.5,** no significant difference was found in the increased percentage of MLSS concentration after nC_{60} 10-day exposure which increased by 12.3, 10.0 and 12.5% (subtracted the adsorbed nC_{60}), for the blank, 0.100 mg/L- and 0.500 mg/L-exposure reactors. **Fig. 5.6** showed almost consistent SVI values of activated sludge before and after nC_{60} exposure in three reactors. Both results above indicated the nC_{60} had no significantly negative effect on the activated sludge under the conditions (i.e., exposure concentration and contact time) studied here.

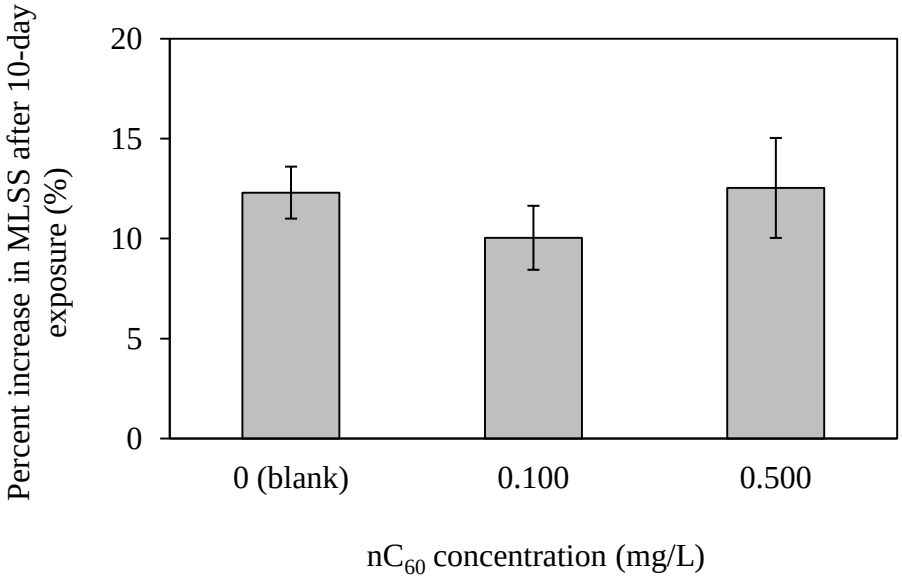

Fig. 5. 5 Percent increase in MLSS concentration after 10-day exposure of nC_{60}.

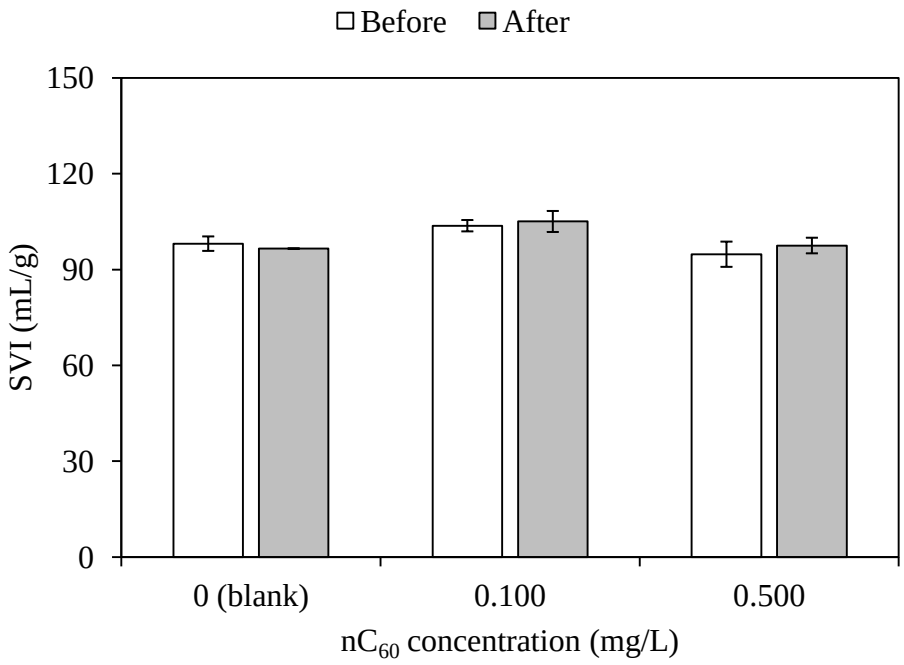

Fig. 5. 6 Change in SVI of activated sludge before and after 10-day exposure of nC_{60}.

5.3.2.4 Adsorption of nC_{60} in the activated sludge

And the nC_{60} adsorption in activated sludge was calculated from the mass balance between the accumulated nC_{60} amount in the exposure reactor and that in the reference reactor. The reference reactor was feed with the wastewater as the exposure reactor but without the activated sludge, to check the nC_{60} losses such as by adsorption to the glassware of reactors. It was calculated to be 7.63 mg (nC_{60})/g (MLSS) for the adsorption amount in the activated sludge at the exposure level of 0.500 mg/L nC_{60} after 10 days. As discussed in the sections above, this adsorption level showed no significant toxicity on the activated sludge. This result was comparable to the published work by Nyberg et al. (2008) that there was no significant effect on the anaerobic sludge at exposure level of 50 mg (nC_{60})/g (anaerobic sludge).

5.3.3 Effect of nC_{60} on nitrification activity.

The sludge nitrification activity and test performance were confirmed using the ATU. The EC_{50} was calculated to be 0.040 mg/L from the data (**Fig. 5.7**) which was close to the published value of 0.025 mg/L (Cui et al., 2005). **Fig. 5.8** shows the

percent nitrification inhibition by two types of nC_{60} at varying concentrations after 3 h, as well as the blank sample for tol/nC_{60}. For the aqu/nC_{60}, no nitrification inhibition was observed up to 8.4 mg/L indicating its low toxicity on nitrifying activated sludge. In the case of the tol/nC_{60}, no obvious effect was found in the blank sample (less than 2%). But ~40% nitrification was inhibited at 8.40 mg/L and the EC_{20} was calculated to 4.89 mg/L for tol/nC_{60}. It clearly showed that the nC_{60} toxicity depended on the preparation method. Kim et al. (2010) found the toxicity of nC_{60} on Japanese medaka embryos dependent on the preparation method and the toxicity increased as an order of toluene exchange (tol/nC_{60}) > DMSO dissolving (DMSO/nC_{60}) > stirring overtime (aqu/nC_{60}).

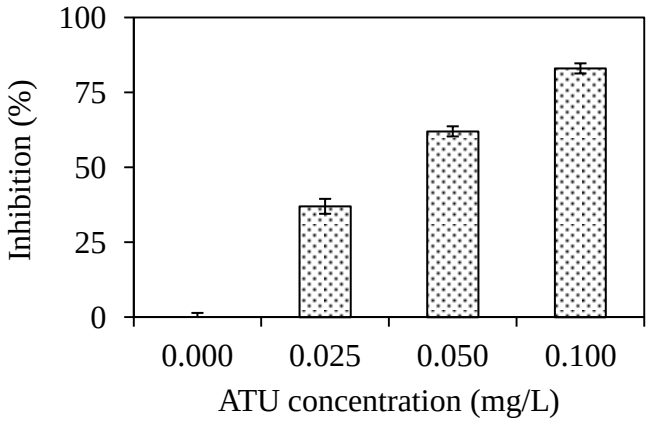

Fig. 5. 7 Nitrification inhibition as a function of ATU concentration.

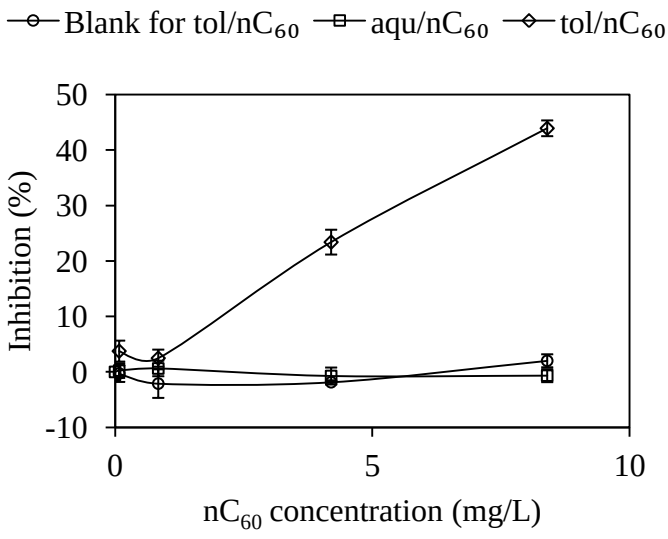

Fig. 5. 8 Nitrification inhibition of nC_{60} as a function of preparation method and exposure concentration.

5.3.4 Effect of nC_{60} on bioluminescent bacteria

Fig. 5.9 (a) shows the percent inhibition due to the exposure to aqu/nC_{60} at different concentrations. No inhibition was observed at the concentration up to 4.2 mg/L for all the incubation time. In contrast, the tol/nC_{60} showed obvious inhibition at > 1.05 mg/L and the toxicity increased with the incubation time (**Fig. 5.9 (b)**). No inhibition was also observed for the blank sample up to 30 min. The EC_{20} of tol/nC_{60} was calculated to 4.96, 4.98 and 3.44 mg/L for 5, 15 and 30 min, respectively.

Both the facts above (section 5.3.3 and 5.3.4) confirmed the low toxicity of aqu/nC_{60} and the toxicity dependent on the preparation methods. As shown in Chapter III, the ratio of UV absorbance at 260, 350 and 450 nm varied with the nC_{60} types indicating the difference in the physicochemical characteristics of nC_{60}. Brant et al. (2006) characterized the structure and chemistry of nC_{60} prepared by four methods with and without organic solvent, and reported the shape, crystal structure and chemical composition of nC_{60} depended on the preparation method even with similar size distribution. In addition, the presence of the residual solvent trapped in the centre of nC_{60} aggregate might also result in varying chemical compositions of nC_{60} (Fortner et al., 2005). Therefore, it is necessary to consider the effect of preparation methods on the physicochemical characteristics of nC_{60} when evaluating their toxicity.

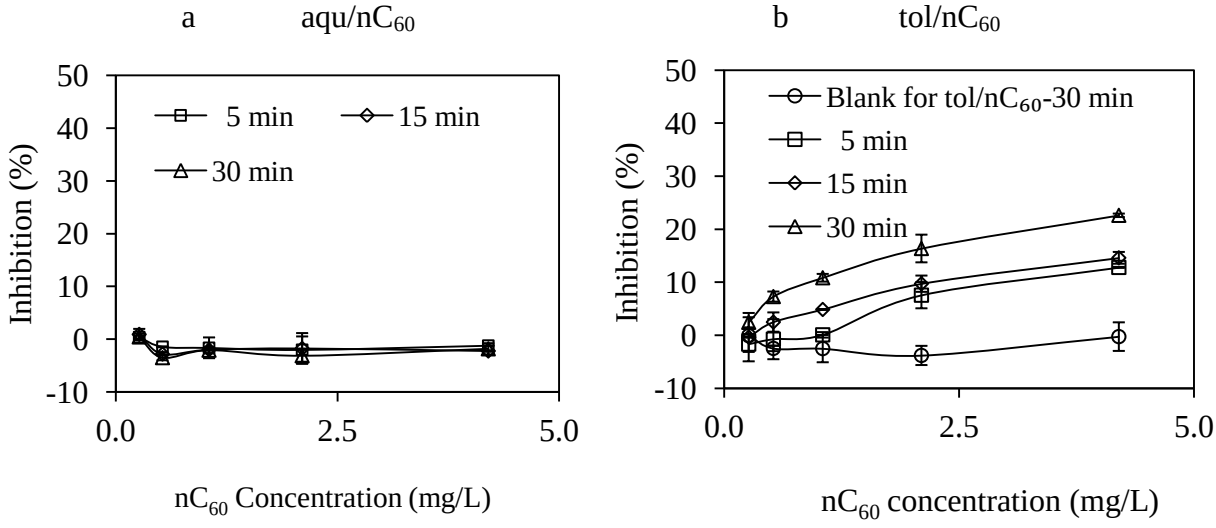

Fig. 5. 9 Bioluminescence inhibition of aqu/nC_{60} (a) and tol/nC_{60} (b) as a function of exposure time and nC_{60} concentration.

5.3.5 Aggregation of nC_{60} in toxicity test medium

The aggregate size is essential information when assessing the toxicity of nanoparticles because of proved correlation (Lyon et al., 2006; Luna-delRisco et al., 2011). The nC_{60} remained stable up to 24 h in the filtrated primary effluent, discussed in detail in Chapter IV. And **Fig. 5.10 (a)** shows the nC_{60} size with time in medium for nitrification inhibition test. After the incubation time of 3 h the aggregate remained stable with only several nm of increase in size for both nC_{60}. It can be explained by the low ionic strength of this medium (~16 mM) which was much lower than the reported threshold destabilizaiton concentraion of ~ 120 mM for the nC_{60} (Chen and Elimelech, 2009). In contrast, the obvious increase in size was found in medium with high ionic strength (~342 mM) for the Microtox® test (**Figure 5.10 (b)**). Therefore, the results obtained from the Microtox® test might be affected by the aggregation in size.

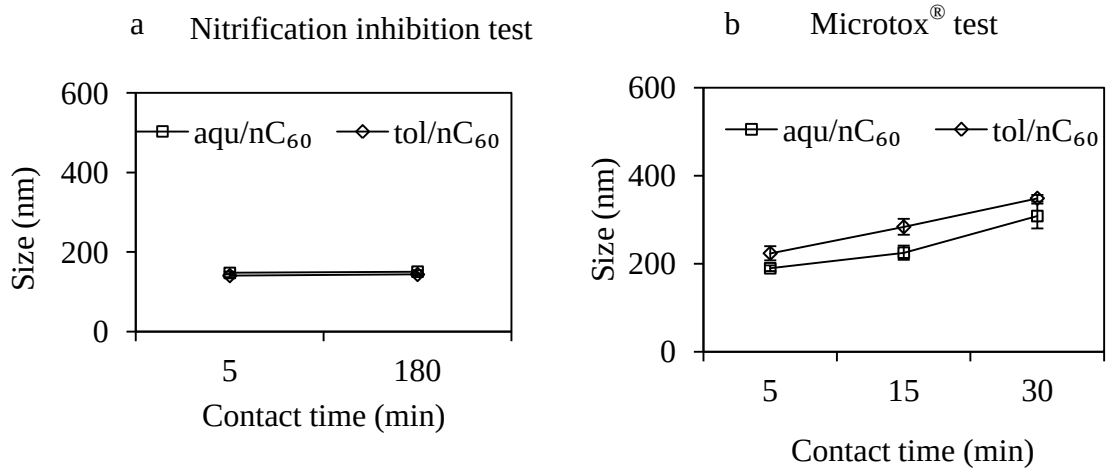

Fig. 5. 10 Change in nC_{60} size in medium for nitrification inhibition (a) and Microtox® test (b).

5.4 Conclusions

Recent studies reported the antibacterial effect of nC_{60} indicating the potential toxicity on the activated sludge. However, very few information is available on the effects of nC_{60} on treatment performance of activated sludge process. To our best knowledge, this was the first study to investigate the toxicity of nC_{60} on the

activated sludge using the nitrifying sludge which directly affects the removal of NH_4^+–N in wastewater. In this chapter, the SBR was used to investigate the effect of aqu/nC_{60} on treatment performance of activated sludge process. The toxicity of aqu/nC_{60} on activated sludge was indicated using the nitrifying sludge and bioluminescent bacteria. In addition, the tol/nC_{60} was also used to investigate the effect of preparation methods on nC_{60} toxicity. The main results as follows:

(1) After exposure of 0.100 and 0.500 mg/L nC_{60} for 10 days, no significant effect was observed on the water quality of treated wastewater by the SBR. And the analysis of sludge growth and settlement properties did not show significant toxicity of the nC_{60} on the activated sludge under the conditions tested in this study. It might be due to the low toxicity of aqu/C_{60} prepared by the extended mixture technique, and the protection effect of great extracellular polymeric substances on the activated sludge from nC_{60} toxicity. According to the mass balance, the adsorption amount of nC_{60} was calculated to be 7.63 mg (nC_{60})/g (MLSS) at the exposure level of 0.500 mg/L nC_{60} after 10 days. Therefore at this adsorption level the nC_{60} showed no significant effect on the treated performance by the SBR and the activated sludge.

(2) The aqu/nC_{60} presented no significant toxicity to the nitrification sludge and bioluminescent bacteria at 8.4 mg/L (maximum concentration studied). In contrast, the EC_{20} of tol/nC_{60} was obtained to be 4.89 mg/L (3 h) for the nitrification inhibition and 3.44 mg/L (30 min) for Microtox® test, respectively. Both the nitrification inhibition and Microtox® test showed the nC_{60} toxicity was greatly affected by the preparation method. This might be attributed to the difference in the physicochemical characteristics of nC_{60} prepared by different methods. Therefore, it is necessary to consider the effect of preparation methods on the physicochemical characteristics of nC_{60} when evaluating their toxicity.

(3) The nC_{60} could keep stable in feed solution of SBR process and in mediums of nitrification inhibition test during the incubation periods. In contrast, the nC_{60} size increased by around one time after 30 min of incubation in the Microtox® test due to high ionic strength. Therefore, the results obtained from the Microtox® test might be affected by the aggregation in size.

5.5 References

Brant, J.A., Labille, J., Bottero, J.Y., Wiesner, M.R., 2006. Characterizing the impact of preparation method on fullerene cluster structure and chemistry. Langmuir 22 (8), 3878–3885.

Chen, K.L., Elimelech, M., 2009. Relating colloidal stability of fullerene (C_{60}) nanoparticles to nanoparticle charge and electrokinetic properties. Environmental Science & Technology 43 (19), 7270–7276.

Comte, S., Guibaud, G., Baudu, M., 2008. Biosorption properties of extracellular polymeric substances (EPS) towards Cd, Cu and Pb for different pH values. Journal of Hazardous Materials 151 (1), 185–93.

Cui, R., Chung, W.J., Jahng, D., 2005. A rapid and simple respirometric biosensor with immobilized cells of Nitrosomonas europaea for detecting inhibitors of ammonia oxidation. Biosensors & Bioelectronics 20 (9), 1788–1795.

Dalzell, D.J.B., Alte, S., Aspichueta, E., de la Sota, A., Etxebarria, J., Gutierrez, M., Hoffmann, C.C., Sales, D., Obst, U., Christofi, N., 2002. A comparison of five rapid direct toxicity assessment methods to determine toxicity of pollutants to activated sludge. Chemosphere 47 (5), 535–545.

Fang, J.S., Lyon, D.Y., Wiesner, M.R., Dong, J.P., Alvarez, P.J.J., 2007. Effect of a fullerene water suspension on bacterial phospholipids and membrane phase behavior. Environmental Science & Technology 41 (7), 2636–2642.

Fortner, J.D., Lyon, D.Y., Sayes, C.M., Boyd, a M., Falkner, J.C., Hotze, E.M., Alemany, L.B., Tao, Y.J., Guo, W., Ausman, K.D., Colvin, V.L., Hughes, J.B., 2005. C_{60} in water: nanocrystal formation and microbial response. Environmental Science & Technology 39 (11), 4307–4316.

Ganesh, R., Smeraldi, J., Hosseini, T., Khatib, L., Olson, B.H., Rosso, D., 2010. Evaluation of nanocopper removal and toxicity in municipal wastewaters. Environmental Science & Technology 44 (20), 7808–7813.

Ghosh, G.C., Okuda, T., Yamashita, N., Tanaka, H., 2009. Occurrence and elimination of antibiotics at four sewage treatment plants in Japan and their effects on bacterial ammonia oxidation. Water Science and Technology 59 (4), 779–786.

Kang, S., Mauter, M.S., Elimelech, M., 2009. Microbial cytotoxicity of carbon-based nnomaterials: implications for river water and wastewater effluent. Environmental Science & Technology 43 (7), 2648–2653.

Kim, K.T., Jang, M.H., Kim, J.Y., Kim, S.D., 2010. Effect of preparation methods on toxicity of fullerene water suspensions to Japanese medaka embryos. Science of the Total Environment 408 (22), 5606–5612.

Li, Q., Mahendra, S., Lyon, D.Y., Brunet, L., Liga, M.V., Li, D., Alvarez, P.J.J., 2008. Antimicrobial nanomaterials for water disinfection and microbial control: potential applications and implications. Water Research 42 (18), 4591–4602.

Liang, Z.H., Das, A., Hu, Z.Q., 2010. Bacterial response to a shock load of nanosilver in an activated sludge treatment system. Water Research 44 (18), 5432–5438.

Luna-delRisco, M., Orupold, K., Dubourguier, H.C., 2011. Particle-size effect of CuO and ZnO on biogas and methane production during anaerobic digestion. Journal of Hazardous Materials 189 (1-2), 603–608.

Lyon, D.Y., Adams, L.K., Falkner, J.C., Alvarez, P.J.J., 2006. Antibacterial activity of fullerene water suspensions: effects of preparation method and particle size. Environmental Science & Technology 40 (14), 4360–4366.

Lyon, D.Y., Brunet, L., Hinkal, G.W., Wiesner, M.R., Alvarez, P.J.J., 2008. Antibacterial activity of fullerene water suspensions (nC_{60}) is not due to ROS-mediated damage. Nano Letters 8 (5), 1539–1543.

Lyon, D.Y., Fortner, J.D., Alvarez, P.J., 2005. Fullerene water suspensions display antibacterial properties. Abstracts of Papers of the American Chemical Society 230, U1522–U1522.

Mu, H., Chen, Y.G., Xiao, N.D., 2011. Effects of metal oxide nanoparticles (TiO_2, Al_2O_3, SiO_2 and ZnO) on waste activated sludge anaerobic digestion. Bioresource Technology 102 (22), 10305–10311.

Nyberg, L., Turco, R.F., Nies, L., 2008. Assessing the impact of nanomaterials on anaerobic microbial communities. Environmental Science & Technology 42 (6), 1938–1943.

Radniecki, T.S., Stankus, D.P., Neigh, A., Nason, J.A., Semprini, L., 2011. Influence of liberated silver from silver nanoparticles on nitrification inhibition of *nitrosomonas europaea*. Chemosphere 85 (1), 43–49.

Ren, S.J., 2004. Assessing wastewater toxicity to activated sludge: recent research and developments. Environment International 30 (8), 1151–1164.

Sayes, C.M., Fortner, J.D., Guo, W., Lyon, D., Boyd, A.M., Ausman, K.D., Tao, Y.J., Sitharaman, B., Wilson, L.J., Hughes, J.B., West, J.L., Colvin, V.L., 2004. The differential cytotoxicity of water-soluble fullerenes. Nano Letters 4 (10), 1881–1887.

Tong, Z.H., Bischoff, M., Nies, L., Applegate, B., Turco, R.F., 2007. Impact of fullerene (C_{60}) on a soil microbial community. Environmental Science & Technology 41 (8), 2985–2991.

Zhu, S.Q., Oberdorster, E., Haasch, M.L., 2006. Toxicity of an engineered nanoparticle (fullerene C_{60}) in two aquatic species, Daphnia and fathead minnow. Marine Environmental Research 62, S5–S9.

Chapter VI

MODELLING THE FATE OF nC_{60} IN THE ACTIVATED SLUDGE PROCESS

6.1 Introduction

With the rapid increase in the consumption and production of nC_{60} nanoparticles, they will inevitability enter into the environment via intended or unintended manner (Li et al., 2008). The wastewater treatment plant might be the potential barrier to prevent these nanoparticles from discharge into water environment. One study estimated the environmental concentration of nC_{60} to be ng/L level in the treated wastewater (Gottschalk et al., 2009). Farre et al. (2010) reported the nC_{60} concentration in the µg/L level in the suspended solids of wastewater effluent, although no information was determined on their origins. However, it is still unclear about the fate of nC_{60} during the wastewater treatment process partially due to the limit on the analytical techniques for quantifying the nC_{60} in the environmental samples. Therefore, the modelling method combined the data from batch experiment is a promising way to estimate the fate and potential risk of nC_{60} during the wastewater treatment process.

The objective of this study was to estimate the nC_{60} fate in the activated sludge process at the level of environmental concentrations using a fate model. The Freundlich adsorption coefficients were used to determine the nC_{60} concentration in the treated effluent and excess sludge. The effects of HRT, SRT and MLVSS on the nC_{60} treatment were investigated, as well as the relative contribution of each unit (i.e., primary and secondary treatments) for the nC_{60} removal. In addition, the risk assessments for the nC_{60} toxicity to the water environment and activated sludge were also conducted by comparing the results from the fate model with the calculated predicted no effect concentrations (PNEC) values.

6.2 Description of fate model

6.2.1 Fate model

This model was generally used for the fate studies of hydrophobic chemical in the activated sludge process. A steady-state mass balance was established by each process during the wastewater treatment as follows (Rittmann and McCarty, 2001; Benn and Westerhoff, 2008),

$$\text{In} = \text{Volatilization} - \text{Adsorption} - \text{Biodegradation} - \text{Out} \quad (6.1)$$

According to the properties of nC_{60}, the removal due to the volatilization and biodegradation could be neglected. So the mass balance equation could be simplified into,

$$\text{In} = \text{Adsorption} - \text{Out} \quad (6.2)$$

In this study, the model was developed by introducing the primary treatment. The mass balance could be separated into two control volumes, i.e., primary and secondary treatments, as shown in **Fig. 6.1.**

For the primary treatment, the mass balance was as follows,

$$\text{In} = \text{Adsorption (excess primary sludge)} - \text{Out (primary effluent)} \quad (6.3)$$

By introducing the parameters, and the two phases (liquid and solid) in primary effluent, the Eq. (6.3) was changed into,

$$Q \times C_0 = Q \times C_{L1} + Q \times SS_1 \times C_{SS1} + Q \times (SS_0 - SS_1) \times C_{EPS} \quad (6.4)$$

The meanings of all the parameters were explained in **Fig. 6.1**. The Freundlich coefficient was used as the portioning coefficient for the nC_{60} between the liquid phase and solid phase (suspended solid) in influent. According to the results of Chapter IV, the Freundlich model could well fit the experimental data of nC_{60} adsorption on primary sludge. Although the HRT of primary clarifier tank is usually in the range of 1 to 5 h, which is shorter than the equilibrium time of 12 h for the nC_{60} adsorption on the primary sludge, the equilibrium has been already reached during the wastewater discharge from the source to WWTP. Therefore, it is the steady-state system in the primary clarifier tank. And the nC_{60} concentration in the suspended solids in the primary effluent (C_{SS1}) equals that in the excess primary sludge (C_{EPS}). By introducing the Freundlich coefficient for the primary sludge (k_1) and the removal efficiency of suspended solids during the primary treatment (R_{SS}), the Eq (6.4) was changed into,

$$C_0 = C_{L1} + SS_0 \times (1–R_{SS}) \times k_1 \times C_{L1}^{1/n1} + SS_0 \times R_{SS} \times k_1 \times C_{L1}^{1/n1} \quad (6.5)$$

For the secondary treatment, the mass balance was as follows,

Out (primary effluent) = Adsorption (excess activated sludge) + Out (secondary effluent) (6.6)

The removal by adsorption in the excess activated sludge (EAS) was equal to the density of the compound in the activated sludge times the sludge wasting rate. By introducing the parameters and two phases (liquid and solid), the Eq. (6.6) was changed into,

$$Q \times C_{L1} + Q \times SS_1 \times C_{SS1} = Q \times C_{L2} + Q \times SS_2 \times C_{SS2} + (MLVSS \times V \times C_{EAS})/SRT \quad (6.7)$$

The Freundlich coefficient was also used as the portioning coefficient here. According to the results of Chapter IV, the Freundlich model could well fit the experimental data of nC_{60} adsorption on activated sludge. The HRT (5 – 12 h) of secondary treatment was usually shorter than the equilibrium time of 12 h for the nC_{60} adsorption on the activated sludge. However, according to the adsorption kinetics (Fig. 4.2.2) in Chapter IV, at a lower initial nC_{60} concentration, the adsorption of nC_{60} on the activated sludge reached equilibrium sooner. For the initial nC_{60} concentration of 0.100 and 0.300 mg/L, the adsorption has already reached the equilibrium after around 6 h. The environmental concentration was estimated to be further lower than this level, so the nC_{60} adsorption on the activated sludge could also reach equilibrium during the conventional HRT. And the nC_{60} concentration in the suspended solid in the secondary effluent (C_{SS2}) equals that in the excess activated sludge (C_{EAS}). Then the Eq. (6.7) was changed into,

$$Q \times C_{L1} + Q \times SS_1 \times k_1 \times C_{L1}^{1/n1} = Q \times C_{L2} + Q \times SS_2 \times k_2 \times C_{L2}^{1/n2} + (MLVSS \times V \times C_{EAS})/SRT \quad (6.8)$$

By introducing the HRT and SS_0, the equation was arranged into,

$$C_{L1} + SS_0 \times (1 – R_{SS}) \times k_1 \times C_{L1}^{1/n1} = C_{L2} + SS_2 \times k_2 \times C_{L2}^{1/n2} + (MLVSS \times HRT \times k_2 C_{L2}^{1/n2})/SRT \quad (6.9)$$

Here the SS_0 and SS_2 were set to be 0.15 g/L and 0.002 g/L, respectively, according to the operational conditions of WWTPs where the samples were collected in the former chapters. And then the Eqs (6.5) and (6.9), were changed into,

$$C_0 = C_{L1} + 0.15 \times (1–R_{SS}) \times k_1 \times C_{L1}^{1/n1} + 0.15 \times R_{SS} \times k_1 \times C_{L1}^{1/n1} \quad (6.10)$$

$$C_{L1} + 0.15 \times (1 - R_{SS}) \times k_1 \times C_{L1}^{1/n1} = C_{L2} + 0.002 \times k_2 \times C_{L2}^{1/n2} + (MLVSS \times HRT \times k_2 C_{L2}^{1/n2})/SRT \quad (6.11)$$

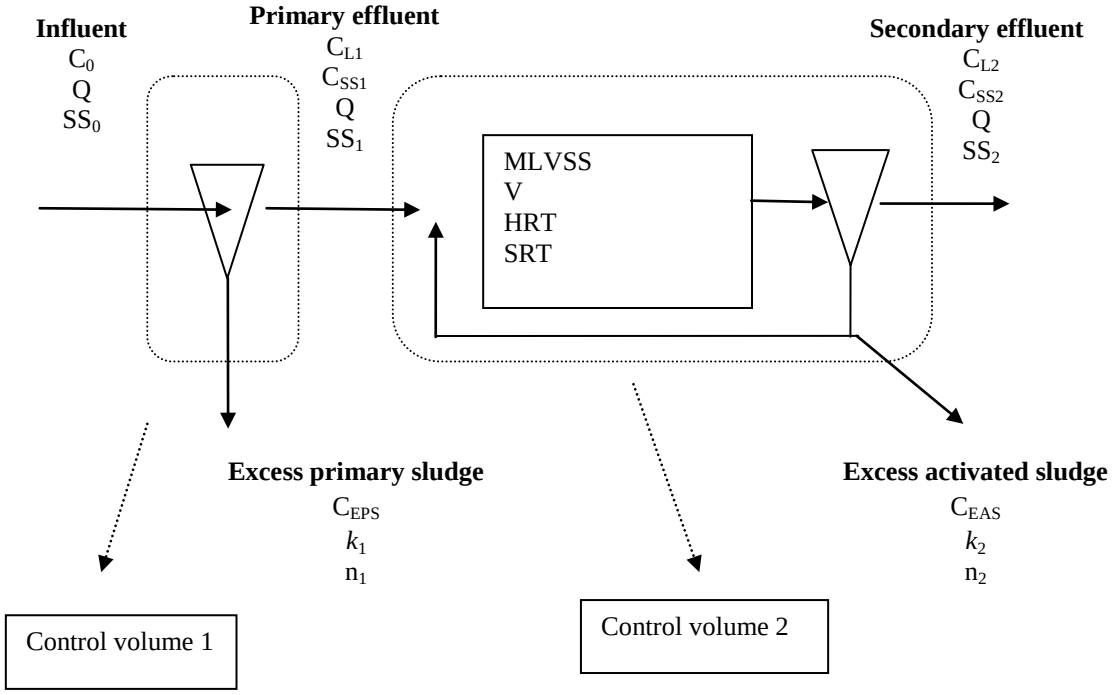

Fig. 6. 1 The schematic of conventional activated sludge process**.**

C_0: the nC_{60} concentration in influent (mg/L)

Q: the influent flow rate (L/day)

SS_0: the suspended solid concentration in influent (g/L)

C_{L1}: the nC_{60} concentration in the liquid phase of primary effluent (mg/L)

C_{SS1}: the nC_{60} concentration in the suspended solid of primary effluent (mg/L)

SS_1: the suspended solid concentration in primary effluent (g/L)

C_{L2}: the nC_{60} concentration in the liquid phase of secondary effluent (mg/L)

C_{SS2}: the nC_{60} concentration in the suspended solids of secondary effluent (g/L)

SS_2: the suspended solid concentration in secondary effluent (g/L)

C_{EPS}: the nC_{60} concentration in the primary sludge (mg/g)

k_1: the Freundlich coefficient for the nC_{60} on the primary sludge

n_1: the Freundlich constant for the nC_{60} on the primary sludge

C_{EAS}: the nC_{60} concentration in the activated sludge (mg/g)

k_2: the Freundlich coefficient for the nC_{60} on the activated sludge

n_2: the Freundlich constant for the nC_{60} on the activated sludge

MLVSS: the activated sludge concentration in the aeration tank

V: the volume of aeration tank (L)

HRT: the hydraulic retention time (h)

SRT: the sludge retention time (day)

6.2.2 Experimental design and parameters for model simulations

The ranges of different parameters were determined according to the operational conditions of WWTPs where the sludge samples were collected in this study. The suspended solid (SS) concentration in the influent was set to 0.15 g/L; the removal efficiency of SS during the primary treatment ranged from 50 to 90%; MLVSS from 1 to 3 g/L; HRT from 5 to 12 h, and SRT from 5 to 30 day. In addition, the occurrence concentration of nC_{60} in the influent was estimated to be approximate 0.020 μg/L in Japan, detailed in Chapter III. Therefore, the nC_{60} concentration in influent was set to be from 0.002 to 0.200 μg/L. The effect of SS removal on the nC_{60} removal during primary treatment was investigated. And the effects of HRT, SRT and MLVSS on nC_{60} removal during secondary treatment were also studied. When investigating the effect of one influencing factor, other factors were kept constant. And detailed parameter and experimental design for model simulation were shown in **Table 6.1.** In addition, the contribution of primary and secondary treatments on nC_{60} removal was calculated under a conventional condition of activated sludge process. The risk assessments for the nC_{60} toxicity to the water environment and activated sludge were also conducted by comparing the results from the fate model with the calculated predicted no effect concentrations (PNEC) values.

Table 6. 1 The parameters for the fate model and experimental design

Scenario	Experiment	nC_{60} conc. in influent (μg/L)	R_{SS} (%)	Primary treatment	Secondary treatment		
				MLVSS (g/L)	MLVSS (g/L)	HRT (h)	SRT (day)
Only primary treatment	Effect of SS removal	0.200	50	0.15			
		0.020	70				
		0.002	90				
Primary + Secondary treatment	Effect of HRT	0.200	70		2	5	15
		0.020				8	
		0.002				12	
	Effect of SRT	0.200	70	0.15	2	8	5
		0.020					15
		0.002					30
	Effect of MLVSS	0.200	70	0.15	1	8	15
		0.020			2		
		0.002			3		
	Contribution of each treatment unit	0.200	70	0.15	2	8	15
		0.020					
		0.002					

R_{SS} (%): Removal efficiency of suspended solid (SS) during the primary treatment.

6.3 Results and discussions

6.3.1 nC_{60} removal during the primary treatment as a function of SS removal

Fig. 6.2 shows the effect of SS removal and nC_{60} initial concentrations on the nC_{60} removal efficiency during the primary treatment. At the nC_{60} initial concentration of 0.002 µg/L and the SS concentration of 0.15 g/L in influent, the nC_{60} removal efficiency increased from 36 to 64% with the increase of SS removal from 50 to 90%. The increased removal of nC_{60} could be attributed to the increased discharge by adsorption on the excess primary sludge. The nC_{60} removal efficiency decreased as the nC_{60} initial concentration increased. According to the results in Chapter IV, the 1/n value of Freundlich model for primary sludge was 0.703 which was less than 1. It indicated at higher nC_{60} concentration at equilibrium time, the adsorption isotherm departed from linear relationship and shifted to the X axis which consequently decreased the percent removal by the adsorption on the primary sludge.

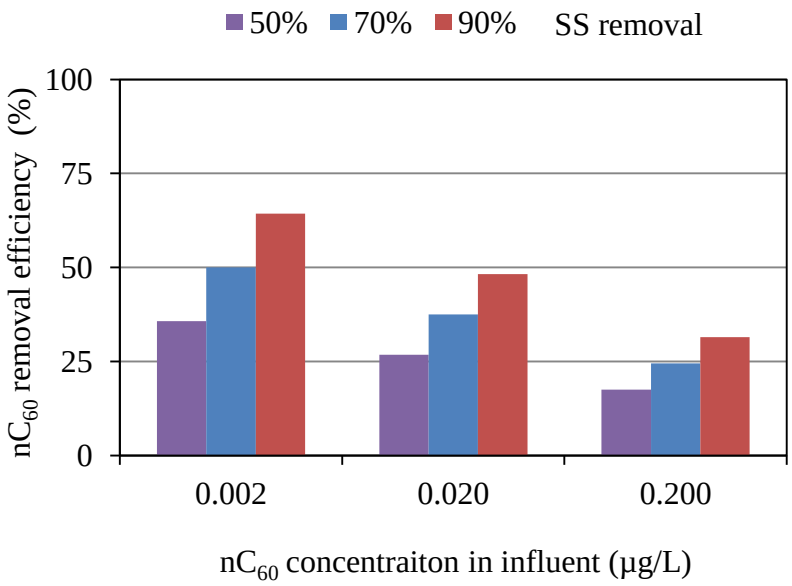

Fig. 6. 2 nC_{60} removal efficiency during the primary treatment as a function of SS removal and initial nC_{60} concentrations.

6.3.2 Effects of HRT, SRT and MLVSS on nC_{60} removal during the secondary treatment

The nC_{60} removal during the secondary treatment increased with increase in the HRT as shown in **Fig. 6.3 (a).** Here the nC_{60} adsorption on the activated sludge already reached equilibrium. Therefore, the effect of HRT on the nC_{60} removal would not be due to the change in the contact time for the adsorption. When keeping the volume of aeration tank constant, the increasing HRT decreased the influent flow rate and consequently reduced the nC_{60} load on the activated sludge and increased the removal efficiency in the activated sludge process. And **Fig. 6.3 (b)** shows the effect of SRT on the nC_{60} removal. The shorter SRT increased the nC_{60} removal by increasing the discharge of excess activated sludge, and by increasing the adsorption capacity due to the fresh activated sludge. The higher MLVSS increased the nC_{60} removal, as shown in **Fig. 6.3 (c)**, which can be attributed to the increase in the adsorption capacity due to higher concentration of activated sludge. Among all the conditions in **Fig. 6.3 (a-c),** the nC_{60} removal efficiency increased at higher initial concentrations. According to **Fig. 6.2**, the nC_{60} removal efficiency during primary treatment decreased greatly at higher nC_{60} initial concentration which resulted in the higher concentration of nC_{60} in the primary effluent. As a result, the nC_{60} adsorption on the activated sludge increased with the increase in the nC_{60} concentration in the primary effluent.

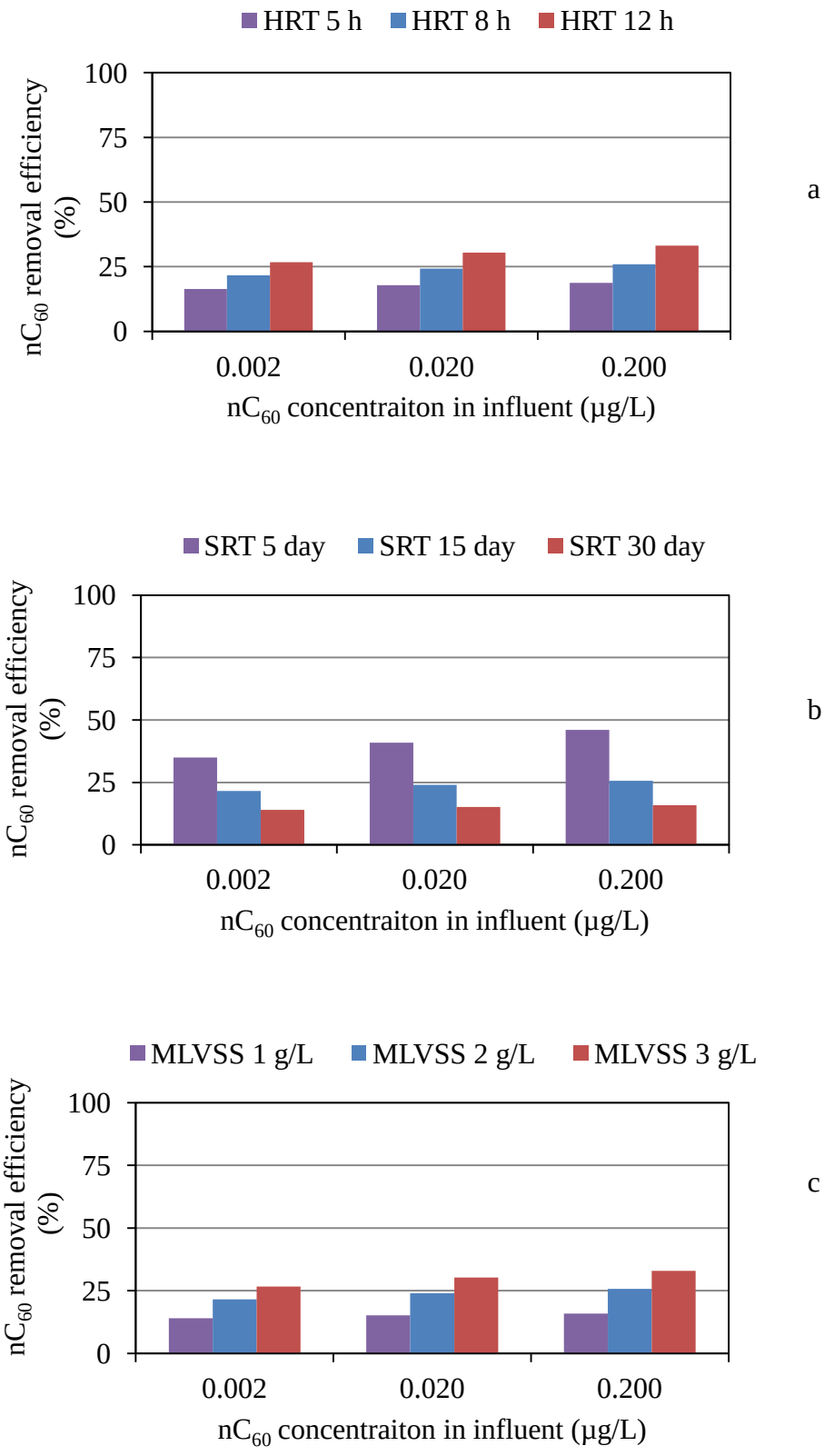

Fig. 6. 3 Effect of HRT (a), SRT (b) and MLVSS (c) on the nC_{60} removal efficiency during the secondary treatment.

6.3.3 Contribution of each unit on the nC_{60} removal in the activated sludge process

The contribution of each unit on the nC_{60} removal in the activated sludge process under a conventional operational condition was calculated at different nC_{60} initial concentrations, as shown in **Fig. 6.4.** At the initial nC_{60} concentrations of 0.002 µg/L, the nC_{60} removal efficiencies were approximate 50 and 21% during the primary and secondary treatment, respectively. And around 28 and 1% of nC_{60} remained in the liquid phase and SS in the secondary effluent. As discussed in **section 6.3.1 and 6.3.2**, the lower removal efficiency of nC_{60} during primary treatment at higher nC_{60} initial concentration resulted in the increase in nC_{60} removal efficiency during the secondary treatment, which was also seen in **Fig. 6.4.** However, the increase in nC_{60} removal efficiency during the secondary treatment was lower than the decrease in the nC_{60} removal efficiency during the primary treatment. As a result, the total removal efficiency of nC_{60} in the wastewater treatment process decreased from 72 to 50% as the nC_{60} initial concentration increased from 0.002 to 0.200 µg/L. This result showed that ~28 to 50% of nC_{60} would be released into the water environment under conventional operational condition. It indicated the potential exposure and risk of nC_{60} to the water environment and human health.

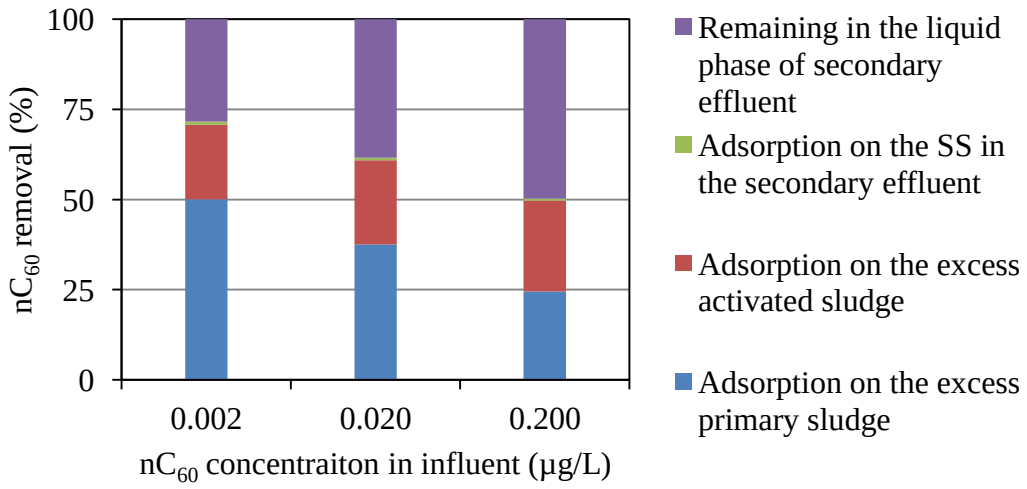

Fig. 6. 4 Contribution of each unit on the nC_{60} removal in the activated sludge process at different initial nC_{60} concentrations. Condition as follows: SS_0 0.15 g/L; R_{SS} 70%; HRT 8 h; SRT 15 day; MLVSS 2 g/L; nC_{60} 0.002, 0.020, and 0.200 µg/L.

6.3.4 Risk assessment

Table 6.2 summarized the results of nC_{60} toxicity from literature and this study. The no observed effect concentration (NOEC) of nC_{60} to *Daphina Magna* ranged from 0.18 to 0.2 mg/L, while LC_{50} was from 0.46 to >35 mg/L due to the difference in the nC_{60} structure by different preparation methods. And the NOEC of nC_{60} to the sludge ranged from 7.63 to 50 mg/g. The PNEC of nC_{60} was calculated using the lowest concentration available with the assessment factors of 1000 and 10 (Gottschalk et al., 2009; European chemical bureau, 2003). Therefore, the predicted no effect concentration (PNEC) of nC_{60} were calculated to be 0.18 µg/L and 0.763 mg/g for the aquatic organism and activated sludge, respectively. Under the operational condition of activated sludge process as shown in **Fig. 6.4**, the nC_{60} concentration in secondary effluent would not exceed the PNEC for the aquatic organism until the nC_{60} in influent increase to be 0.35 µg/L. On the other hand, if the nC_{60} concentration in influent increases to be 0.16 mg/L, the adsorption of nC_{60} in activated sludge will exceed the PNEC for the activated sludge. And the risk quotient was calculated to be lower than 1, indicating no significant risk to the water environment at current exposure and discharge level.

However, significant toxicity of nC_{60} was observed on the human cell lines at µg/L level with the LC_{50} values of 2 to 50 µg/L for human dermal fibroblasts, human liver carcinoma and neuronal astrocytes (Sayes et al., 2004; 2005). Considering the high assessment factor due to the uncertainties in extrapolation for the human being, the remaining nC_{60} in treated wastewater might pose the potential risk on the human health.

Table 6. 2 Data for nC_{60} toxicity from literature and this study

Test target	NOEC	LC_{50}	References	Assessment factor	PNEC (Calculated)
Daphnia Magna		>35 mg/L	(Zhu et al., 2006)	1000	0.18 μg/L
Daphnia Magna		0.8 mg/L			
Daphnia Magna	0.18 mg/L	0.46 mg/L	(Lovern and Klaper, 2006)		
Daphnia Magna	0.2 mg/L	7.9 mg/L			
Anaerobic sludge (digestion activity and microbial community)	50 mg/g		(Nyberg et al., 2008)	10	0.763 mg/g
Activated sludge (treatment performance and sludge properties)	7.63 mg/g		This study		

6.4 Conclusions

A fate model based on the steady-state mass balance was used to investigate the nC_{60} fate in the activated sludge process. The model was developed in this study by combing the primary treatment with secondary treatment. The Freundlich adsorption coefficients, obtained from the Chapter IV, were used to determine the nC_{60} concentration in the liquid and solid phases in wastewater. The effect of SS removal during the primary treatment on the nC_{60} removal efficiency was investigated. The effects of HRT, SRT and MLVSS were investigated as well as the relative contribution of each unit (i.e., primary and secondary treatments) for the nC_{60} removal. In addition, the risks of nC_{60} to the water environment and activated sludge were evaluated using the results from the fate model and calculated PNEC. The main conclusions as follows:

(1) The nC_{60} removal efficiency increased with increase in the SS removal during the primary treatment due to the increased discharge of nC_{60} with the excess primary sludge. At the initial nC_{60} concentration of 0.002 μg/L and the SS concentration of

0.15 g/L in influent, the nC_{60} removal increased from 36 to 64% with the increase of SS removal from 50 to 90%.

(2) The increase in HRT, MLVSS and decrease in SRT contributed to the removal of nC_{60} by increasing the discharge of excess activated sludge and adsorption capacity by the fresh sludge.

(3) Under the conventional operational condition (SS_0 0.15 g/L; R_{SS} 70%; HRT 8 h; SRT 15 day and MLVSS 2 g/L), the nC_{60} removal efficiency decreased from 50 to 24% during the primary treatment, increased from 21 to 25% during the secondary treatment as the nC_{60} initial concentration increased from 0.002 to 0.200 μg/L. However, approximate 28–50% of nC_{60} still remained in the liquid phase of secondary effluent as well as 1% of nC_{60} adsorbed on the SS in the effluent indicating the potential risk to water environment and human health.

(4) The PNEC of nC_{60} were calculated to be 0.18 μg/L and 0.763 mg/g for the aquatic organism and activated sludge, respectively. Under the conventional operational condition, the nC_{60} concentration in secondary effluent would not exceed the PNEC for the aquatic organism until the nC_{60} in influent increase to be 0.35 μg/L. If the nC_{60} concentration in influent increase to be 0.16 mg/L, the adsorption of nC_{60} in activated sludge will exceed the PNEC for the activated sludge. These exposure levels of the nC_{60} were much higher than the estimated nC_{60} concentration of 0.020 μg/L in raw wastewater based on the production amount of C_{60} nanoparticles (Chapter III). And the risk quotient was calculated to be lower than 1, indicating no significant risk to the water environment at current exposure and discharge level.

However, due to high toxicity on the human cell line (only μg/L level) and high assessment factor due to the uncertainties in extrapolation for the human being, the remaining nC_{60} in treated wastewater might pose the potential risk on human health. Also, the rapid increase in C_{60}'s application and use will increase the potential of higher exposure. Therefore it is necessary to further investigate the fate of nC_{60} during different wastewater treatment processes.

6.5 References

Benn, T.M., Westerhoff, P., 2008. Nanoparticle silver released into water from commercially available sock fabrics. Environmental Science & Technology 42 (11), 4133–4139.

European chemical bureau, 2003. Technical guidance document on risk assessment.

Farre, M., Perez, S., Gajda-Schrantz, K., Osorio, V., Kantiani, L., Ginebreda, A., Barcelo, D., 2010. First determination of C_{60} and C_{70} fullerenes and N-methylf ulleropyrrolidine C_{60} on the suspended material of wastewater effluents by liquid chromatography hybrid quadrupole linear ion trap tandem mass spectrometry. Journal of Hydrology 383 (1-2), 44–51.

Gottschalk, F., Sonderer, T., Scholz, R.W., Nowack, B., 2009. Modeled environmental concentrations of engineered nanomaterials (TiO_2, ZnO, Ag, CNT, Fullerenes) for different regions. Environmental Science & Technology 43 (24), 9216–9222.

Li, Q., Mahendra, S., Lyon, D.Y., Brunet, L., Liga, M.V., Li, D., Alvarez, P.J.J., 2008. Antimicrobial nanomaterials for water disinfection and microbial control: potential applications and implications. Water Research 42 (18), 4591–4602.

Lovern, S.B., Klaper, R., 2006. Daphnia magna mortality when exposed to titanium dioxide and fullerene (C_{60}) nanoparticles. Environmental Toxicology and Chemistry 25 (4), 1132–1137.

Nyberg, L., Turco, R.F., Nies, L., 2008. Assessing the impact of nanomaterials on anaerobic microbial communities. Environmental Science & Technology 42 (6), 1938–1943.

Rittmann, B.E., McCarty, P.L., 2001. Environmental biotechnology. McGraw-Hill Boston.

Sayes, C.M., Fortner, J.D., Guo, W., Lyon, D., Boyd, A.M., Ausman, K.D., Tao, Y.J., Sitharaman, B., Wilson, L.J., Hughes, J.B., West, J.L., Colvin, V.L., 2004. The differential cytotoxicity of water-soluble fullerenes. Nano Letters 4 (10), 1881–1887.

Sayes, C.M., Gobin, A.M., Ausman, K.D., Mendez, J., West, J.L., Colvin, V.L. (2005). Nano-C 60 cytotoxicity is due to lipid peroxidation. Biomaterials 26, 7587–7595.

Zhu, S.Q., Oberdorster, E., Haasch, M.L., 2006. Toxicity of an engineered nanoparticle (fullerene C_{60}) in two aquatic species, Daphnia and fathead minnow. Marine Environmental Research 62, S5–S9.

CHAPTER VII

CONCLUSIONS AND RECOMMENDATIONS

7.1 Conclusions

Fullerene C_{60} nanoparticles, with unique physical-chemical properties, are attracting strong commercial and scientific interest in wide fields. The growing production and use of C_{60} will inevitably result in their entry into the environment. Reported toxicity to the microorganism raises recent concerns about environmental risks and human health. The occurrence of aqueous C_{60} aggregate (nC_{60}) in cosmetics and even treated effluent showed high potential of their discharge into the water environment via the wastewater treatment plant. However, it is still unclear the fate and toxicity of the nC_{60} in the activated sludge process. This study for the first time investigated the aggregation behavior of nC_{60} in wastewater and adsorption behavior on different wastewater sludges by studying the adsorption kinetics and equilibrium, and elucidated the adsorption mechanism by correlating the nC_{60} adsorption with properties of wastewater sludges. In addition, this study investigated the toxicity of nC_{60} on the activated sludge as well as the potential effect on the performance of wastewater treatment. The main findings of this study were described by each chapter as follows:

In Chapter III, two types of nC_{60} were prepared using the toluene exchange (tol/nC_{60}) and extended stirring (aqu/nC_{60}) techniques for the fate and toxicity studies. And the nC_{60} extraction in wastewater was evaluated using the liquid-liquid extraction (LLE) or solid phase extraction (SPE) methods. And the method detection and quantification limits of nC_{60} in wastewater samples were determined using the HPLC-UV/vis system with the LLE or SPE. The main conclusions were as follows:

(1) Two types of nC_{60} demonstrated very similar size distribution with an average size of 154 and 144 nm for aqu/nC_{60} and tol/nC_{60}, respectively. Both nC_{60} were negatively charged in Milli-Q water at pH 5.6.

(2) The LLE of nC_{60} from wastewater samples could give a high recovery of > 90% and good linear correlation (R^2 > 0.99) at the concentration ranged from 2 to 500 μg/L. The method detection limit was determined to be 1.07 μg/L for wastewater samples.

(3) The SPE of nC_{60} from wastewater samples could give a recovery of > 64% and good linear correlation (R^2 > 0.99) at the concentration ranged from 0.05 to 5.17 μg/L. The method detection limit of 0.03 μg/L for wastewater samples was 10 times lower than the reported ones primarily due to the high extraction efficiency of HLB cartridge and high concentration factor.

(4) The nC_{60} concentration in the domestic influent wastewater from a domestic WWTP was measured using the optimized SPE method with HPLC-UV/vis system. The nC_{60} was not detected. Based on the annual wastewater and the production of C_{60} in Japan, the nC_{60} concentration was estimated to be 0.020 μg/L in the raw wastewater. The real concentration in the liquid phase in wastewater could be much lower, given the adsorption on the suspended solids in the raw wastewater.

Chapter IV investigated the fate of nC_{60} in the activated sludge process. It included two parts: the size aggregation of nC_{60} in wastewater, and their adsorption behavior on the wastewater sludge.

The effects of pH, ionic strength and dissolved organic matter (DOM) on nC_{60} aggregation in wastewater were studied by measuring the size, size distribution and ζ potential. The main conclusions were as follows:

(1) The nC_{60} remained relatively stable up to 24 h under environmentally relevant values of ionic strength and pH. This finding suggested the potential for nC_{60} discharge from wastewater treatment plants in effluent and subsequent long-distance transport in water environment.

(2) At high ionic strength (>100 mM) or under acidic conditions (pH 3), such as the condtions found in seawater or industrial wastewater, the absolute ζ potential of the nC_{60} was reduced to ≲20 mV from an initial ~30 mV, increasing the size of aggregates up to the micrometer scale.

(3) The nC_{60} aggregation behavior varied among wastewater samples. Compared with the aggregation behavior in the filtered secondary effluent and aeration tank liquor, that in the filtered primary effluent was obviously inhibited. The aggregation rate of nC_{60} greatly varied with the DOM amounts in water even at nearly the same ζ potential. This result clearly indicated the steric stabilization on the nC_{60} aggregation due to the DOM isolated from wastewater, in addition to electrostatic effect.

(4) These results showed the aquatic conditions could affect the aggregation behavior of nC_{60} in wastewater which might consequently influence their fate during the wastewater treatment process.

The second part investigated the adsorption behavior of nC_{60} on the different sludge samples. And the adsorption mechanism was explained by modeling the adsorption isotherm and kinetics, analyzing the correlation of nC_{60} adsorption coefficients and properties of sludge samples, as well as the effect of influencing factors on the adsorption on sludge. The main conclusion as follows:

(1) The adsorption reached equilibrium after 12 h at an MLSS level of 1000 mg/L for both the primary and activated sludges. The process well followed the Freundlich isotherm model indicating the nC_{60} adsorption occurred at multi-layer and on the heterogeneous surface of the activated sludge. The high correlation with linear partitioning model suggested the partitioning process played an important role in the adsorption process on the sludge such as the hydrophobic-hydrophobic interactions.

(2) The activated sludge had a much higher Freundlich coefficient (k_F) and linear partitioning coefficient (k_d) than those for the primary sludge indicating their higher adsorption capacity. It could be attributed to the higher hydrophobicity and lower absolute ζ potential which could contribute to the adsorption of nC_{60} by increasing the attractive force and reducing the repulsive forces, respectively.

(3) The pH values greatly affected the adsorption on the activate sludge, decreasing the adsorption of nC_{60} from 86% at pH 3 to 26% at pH 11 after 1 h of mixture. At an ionic strength of 0 to10 mM, there was no significant effect on nC_{60} adsorption. At

MLSS concentrations of 1000 and 2000 mg/L, which are common in conventional activated sludge treatment, the reduction of nC_{60} in the aqueous phase after 1 h of mixture reached up to 48 and 74%, respectively, demonstrating high removal efficiency.

(4) The adsorption mechanism was further investigated by analyzing the correlation between the adsorption coefficient and the surface properties of activated sludge samples. The adsorption coefficients of k_F and k_d showed consistent correlations with the surface properties: positive correlation with relative hydrophobicity and ζ potential, negative with sludge size. The results showed both the electrostatic repulsions and hydrophobic attractions were involved in the nC_{60} adsorption on activated sludge, as well as the sludge size.

In Chapter V, the sequencing batch reactor was used to investigate the effect of aqu/nC_{60} on treatment performance of activated sludge process. The toxicity of aqu/nC_{60} on activated sludge was indicated using the nitrifying sludge and bioluminescent bacteria. In addition, the tol/nC_{60} was also used to investigate the effect of preparation methods on nC_{60} toxicity. The main conclusions as follows:

(1) After exposure of 0.100 and 0.500 mg/L nC_{60} for 10 days, no significant effect was observed on the water quality of treated wastewater by the SBR. And the analysis of sludge growth and settlement properties did not show significant toxicity of the nC_{60} on the activated sludge under the conditions tested in this study. The adsorption amount of nC_{60} was calculated to be 7.63 mg (nC_{60})/g (MLSS) at the exposure level of 0.500 mg/L nC_{60} after 10 days. Therefore, at this adsorption level, the nC_{60} had no significant effect on the treated performance in the SBR and the activated sludge.

(2) The aqu/nC_{60} presented no significant toxicity to the nitrification sludge and bioluminescent bacteria at 8.4 mg/L (maximum concentration studied). In contrast, the EC_{20} of tol/nC_{60} was obtained to be 4.89 mg/L (3 h) for the nitrification inhibition and 3.44 mg/L (30 min) for Microtox® test, respectively. Both the nitrification inhibition and Microtox® test showed the nC_{60} toxicity was greatly affected by the preparation method. This might be attributed to the difference in

the physicochemical characteristics of nC_{60} prepared by different methods. Therefore, it is necessary to consider the effect of preparation methods on the physicochemical characteristics of nC_{60} when evaluating their toxicity.

(3) The nC_{60} could keep stable in feed solution of SBR process and in mediums of nitrification inhibition test during the incubation periods. In contrast, the nC_{60} size increased by around one time after 30 min of incubation in the Microtox® test due to high ionic strength. The results obtained from the Microtox® test might be affected by the aggregation in size. Therefore, the size aggregation in the test media needed to be considered when evaluating the toxicity.

In Chapter VI, a fate model based on the steady-state mass balance was developed by combing the primary and secondary treatment and then used to investigate the nC_{60} fate in the activated sludge process. The effect of suspended solid (SS) removal during the primary treatment on the nC_{60} removal efficiency was investigated. And this part also investigated the effects of HRT, SRT and MLVSS as well as the relative contribution of each unit (i.e., primary and secondary treatments) for the nC_{60} removal. In addition, the risk of nC_{60} to the water environment and activated sludge was evaluated using the results from the fate model and calculated predicted no effect concentrations (PNEC). The main conclusions were as follows:

(1) The nC_{60} removal efficiency increased with increase in the SS removal during the primary treatment. At the initial nC_{60} concentration of 0.002 μg/L and the SS concentration of 0.15 g/L in influent, the nC_{60} removal increased from 36 to 64% with the increase of SS removal from 50 to 90%.

(2) The increase in HRT, MLVSS and decrease in SRT could contribute to the removal efficiency of nC_{60} by increasing the discharge of excess activated sludge and adsorption capacity by the fresh sludge.

(3) Under the conventional operational conditions (SS_0 0.15 g/L; R_{SS} 70%; HRT 8 h; SRT 15 day and MLVSS 2 g/L), the nC_{60} removal efficiency decreased from 50 to 24% during the primary treatment, increased from 21 to 25% during the secondary treatment as the nC_{60} initial concentration increased from 0.002 to 0.200 μg/L. Around 28–50% of nC_{60} still remained in the liquid phase of secondary effluent as

well as 1% adsorbed on the SS in the effluent indicating the potential risk to water environment and human health.

(4) The PNEC of nC_{60} were calculated to be 0.18 μg/L and 0.763 mg/g for the aquatic organism and activated sludge, respectively. Under the conventional operational condition of activated sludge process, the nC_{60} concentration in secondary effluent and activated sludge would not exceed the PNEC until the nC_{60} in influent increases to be 0.35 μg/L and 0.16 mg/L, respectively. And the risk quotient was calculated to be lower than 1, indicating no significant risk to the water environment at current exposure and discharge level.

However, due to high toxicity of nC_{60} on the human cell line and high assessment factor due to the uncertainties in the extrapolation for the human beings, the remaining nC_{60} in treated wastewater might pose the potential risk on human health. Also, the rapid increase in C_{60}'s production and use will increase the potential of higher exposure to human beings. Therefore, it is necessary to further investigate the fate of nC_{60} during different wastewater treatment processes.

7.2 Recommendations

1) The established MQL in this study is not significantly lower than PNEC value for aquatic organisms. Need to decrease the quantification limit for the risk assessment and occurrence studies in future.

2) nC_{60} would adsorb on the wastewater sludge and suspended solid in wastewater. Therefore, the establishments of extraction and quantification methods for nC_{60} in the solid phase are recommended for better understanding the nC_{60}'s fate during wastewater treatment process.

3) The fate prediction and occurrence measurement here only focused the liquid phase of primary effluent. It is necessary to combine the studies of both liquid and solid phases because of high adsorption and high potential distribution of nC_{60} on the solid phase.

4) nC_{60} would accumulate in wastewater sludge during wastewater treatment. It is necessary to investigate the nC_{60} fate during anaerobic digestion process.

5) nC_{60} adsorption would be affected by the surface properties of sludge, which depend on the operational condition of treatment processes. It is recommended to investigate the fate of nC_{60} in different biological treatment not only aerobic but also anaerobic ones.

ACKNOWLEDGEMENT

First and foremost, I would like to express my sincere appreciation to my supervisor, Professor Hiroaki Tanaka, Department of environmental engineering, Kyoto University. I am deeply grateful to him for providing the opportunity to pursue the Ph.D degree in Kyoto University, the instructive advice on how to conduct a new scientific field, and large support during the whole study period. I am also grateful to Professor Minoru Yoneda and Professor Sadahiko Itoh for their valuable comments and precious time for this dissertation.

I would like to express my thanks to Assistant Professor Norihide Nakada. I appreciate for his valuable discussion and support for the experimental setup and sampling as well as the preparation of manuscripts. I would like to thank Lecture Naoyuki Yamashita for his continuous and valuable help on this dissertation.

Great appreciation should also be given to Professor Yoshihisa Shimizu and Associate Professor Tomonari Matsuda for their suggestion and help on this dissertation. I also greatly thank Associate Professor Makoto Yasojima and Mr. Ryoji Nakajima in Shimadzu Techno-research lnc. for their help and support on the joint research. And also great thank goes to Dr. Wang Chao in the Technological and Higher education Institute of Hong Kong.

Special thanks also go to all the staffs and students in Research Center for Environmental Quality Management, Kyoto University. Specially, I would like to thank Mrs. Kazumi Hattori for his kind help on the research and my life in Japan. And particular thanks also go to Mr. Hanamoto and Mr. Narumiya for their great helps. Thanks also are given to all the Postdoc, Ph.D, Master and Bachelor students for giving me the kind help on the research and very pleasant life in Japan.

I also thank the MEXT (Ministry of Education, Culture, Sports, Science, and Technology), Japan, and GCOE-HSE program for the support to finish the doctoral research.

Finally, I would like to thank my family for their continuous support. Especially it is never too much to express my thanks and love to my wife, Qian Liu, for her support and understanding.